

**Fault Detection and Isolation of Two Time-Scaled
Singularly Perturbed Systems**

Fei Gong

A Thesis
in
The Department
of
Electrical and Computer Engineering

Presented in Partial Fulfillment of the Requirements
for the Degree of Master of Applied Science (Electrical Engineering) at
Concordia University
Montreal, Quebec, Canada

February 2006

@ Fei Gong, 2006



Library and
Archives Canada

Bibliothèque et
Archives Canada

Published Heritage
Branch

Direction du
Patrimoine de l'édition

395 Wellington Street
Ottawa ON K1A 0N4
Canada

395, rue Wellington
Ottawa ON K1A 0N4
Canada

Your file *Votre référence*
ISBN: 0-494-14257-X
Our file *Notre référence*
ISBN: 0-494-14257-X

NOTICE:

The author has granted a non-exclusive license allowing Library and Archives Canada to reproduce, publish, archive, preserve, conserve, communicate to the public by telecommunication or on the Internet, loan, distribute and sell theses worldwide, for commercial or non-commercial purposes, in microform, paper, electronic and/or any other formats.

The author retains copyright ownership and moral rights in this thesis. Neither the thesis nor substantial extracts from it may be printed or otherwise reproduced without the author's permission.

AVIS:

L'auteur a accordé une licence non exclusive permettant à la Bibliothèque et Archives Canada de reproduire, publier, archiver, sauvegarder, conserver, transmettre au public par télécommunication ou par l'Internet, prêter, distribuer et vendre des thèses partout dans le monde, à des fins commerciales ou autres, sur support microforme, papier, électronique et/ou autres formats.

L'auteur conserve la propriété du droit d'auteur et des droits moraux qui protègent cette thèse. Ni la thèse ni des extraits substantiels de celle-ci ne doivent être imprimés ou autrement reproduits sans son autorisation.

In compliance with the Canadian Privacy Act some supporting forms may have been removed from this thesis.

Conformément à la loi canadienne sur la protection de la vie privée, quelques formulaires secondaires ont été enlevés de cette thèse.

While these forms may be included in the document page count, their removal does not represent any loss of content from the thesis.

Bien que ces formulaires aient inclus dans la pagination, il n'y aura aucun contenu manquant.


Canada

ABSTRACT

Fault Detection and Isolation of Two Time-Scaled Singularly Perturbed Systems

Fei Gong

Singular perturbations technique is a means of taking into account neglected high-frequency and parasitic phenomena into modeling systems by decoupling the representation into separate slow and fast time-scales. The practical advantages of a singular perturbation in model order are significant, since the order of every real dynamical system is higher than that of the model used to represent the system.

This thesis focus is emphasized on the fault diagnosis of two time-scaled singularly perturbed systems. By decoupling the original full-order system into higher-order slow and fast subsystem models, our goal is to design a composite diagnoser based on diagnosers designed for the two subsystems to detect and isolate the faults in the original full-order system. Based on a power series expansion of the exact slow manifold associated with the original model around $\varepsilon = 0$, higher-order corrections of the manifold are obtained. Conditions are formulated for which a composite diagnoser can be designed for the original full-order system. Satisfying the conditions of a geometric approach, this composite diagnoser is used to diagnose the faults in the original full-order system. The illustrated methodology is applied to a two time-scale aircraft longitudinal dynamical model as well as the four degree of freedom gyroscope.

Acknowledgements

I would like to express my gratitude to all those who gave me the possibility to complete this thesis.

I am deeply indebted to my supervisor Dr. K. Khorasani whose help, stimulating suggestions and encouragement helped me in all the time of research for and writing of this thesis.

I want to thank my best friends Baoxin Zhao and Erica Gong for helping me get through the difficult times, and for all the emotional support, entertainment, and caring they provided.

Finally, I would like to give my special thanks to my parents whose love enabled me to complete this work.

TABLE OF CONTENTS

Chapter 1	Introduction.....	1
1.1	Fault Diagnosis Methodology.....	2
1.2	Singular Perturbation Methods in Control Analysis and Design.....	5
1.2.1	Order Reduction, Initial Value, and Boundary Value Problems.....	6
1.2.2	Stability and Stabilizability.....	7
1.2.3	Linear Feedback Control.....	8
1.2.4	Optimal Control.....	9
1.2.5	Nonlinear Systems.....	11
1.3	Contributions of the Thesis.....	13
1.4	Outline of the Thesis.....	14
Chapter 2	Fault Diagnosis Using Analytical and Knowledge-based Redundancy: A Review.....	16
2.1	Principles of Model-based FDI.....	17
2.2	Robust Residual Generation in Linear Systems.....	21
2.3	Adaptive Residual Generation in Linear Systems.....	24
2.4	Robust Residual Generation in Nonlinear Systems.....	26
2.5	Adaptive Residual Generation in Nonlinear Systems.....	29
2.6	Knowledge-based Residual Generation in Dynamic Systems.....	32
2.7	Conclusion.....	36
Chapter 3	Model Order Reduction and Composite Observer.....	37
3.1	Preliminaries.....	37

3.2	Uncorrected Slow and Fast Models	39
3.3	High-order Slow and Fast Models	42
3.4	Composite Observer Based on Uncorrected Models	45
3.5	Composite Observer Based on First-order Corrected Models	47
3.6	Conclusion.....	53
Chapter 4 A Geometric Approach to Fault Diagnosis.....		54
4.1	Preliminaries	54
4.2	Failure Modeling and Problem Formulation.....	55
4.3	A Geometric Approach to Actuator Fault Detection and Isolation.....	56
4.3.1	A Geometric Formulation and Solution to the BJDFP	56
4.3.2	Application to Singularly-Perturbed Systems.....	58
4.4	Simulation Results	59
4.4.1	Results with $\varepsilon = 0.01$	61
4.4.2	Results with $\varepsilon = 0.5$:.....	66
4.5	Conclusion.....	69
Chapter 5 Validation of the Proposed FDI Schemes to Two Applications		72
5.1	Two Time-scale Aircraft Longitudinal Dynamics	72
5.1.1	System Model	72
5.1.2	Composite Observer Design	82
5.1.3	Actuator Fault Diagnosis and Simulation Results	85
5.2	The Four Degree of Freedom (DOF) Gyroscope.....	86
5.2.1	System Model [40].....	86
5.2.3	Composite Observer Design	94

5.2.4	Actuator Fault Diagnosis and Simulation Results	97
5.3	Conclusion.....	99
Chapter 6	Conclusions and Future Work.....	102
6.1	Conclusions and Contributions	102
6.2	Future Direction of Research	104

LIST OF FIGURES

Figure 2-1 System Structure of a regional self-organizing scheme [34]	33
Figure 2-2 Sliding data window [34]	34
Figure 2-3 Two neighbor regions [34]	34
Figure 4-1 The state responses x_1, x_2, x_3, x_4 with $x_1^0 = 1, x_2^0 = 0, x_3^0 = 1, x_4^0 = 1$	61
Figure 4-2 Detection and identification of the actuator fault in the slow and fast subsystems at $\varepsilon = 0.01$ and $\varepsilon = 0.5$	65
Figure 4-3 The fault in the original system and the residuals with different observers gain at $\varepsilon = 0.01$	66
Figure 4-4 The fault in the original full-order system and the residuals for different observers with gains at $\varepsilon = 0.5$	70
Figure 5-1 Two Time-scale Aircraft Longitudinal Dynamics [39].....	74
Figure 5-2 Aircraft response in slow Figure 5-3 Aircraft response in fast	75
Figure 5-4 The exact solution vs. the uncorrected solution and 1 st -order corrected solution at $\varepsilon = 0.01$ and $u(t) = 1, x_1^0 = 100 \text{ feet / sec}, x_2^0 = 1 \text{ rad}$	79
Figure 5-5 The exact solution vs. uncorrected solution and the 1 st -order corrected solution at $\varepsilon = 0.05$ and $u(t) = 1, x_1^0 = 100 \text{ feet / sec}, x_2^0 = 1 \text{ rad}$	81
Figure 5-6 The responses of V and q for the closed-loop system with the composite full- order model observer G	84
Figure 5-7 The responses of V and q for the closed-loop system with the composite observer G_{or}	84
Figure 5-8 The faults in the slow and fast subsystems and the residuals associated with the uncorrected models	87

Figure 5-9 The fault in the original system and the residuals using different observer gain	88
Figure 5-10 The Four Degree of Freedom Gyroscope [40]	91
Figure 5-11 All gimbals free configuration ($q_{2_0} = 0, q_{3_0} = 0$) [40]	92
Figure 5-12 Performance comparison of the output responses (q_3, q_4) of the closed-loop system with the composite observer G (solid lines) and the observer G_{or} (dashed lines) directly designed for the original full-order system	96
Figure 5-13 The actuator fault in the original system and the residuals of different generators	101

LIST OF SYMBOLS

ε	A singular perturbation parameter
τ	The fast time scale
M_ε	An invariant n-dimensional manifold of the full-order singularly perturbed system
M_i	The i th-order corrected manifold
ϕ	The differentiable function of the manifold M_ε
ϕ_i	The i th term of ϕ
x_s^i	The state variables of the i th-order corrected slow model
u_s	The input of the slow model
x_f^i	The state variables of the i th-order corrected fast model
u_f	The input of the fast model
\hat{A}_{ij}	Matrix element of \hat{A}
G_i	The $(1,i)$ th matrix element of the observer gain matrix G of the full-order model
G_s^i	The observer gain matrix of the i th-order corrected slow model
G_f^i	The observer gain matrix of the i th-order corrected fast model
e_s^i	The error which is defined as $\hat{x}_s^i - x_s^i$
e_f^i	The error which is defined as $\hat{x}_f^i - x_f^i$
L_i	The effect of fault in the i th actuator which is equal to the i th column of B
f_i	The fault in the i th actuator
f_{sj}^i	The fault in the j th actuator of the i th-order corrected slow model
f_{fj}^i	The fault in the j th actuator of the i th-order corrected fast model

Chapter 1

Introduction

Modern control systems are becoming more and more complex. In order to maintain a high level of safety, performance and reliability in controlled processes, it is important that system errors, component faults and abnormal system operations are detected promptly and that the source and severity of each malfunction is diagnosed so that corrective actions can be taken.

The modeling of many systems calls for high-order dynamic equations. The presence of some parasitic parameters such as small time constants and moments of inertia are often the source for the increased order and “stiffness” of these systems. The stiffness, attributed to the simultaneous occurrence of “slow” and “fast” phenomena, gives rise to time scales. The systems in which the suppression of a small parameter is responsible for the degeneration of the system order are labeled as singularly perturbed systems, which are a special representation of the general class of time-scale systems.

In this thesis, we propose new considerations to design residuals for both slow and fast subsystems and the original system in order to detect and isolate faults in a singularly perturbed system possessing two separable time scales. The system model and composite

observer designs are investigated in detail, which are very useful not only for the problem of fault diagnosis but also for that of system control.

1.1 Fault Diagnosis Methodology

A “fault” is to be understood as an unexpected change of system function, although it may not represent physical failure or breakdown [1]. Such a fault or malfunction hampers or disturbs the normal operation of an automatic system, thus causing an unacceptable deterioration of the performance of the system or even leading to dangerous situations. A fault must be diagnosed as early as possible even it is tolerable at its early stage, to prevent any serious consequences.

A monitoring system that detects faults and diagnosis their location and significance in a system is called a “fault diagnosis system”. Such a system normally consists of the following tasks [1]:

Fault detection: to make a binary decision, either that something has gone wrong or that everything is fine.

Fault isolation: to determine the location of the fault, e.g., which sensor or actuator has become faulty.

Fault identification: to estimate the size and type or nature of the fault.

Hence, fault diagnosis is very often considered as fault detection and isolation, and is abbreviated as FDI.

A wide range of fault diagnosis approaches have been proposed in the literature which can be broadly divided into model-based techniques (analytical redundancy

approach), knowledge-based methodologies, empirical or signal processing techniques and artificial intelligence methods [2].

For the model-based approach, quantitative models (differential equations, state space methods, transfer functions, etc.) are used which generally utilize results from the field of control theory. The general and conceptual structure of a model-based fault diagnosis system comprises two main stages of residual generation and decision making [3]. A residual is fault indicator or an accentuating which reflects the faulty situation of the monitored system. The core element of model-based fault diagnosis methods is to generate residual as a fault indicating signal. A residual generator uses available input and output information of the system and generates a residual vectors, which should be normally zero or close to zero when no fault is present, but is distinguishably different from zero when a fault occurs. The residuals are examined for the likelihood of faults, and a decision rule is then applied to determine if any fault has occurred. Survey papers by Frank [4], Gertler [5], Isermann [6] and Willsky [7] present excellent overviews of the model-based fault diagnosis algorithms.

The model-based approach to fault diagnosis can be brought down to a few basic concepts: the observer-based method, the parity space method, and the parameter identification method. The basic idea behind the observer or filter-based approaches is to estimate the states of the system from the measurements by using either Luenberger observer in a deterministic setting or Kalman filter in a stochastic setting. The output estimation error is the used as a residual. The flexibility in selecting the observer gain has been fully exploited in the literature yielding a rich a variety of FDI schemes. Another common and important model-based technique is parity relation method. The basic idea

of the parity relation approach is to provide a proper check of the parity (consistence) of the measurements of the monitored system through two types of redundancies: direct redundancy which makes use of relationships among redundant sensor outputs, or temporal redundancy which counts on dynamic relationships between outputs and inputs. The model-based parameter estimation method makes use of the fact that the dynamic sofa systems are characterized by the physical parameters of the system. It detects the fault through estimation of the parameters of the mathematical model of the system. If the estimates of the parameters deviate from the nominal values, it may be declared that a fault has occurred.

Model-based FDI makes use of mathematical models of the supervised system. However, a perfectly accurate and complete mathematical model of a physical system is never available. Hence, there is always a mismatch between actual process and its mathematical model even when there are no process faults. The effect of modeling uncertainties is therefore the most crucial point in the model-based FDI concept. To overcome the difficulties introduced by modeling uncertainty, a model-based FDI has to be made robust. A number of robust model-based FDI methods have been proposed to tackle the problem, for example, the unknown input observer [8], high-gain observer [9], adaptive observer [10], and optimally robust parity relation methods [11,12].

Analytical approach applies to information-rich systems that provide enough sensor information and can satisfactorily be described by mathematical models. In the case of information-poor systems where much less system information and only poor models are available, the knowledge-based approach is selected. To develop knowledge-based diagnosis systems, knowledge about the process structure, process unit functions and

qualitative models of the process units under various faulty conditions are required. Thus, expert systems, neural networks [13] and fuzzy logic [14] can be applied. These methods are attractive as they do not require explicit mathematical models of the plant being monitored. The neural network training and fuzzy rule development from plant data actually provide implicit models of the plant being monitored (“data-based models”). In many practical situations, a combination of both the analytical and knowledge-based approach may be the most appropriate solution to the FDI problem [15].

1.2 Singular Perturbation Methods in Control Analysis and Design

Singularly perturbed systems and, more generally, multitime-scale systems, often occur naturally due to the presence of small “parasitic” parameters, typically small time constants, masses, etc., multiplying time derivative or, in more disguised form, due to the presence of large feedback gains and weak coupling effects. The main purpose of the singular perturbation approach to analysis and design is the alleviation of the high dimensionality and ill-conditioning resulting from the interaction of slow and fast dynamic modes.

Singular perturbations are a means of taking into account neglected high-frequency phenomena and considering them in a separate fast time-scale. This is achieved by treating a change in the dynamic order of a system of differential equations through a parameter perturbation designed as ε . The practical advantages of such changes in model order are significant, because the order of every real dynamic system is higher than that of the model used to represent the system. This time-scale approach is asymptotic, that is,

exact in the limit as the parameter ε of the speeds of the slow versus the fast dynamics tends to zero. When ε is small, approximations are obtained from reduced-order models in separate time scales. Singular perturbation and time-scale techniques were introduced to control engineering in the late 1960s and have since become common tools for the modeling, analysis and design for control systems. Fruitful results can be found in survey papers [16, 17] and book [18].

1.2.1 Order Reduction, Initial Value, and Boundary Value Problems

The standard singular perturbation model is in the explicit state space representations in which the derivatives of some of the states are multiplied by a small positive scalar ε , that is,

$$\dot{x} = f(x, z, \varepsilon, t), \quad x(t_0) = x^0, x \in R^n, \quad (1.1)$$

$$\varepsilon \dot{z} = g(x, z, \varepsilon, t), \quad z(t_0) = z^0, z \in R^m, \quad (1.2)$$

where f and g are assumed to be sufficiently many times continuously differentiable functions of their arguments x, z, ε, t . The scalar ε represents all the small parameters to be neglected. When we set $\varepsilon = 0$, the dimension of the state space of (1.1)-(1.2) reduces from $n+m$ to n because the differential equation (1.2) degenerates into the algebraic or transcendental equation

$$0 = g(\bar{x}, \bar{z}, 0, t) \quad (1.3)$$

where the bar is used to indicate that the variables belong to a system with $\varepsilon = 0$. If and only if the equation (1.3) has $k \geq 1$ distinct real roots

$$\bar{z} = \bar{\phi}_i(\bar{x}, t), \quad i = 1, 2, \dots, k \quad (1.4)$$

the model (1.1)-(1.2) is in the space standard form. This assumption ensures that a well-defined n -dimensional reduced model will correspond to each roots of (1.4). The reduced model

$$\dot{\bar{x}} = \bar{f}(\bar{x}, t), \quad \bar{x}(t_0) = x^0 \quad (1.5)$$

is called a quasi-steady-state model, because z , whose velocity $\dot{z} = g/\varepsilon$ can be large when ε is small, may rapidly converge to a root of (1.3), which is the quasi-steady-state form of (1.2). By contrast with the original variable z , starting at t_0 from a prescribed z^0 , there may be a large discrepancy between the initial value of the quasi-steady-state \bar{z}

$$\bar{z}(t_0) = \bar{\phi}(\bar{x}(t_0), t_0) \quad (1.6)$$

and the prescribed initial condition z^0 . The approximation

$$z = \bar{z}(t) + O(\varepsilon) \quad (1.7)$$

establishes that during an initial (“boundary layer”) interval $[t_0, t_1]$ the original variable z approaches \bar{z} and then, during $[t_1, T]$, remains close to \bar{z} .

1.2.2 Stability and Stabilizability

For a linear system with a control input $u(t) \in R^r$ and an output $y(t) \in R^p$; namely,

$$\begin{bmatrix} \dot{x} \\ \varepsilon \dot{z} \end{bmatrix} = \begin{bmatrix} A_{11} & A_{12} \\ A_{21} & A_{22} \end{bmatrix} \begin{bmatrix} x \\ z \end{bmatrix} + \begin{bmatrix} B_1 \\ B_2 \end{bmatrix} u, \quad \begin{bmatrix} x(t_0) \\ z(t_0) \end{bmatrix} = \begin{bmatrix} x^0 \\ z^0 \end{bmatrix}, \quad (1.8)$$

$$y = \begin{bmatrix} C_1 & C_2 \end{bmatrix} \begin{bmatrix} x \\ z \end{bmatrix}, \quad (1.9)$$

the system (1.8) is controllable if there exists a control $u(t)$ that transfer $x(t), z(t)$ from any bounded initial state $x(t_0), z(t_0)$ to any bounded terminal state $x(T), z(T)$ in a finite time $T - t_0$. Similarly, the system (1.8)-(1.9) is observable if the initial state $x(t_0), z(t_0)$ can be determined from the measurement of the input $u(t)$ and the output $y(t)$ over the period $[t_0, T]$.

A necessary and sufficient condition [18] for the i th eigenvalue λ_i of the system (1.8)-(1.9) to be controllable is

$$\text{rank}[\lambda_i I_{n+m} - A : B] = n + m, \quad (1.10)$$

and that for the i th eigenvalue λ_i of the system (1.8)-(1.9) to be observable is

$$\text{rank} \begin{bmatrix} \lambda_i I_{n+m} - A \\ C \end{bmatrix} = n + m. \quad (1.11)$$

1.2.3 Linear Feedback Control

To construct a state-feedback control for the singularly perturbed linear time-invariant system (1.8)-(1.9), the system is approximately decomposed into a slow system model and a fast system model as

$$\dot{x}_s(t) = A_s x_s(t) + B_s u_s(t), \quad x_s(t_0) = x^0, \quad (1.12)$$

$$\varepsilon \dot{z}_f(t) = A_{22} z_f(t) + B_2 u_f(t), \quad z_f(t_0) = z^0 - z_s(t_0), \quad (1.13)$$

where

$$A_s = A_{11} - A_{12}(A_{22})^{-1}A_{21}, \quad B_s = B_1 - A_{12}(A_{22})^{-1}B_2. \quad (1.14)$$

It is appropriate to consider the following decomposition of the feedback control where

$$u_s = K_0 x_s, \quad u_f = K_2 z_f \quad (1.15)$$

are separately designed for the slow and fast systems (1.12) and (1.13). A composite control for the full-order system (1.8)-(1.9) takes the realizable feedback form [18]:

$$u = K_0 x + K_2 [z + A_{22}^{-1} (A_{21} x + B_2 K_0 x)] = K_1 x + K_2 z, \quad (1.16)$$

where

$$K_1 = (I_r + K_2 A_{22}^{-1} B_2) K_0 + K_2 A_{22}^{-1} A_{21}. \quad (1.17)$$

1.2.4 Optimal Control

We apply the Hamiltonian condition to the problem of finding a control $u(t)$ that steers the state x, z of the singularly perturbed system

$$\dot{x} = f(x, z, t, \varepsilon, u), \quad x \in R^n, u \in R^r \quad (1.18)$$

$$\varepsilon \dot{z} = g(x, z, t, \varepsilon, u), \quad z \in R^m \quad (1.19)$$

from x_0, z_0 at $t=0$ to x_1, z_1 at $t=1$, that is

$$x(0) = x_0, z(0) = z_0, x(1) = x_1, z(1) = z_1 \quad (1.20)$$

while minimizing the cost function

$$J = \int_0^1 V(x, z, t, \varepsilon, u) dt. \quad (1.21)$$

This problem can be simplified by neglecting ε in two different ways. First, an optimality condition can be formulated for the exact problem and simplified by setting $\varepsilon = 0$. The result will be a reduced optimality condition. Second, by neglecting ε in the system (1.18)-(1.19), the same type of optimality condition can be formulated for the reduced system.

By using the Lagrangian, a necessary optimality condition for the exact problem is given as

$$N = V + p^T (\dot{x} - f) + q^T (\varepsilon \dot{z} - g), \quad (1.22)$$

where p and q are the multipliers associated with x and z respectively.

The reduced problem is obtained by setting $\varepsilon = 0$ in (1.18), (1.19) and (1.22), and dropping the requirement that $z(0) = z_0, z(1) = z_1$; that is, the reduced problem is defined as

$$\dot{x}_s = f(x_s, z_s, t, 0, u_s), \quad x_s(0) = x_0, \quad (1.23)$$

$$0 = g(x_s, z_s, t, 0, u_s), \quad x_s(1) = x_1, \quad (1.24)$$

$$J_s = \int_0^1 V(x_s, z_s, t, 0, u_s) dt \quad (1.25)$$

The Lagrangian for the reduced problem (1.23)-(1.25) is

$$\begin{aligned} N_s = & V(x_s, t, 0, u_s) + p_s^T [\dot{x}_s - f(x_s, z_s, t, 0, u_s)] \\ & - q_s^T g(x_s, z_s, t, 0, u_s) \end{aligned} \quad (1.26)$$

The more common Hamiltonian form is obtained via the Hamiltonian function

$$N_H = V + p^T f + q^T g. \quad (1.27)$$

Let us apply the Hamiltonian condition to the problem

$$\dot{x} = A_{11}x + A_{12}z + B_1u, \quad x(0) = x_0, x(1) = x_1 \quad (1.28)$$

$$\varepsilon \dot{z} = A_{21}x + A_{22}z + B_2u, \quad z(0) = z_0, z(1) = z_1 \quad (1.29)$$

$$y = C_1x + C_2z \quad (1.30)$$

$$J = \frac{1}{2} \int_0^1 (y^T y + u^T R u) dt, R > 0 \quad (1.31)$$

Using the Hamiltonian

$$N_H = \frac{1}{2}y^T y + \frac{1}{2}u^T R u + p^T (A_{11}x + A_{12}z + B_1u) + q^T (A_{21}x + A_{22}z + B_2u) \quad (1.32)$$

one can obtain [18]

$$u = -R^{-1}(B_1^T p + B_2^T q), \quad (1.33)$$

$$\dot{p} = -A_{11}^T p - A_{21}^T q - C_1^T C_1 x - C_1^T C_2 z, \quad (1.34)$$

$$\varepsilon \dot{q} = -A_{12}^T p - A_{22}^T q - C_2^T C_1 x - C_2^T C_2 z. \quad (1.35)$$

1.2.5 Nonlinear Systems

Consider a nonlinear autonomous singularly perturbed system

$$\dot{x} = f(x, z), \quad x \in R^n \quad (1.36)$$

$$\varepsilon \dot{z} = g(x, z), \quad z \in R^m \quad (1.37)$$

which has an isolated equilibrium at the origin. Stability of the equilibrium of (1.36)-(1.37) is investigated by examining the stability of the reduced (slow) system

$$\dot{x} = f(x, h(x)) \quad (1.38)$$

where $z=h(x)$ is an isolated root of $0=g(x,z)$, and the stability of the boundary-layer (fast) system

$$\frac{d\eta}{d\tau} = g(x, \eta(\tau)), \quad \eta = z - h(x), \quad \tau = \frac{t}{\varepsilon} \quad (1.39)$$

and in (1.39) x is treated as a fixed value. If $x=0$ is an asymptotically stable equilibrium of the reduced system (1.38), $\eta=0$ is an asymptotically stable equilibrium of the boundary-layer system (1.39). Furthermore, if f and g satisfy certain growth conditions,

then the origin is an asymptotically stable equilibrium of the singularly perturbed system (1.36)-(1.37) [18].

For the nonlinear autonomous systems

$$\dot{x} = f(x, z, u), \quad x \in R^n \quad (1.40)$$

$$\varepsilon \dot{z} = g(x, z, u), \quad z \in R^m \quad (1.41)$$

where u is a control input, the composite control procedure is to choose u as the sum of slow and fast controls

$$u = u_s + u_f \quad (1.42)$$

where u_s is a feedback function of x ,

$$u_s = \Gamma_s(x) \quad (1.43)$$

and u_f is a feedback function of x and z

$$u_f = \Gamma_f(x, z). \quad (1.44)$$

The fast feedback function $\Gamma_f(x, z)$ is designed to satisfy two crucial requirements. First, when the feedback control (1.42) is applied to (1.40)-(1.41), the closed-loop system should remain a standard singularly perturbed system. The second requirement is that $\Gamma_f(x, z)$ be “inactive” for $z = h(x, u_s)$, i.e.

$$\Gamma_f(x, h(x, \Gamma_s(x))) = 0. \quad (1.45)$$

Once $\Gamma_s(x)$ has been chosen, the boundary layer model of the closed-loop system is defined as

$$\frac{dz}{d\tau} = g(x, z, \Gamma_s(x) + u_f) \quad (1.46)$$

where x is treated as a fixed parameter.

Control applications of singular perturbation techniques are divided into three groups:

The first group comprises the use of singular perturbation in new control problems. One of these stresses the geometric aspect of two-time-scale systems and provides an interpretation of the important concept of zero dynamics [19]. Multi-time-scale behavior is also analyzed in high-gain observers, which are employed for stabilization of nonlinear systems [20].

The second group encompasses extensions and refinements of earlier theoretical concepts. More general singularly perturbed optimal control problems have been solved with a broader definition of the reduced problem based on averaging [21, 22]. Analytical tools for multi-time-scale analysis have also been advanced.

The third group includes diverse problem-specific applications. For example, to examine control issues of a robot manipulator modeled with link structural flexibility, [23] utilized a two time-scale approach by which asymptotic motion tracking can be effectively achieved and the force regulation error can be made arbitrarily small. And [24] adopted the hybrid position/force control for flexible link robot arm. A multi-time scale fuzzy logic controller is applied whereby using this methodology the control of the force and the position of the end point are possible while the end effector moves on the constraint surface.

1.3 Contributions of the Thesis

In this thesis, an observer design method is developed for fault diagnosis for a singularly perturbed system. The problem of Fault Detection and Isolation (FDI) has been

treated through many approaches, but these approaches have not been applied to singularly perturbed systems. Our goal is to design an integrated approach which enables one to detect and isolate faults in singularly perturbed system.

The contributions of the thesis are listed as follows:

- (1) High-order corrections of the slow and fast models of a singularly perturbed system with inputs are developed by equating terms in like powers of ε .
- (2) A full-order observer for the original singularly perturbed system is constructed based on observers designed separately for the slow and fast models.
- (3) The composite observer is designed for detecting high-order and isolating actuator faults in the full-order system.
- (4) The performance of the composite observer with that of the observer directly designed for the original full-order system are compared.

1.4 Outline of the Thesis

In this thesis, to detect and isolate actuator faults in a singularly perturbed system, based on a composite observer design frame work a geometric model-based approach is used.

Chapter 2 reviews the literature approaches and techniques for of fault detection and isolation in automatic processes using analytical and knowledge-based redundancy and presents some recent results.

Chapter 3 studies model order reduction and considers full-order observer for a class of singularly perturbed linear systems. The full order model is separated into slow

and fast subsystems of high-order by equating terms in like powers of ε . Conditions are formulated for which a composite observer approximates the state reconstruction of the original singularly perturbed system by utilizing a full-order observer. The composite observer is synthesized from full-order observers that are designed according to slow and fast for the two high-order subsystem models.

Chapter 4 applies a geometric model-based approach to isolate and detect the actuator faults in a singularly perturbed system. Based on the results of Chapter 3, a composite observer is used as a residual generator to diagnose the actuator faults in the full-order system. The performance of a composite observer and the observer directly designed for the full-order system are also compared.

Chapter 5 applies the preceding ideas to a two time-scale aircraft longitudinal dynamics and a four degree of freedom gyroscope. Though both of these systems are two time-scale, it is shown that the design of composite observer is not always necessary due to different observability and diagnosability of the systems. For each system, we compare the simulation results with different values of ε in order to evaluate the influence of ε on the performance of the FDI system.

Chapter 6 concludes with a discussion for the directions for future research.

Chapter 2

Fault Diagnosis Using Analytical and Knowledge-based Redundancy: A Review

This chapter reviews the approaches for fault detection and isolation in automatic processes using analytical and knowledge-based redundancy, and presents some recent results. It outlines the principles and the most important model-based techniques for residual generation using state estimation, parity space and parameter identification with emphasis upon the latest attempts to achieve robustness. The structural equivalence between the parity space approach and the observer-based approach is shown as a nonlinear function. The theory of robust linear observer-based residual generation for FDI is reviewed from a general point of view. The unknown input observer approach for robust residual generation in uncertain linear systems is extended to a class of nonlinear systems. Adaptive observer schemes are also reviewed. Finally, the knowledge-based

residual generation techniques are outlined to overcome the difficulty associated with the dependence of FDI on system models.

2.1 Principles of Model-based FDI

Model-based fault diagnosis can be defined as the detection, isolation and characterization of faults in components of a system from the comparison of the system's available measurements, with *a priori* information represented by the system's mathematical model. The model-based approach can basically be described as a two step process: generation of a residual that reflects the fault on the basis of a system model; and then evaluation of the residuals with the aid of a decision-maker.

As already introduced in Chapter 1, there are three methods to generate residuals: the observer-based method, the parity space method, and the parameter identification method. A parity residual is generated by computing on-line the known part of model equations. The major drawback of this approach is that the residuals are computed using time derivatives of measured variables. An observer-based residual is a combination of the estimation error on the outputs. The closed-loop structure makes there residual more robust with respect to noise and perturbations than parity ones.

The close relationship between the parity space and the observer-based approach has widely been developed in the linear case and some equivalence results are available. Wuennberg and Frank [25] has generally proved that the residual generation in terms of the parity space approach in the state space form is identical with a dead-beat observer. A derivation of this issue from a different point of view was given by Patton and Chen [26].

The comparison to a wider class of nonlinear MISO systems using high gain observers was recently extended by Christophe and Cocquempot [27].

To show a nonlinear relationship between parity residuals and high gain observer-based residuals, [27] considers dynamic MISO systems which are described by the following continuous time affine nonlinear model:

$$\Sigma : \begin{cases} \dot{x} = f(x) + g(x)u + k_1(x, u, \varphi) \\ y = h(x) + k_2(x, \varphi) \end{cases} \quad (2.1)$$

where φ represents the fault vector, $f(\cdot)$ and $k_1(\cdot)$ are smooth vector fields, $h(\cdot)$ and $k_2(\cdot)$ are smooth functions.

System (2.1) is uniformly observable if and only if, the following application

$$x \rightarrow z = \Psi(x) = \begin{pmatrix} h(x) \\ L_f h(x) \\ \vdots \\ L_f^{n-1} h(x) \end{pmatrix} \quad (2.2)$$

where $L_f h$ denote the Lie derivative of the scalar function h , is a diffeomorphism which transforms system (2.1) into the so-called Observable Canonical Form (OCF):

$$\Sigma_{OCF} : \begin{cases} \dot{z} = Ax + \Gamma(z) + G(z)u + k(z, u, \varphi) \\ y = Cz \end{cases} \quad (2.3)$$

where $k(z, u, 0) = 0$ and

$$A = \begin{bmatrix} 0 & 1 & \cdots & 0 \\ 0 & \ddots & \ddots & 0 \\ \vdots & & \ddots & 1 \\ 0 & \cdots & 0 & 0 \end{bmatrix}, \quad \Gamma(z) = \begin{pmatrix} 0 \\ \vdots \\ 0 \\ \gamma(z) \end{pmatrix}$$

$$G = \begin{pmatrix} g_1(z_1) \\ g_2(z_1, z_2) \\ \vdots \\ g_n(z_1, \dots, z_n) \end{pmatrix}, \quad C = [1 \quad 0 \quad \dots \quad 0]$$

Consider the n successive time derivations of the output y

$$\bar{y}^{(n)} = \Lambda_n(x, \bar{u}^{(n-1)}, \bar{\varphi}^{(n)}) \quad (2.4)$$

The redundancy relations of the parity space method are input/output relations obtained by eliminating the unknown state x in equation (2.2). Existence conditions of the relations depend on the rank of the Jacobian matrix $\frac{\partial \Lambda_n(x, \bar{u}^{(n-1)})}{\partial x}$. Moreover, it has been shown that for uniformly observable nonlinear systems, there exist as many redundancy relations as outputs. This redundancy relation, which is generated using symbolic computation algorithms, can be described as follows

$$w(\bar{y}^{(n)}, \bar{u}^{(n-1)}, \bar{\varphi}^{(n)}) = 0. \quad (2.5)$$

Consider the Taylor expansion of w with respect to φ

$$w(\bar{y}^{(n)}, \bar{u}^{(n-1)}, \bar{\varphi}^{(n)}) = w_c(\bar{y}^{(n)}, \bar{u}^{(n-1)}) - w_e(\bar{y}^{(n)}, \bar{u}^{(n-1)}, \bar{\varphi}^{(n)})$$

with $w_e(\bar{y}^{(n)}, \bar{u}^{(n-1)}, 0) = 0$. In the no fault case ($\varphi = 0$), $w_c(\bar{y}^{(n)}, \bar{u}^{(n-1)}) = 0$. When a fault occurs, it becomes different from 0. As a consequence, $w_e(\bar{y}^{(n)}, \bar{u}^{(n-1)})$ represents the computational expression of a parity residual ρ_p which can be used for fault detection. $w_e(\bar{y}^{(n)}, \bar{u}^{(n-1)}, 0) = 0$ is the evaluation expression of the residual ρ_p .

The parity residual is

$$\rho_p = w_c(\bar{y}^{(n)}, \bar{u}^{(n-1)}) = w_e(\bar{y}^{(n)}, \bar{u}^{(n-1)}, \bar{\varphi}^{(n)}). \quad (2.6)$$

Now consider the observer-based approach. Under the hypothesis that γ and the g_i 's in equation (2.3) are global Lipschitz, an asymptotic high gain observer for system (2.1) is defined by

$$\begin{aligned}\dot{\hat{x}} &= f(\hat{x}) + g(\hat{x})u - \left[\frac{\partial \Psi(\hat{x})}{\partial \hat{x}} \right]^{-1} S_{\infty}^{-1}(\theta) C^T (h(\hat{x}) - y) \\ \hat{y} &= h(\hat{x})\end{aligned}\quad (2.7)$$

with Ψ defined by equation (2.2) and where the gain matrix $S_{\infty}^{-1}(\theta)$ is the unique solution of the algebraic Lyapunov equation:

$$\theta S_{\infty}(\theta) + A^T S_{\infty}(\theta) + S_{\infty}(\theta) A - C^T C = 0 \quad (2.8)$$

where A and C are the canonical form representation of the linearized functions h , and θ is a positive and sufficiently large design parameter. When there is no fault present, the estimation error $e = \hat{y} - y$ converges asymptotically to zero. When a fault occurs, it becomes different from zero. Consequently, e can be used as a residual for the fault detection.

It was shown in [27] that the parity residual ρ_p and the high gain observer-based residual e are linked by a nonlinear differential equation which can be expressed in the following general form

$$\rho_p = -w_{obs2}(\bar{y}^{(n)}, \bar{u}^{(n-1)}, \bar{e}^{(n)}, \theta) \quad (2.9)$$

where

$$w_{obs2}(\bar{y}^{(n)}, \bar{u}^{(n-1)}, \bar{e}^{(n)}, \theta)_{\bar{e}^{(n)}=0, \theta=0} = 0 \quad (2.10)$$

Therefore, the two kinds of residual are linked by a nonlinear function which can be calculated *a priori*.

2.2 Robust Residual Generation in Linear Systems

The model-based FDI techniques have the advantage of making full use of the prior quantitative information of the process dynamics. But due to modeling difficulties, there is always a mismatch between the actual process and its mathematical model. Therefore, to design a robust FDI system in the sense that the FDI function can be insensitive to unknown inputs such as disturbances, and noise on the working system and model uncertainties, is a key challenge in model-based FDI approaches. The robust residual generation problem can be stated as follows [15]: for fault detection, the fault effect on the residual must be distinguishable from the effect of the unknown inputs; for fault isolation, the effects of the faults must, in addition, be distinguishable from each other.

To investigate a systematic and straightforward fault estimation scheme for robust process FDI, Park and Lee [28] developed the basic idea of using a special co-ordinate transformation in the observer design for a linear system with both faults and unknown inputs present.

Assume that the system considered can be expressed by:

$$\begin{aligned} \dot{x} &= Ax + Bu + Dd + Ff \\ y &= Cx \end{aligned} \tag{2.11}$$

where x is the state vector, u is the input vector, d is the unknown input vector, f is the process fault vector, and y is the output vector. Under the assumption that $\text{rank}(D) = l$ and $\text{rank}(F) = q$, one important consideration is to choose a nonsingular matrix:

$$T = \begin{bmatrix} N & D & F \end{bmatrix}, \quad N \in R^{n \times (n-l-q)} \tag{2.12}$$

for a co-ordinate transformation of the original full-order system (2.11), where N is an arbitrary matrix such that T is nonsingular. The given system (2.11) can be partitioned into the following form:

$$\begin{aligned}\dot{\bar{x}} &= \bar{A}\bar{x} + \bar{B}u + \bar{D}d + \bar{F}f \\ y &= \bar{C}\bar{x}\end{aligned}\quad (2.13)$$

where

$$\begin{aligned}x = T\bar{x} &= T \begin{bmatrix} \bar{x}_1 \\ \bar{x}_2 \\ \bar{x}_3 \end{bmatrix}, \bar{A} = T^{-1}AT = \begin{bmatrix} \bar{A}_{11} & \bar{A}_{12} & \bar{A}_{13} \\ \bar{A}_{21} & \bar{A}_{22} & \bar{A}_{23} \\ \bar{A}_{31} & \bar{A}_{32} & \bar{A}_{33} \end{bmatrix}, \\ \bar{B} = T^{-1}B &= \begin{bmatrix} \bar{B}_1 \\ \bar{B}_2 \\ \bar{B}_3 \end{bmatrix}, \bar{D} = T^{-1}D = \begin{bmatrix} 0 \\ I_l \\ 0 \end{bmatrix}, \bar{F} = T^{-1}F = \begin{bmatrix} 0 \\ 0 \\ I_q \end{bmatrix}, \\ \bar{C} = CT &= [CN \quad CD \quad CF]\end{aligned}\quad (2.14)$$

In (2.13), the differential equations corresponding to the state subvectors \bar{x}_2 and \bar{x}_3 , are directly influenced by the unknown input d and the fault f , respectively. Let us choose a nonsingular matrix U with the assumption that $\text{rank}(CD) = l$ and $\text{rank}(CF) = q$, that is

$$U = [CD \quad CF \quad Q], \quad Q \in R^{p \times (p-l-q)} \quad (2.15)$$

where

$$U^{-1} = [U_1 \quad U_2 \quad U_3]^T \quad (2.16)$$

We now obtain

$$\begin{aligned}\dot{\tilde{x}}_1 &= \tilde{A}_1\tilde{x}_1 + \tilde{B}_1u + E_1y \\ \tilde{y} &= \tilde{C}_1\tilde{x}_1\end{aligned}\quad (2.17)$$

where

$$\begin{aligned}
\tilde{A}_1 &= \bar{A}_{11} - \bar{A}_{12}U_1CN - \bar{A}_{13}U_2CN, \\
E_1 &= \bar{A}_{12}U_1 + \bar{A}_{13}U_2, \\
\tilde{C}_1 &= U_3CN, \\
\bar{y} &= U_3y
\end{aligned} \tag{2.18}$$

Under the assumption that the pair $(\tilde{A}_1, \tilde{C}_1)$ is observable or detectable, an observer can be constructed for the unknown input and fault-free system as:

$$\dot{w} = (\tilde{A}_1 - L\tilde{C}_1)w + \bar{B}_1u + L\bar{y} + E_1y. \tag{2.19}$$

The estimation error dynamics for the state \bar{x}_1 from (2.17) and (2.19) becomes

$$\dot{e}_{\bar{x}_1} = (\tilde{A}_1 - L\tilde{C}_1)e_{\bar{x}_1}. \tag{2.20}$$

The state of the original system (2.10) can be estimated as:

$$\hat{x} = T\hat{\bar{x}} = T \begin{bmatrix} \hat{\bar{x}}_1 \\ \hat{\bar{x}}_2 \\ \hat{\bar{x}}_3 \end{bmatrix} = T \begin{bmatrix} w \\ U_1y - U_1CNw \\ U_2y - U_2CNw \end{bmatrix}. \tag{2.20}$$

From the observer (2.19) and (2.21), the estimate of the unknown input d may be evaluated according to

$$\hat{d} = \hat{\bar{x}}_2 - \begin{bmatrix} \bar{A}_{21} & \bar{A}_{22} & \bar{A}_{23} \end{bmatrix} \hat{\bar{x}} - \bar{B}_2u \tag{2.21}$$

and the unknown input estimation error is found to be

$$e_d = U_1CNe_{\bar{x}_1} + (\bar{A}_{21} - \bar{A}_{22}U_1CN - \bar{A}_{23}U_2CN)e_{\bar{x}_1} \tag{2.22}$$

Similarly, an estimate of the fault f is:

$$\hat{f} = \hat{\bar{x}}_3 - \begin{bmatrix} \bar{A}_{31} & \bar{A}_{32} & \bar{A}_{33} \end{bmatrix} \hat{\bar{x}} - \bar{B}_3u \tag{2.23}$$

and the fault estimation error is given by

$$e_f = U_2CNe_{\bar{x}_1} + (\bar{A}_{31} - \bar{A}_{32}U_1CN - \bar{A}_{33}U_2CN)e_{\bar{x}_1}. \tag{2.24}$$

In conclusion, the use of the proposed transformation significantly reduces the order of the resulting observer. The observer information, the state estimate of the unknown input and fault-free system, will be used to reconstruct the shape and magnitude of the fault for the FDI purpose and also to estimate the unknown input. The fault estimates are the basis of FDI. They will also be used to construct an additional control inputs for fault tolerant control with which the original control objective can be achieved without considerable loss of control performance in the face of the actuator faults and failures.

2.3 Adaptive Residual Generation in Linear Systems

One of the major benefits of the unknown input observer-based methodology is that substantial robustness to model uncertainties can be achieved. But there is some weakness in detecting slowly developing faults, especially when large model uncertainties exist. To overcome this difficulty, adaptive observers may be used. In the context of FDI, an adaptive observer is a dynamic system that estimates output and slowly varying parameters at the same time. This means that besides abrupt faults, slowly developing faults as well as slow parameter variations can be estimated on-line. This will enhance the robustness of the residual generator.

An approach to identify the faults in actuators and sensors by the use of an adaptive observer has been presented in [29]. The approach provides the amplitude of faults and can be used for a system with uncertainty that cannot be decoupled from faults or residuals. In [30], Zhang proposed a new approach to design of globally exponential adaptive observers for joint state-parameter estimation in linear time-varying (LTV)

multiple-input-multiple-output (MIMO) systems, and provided some robustness analysis of the adaptive observers in the presence of modeling and measurement noises.

For a LTI MIMO system of the form

$$\dot{x}(t) = A(t)x(t) + B(t)u(t) + P(t)\theta \quad (2.25a)$$

$$y(t) = C(t)x(t) \quad (2.25b)$$

where $x(t) \in R^n, u(t) \in R^l, y(t) \in R^m$ are the state, input, and output of the system respectively, $A(t), B(t), C(t)$ are known time-varying matrices of appropriate dimensions, $\theta \in R^p$ is an unknown parameter vector assumed to be constant, $P(t) \in R^n \times R^p$ is a matrix of known signals. Let us rewrite (2.25a) as

$$\dot{x}(t) = [A(t) - K(t)C(t)]x(t) + B(t)u(t) + K(t)y(t) + \Psi(t)\theta \quad (2.26)$$

with a feedback matrix $K(t)$. Partition $x(t)$ into $x(t) = x_u(t) + x_\theta(t)$ with

$$\dot{x}_u(t) = [A(t) - K(t)C(t)]x_u(t) + B(t)u(t) + K(t)y(t) \quad (2.27)$$

$$\dot{x}_\theta(t) = [A(t) - K(t)C(t)]x_\theta(t) + \Psi(t)\theta \quad (2.28)$$

The observers to estimate $x_u(t)$ and $x_\theta(t)$ are now given by

$$\dot{\hat{x}}_u(t) = [A(t) - K(t)C(t)]\hat{x}_u(t) + B(t)u(t) + K(t)y(t) \quad (2.29)$$

$$\dot{\hat{x}}_\theta(t) = [A(t) - K(t)C(t)]\hat{x}_\theta(t) + \Psi(t)\hat{\theta}(t) + \omega(t) \quad (2.30)$$

According to (2.29) and (2.30), $\hat{x}(t)$ satisfies

$$\dot{\hat{x}}(t) = [A(t) - K(t)C(t)]\hat{x}(t) + B(t)u(t) + K(t)y(t) + \Psi(t)\hat{\theta}(t) + \gamma(t)\dot{\hat{\theta}}(t) \quad (2.31)$$

where

$$\omega(t) = \gamma(t)\dot{\hat{\theta}}(t). \quad (2.32)$$

Under the assumption that there exists a bounded time-varying matrix $K(t) \in R^n \times R^m$ so the system

$$\dot{\eta}(t) = [A(t) - K(t)C(t)]\eta(t) \quad (2.33)$$

is exponentially stable, and the assumption that $\gamma(t) \in R^n \times R^p$ is a matrix of signals generated by the ordinary differential equation (ODE) system

$$\dot{\gamma}(t) = [A(t) - K(t)C(t)]\gamma(t) + \Psi(t) \quad (2.34)$$

Let $\Gamma \in R^p \times R^p$ be any symmetric positive-definite matrix and $\Sigma(t) \in R^m \times R^m$ be some bounded symmetric positive-definite matrix., the ODE system

$$\begin{aligned} \dot{\hat{x}}(t) &= A(t)\hat{x}(t) + B(t)u(t) + \Psi(t)\hat{\theta}(t) \\ &+ [K(t) + \gamma(t)\Gamma\gamma^T(t)C^T(t)\Sigma(t)] \cdot [y(t) - C(t)\hat{x}(t)] \end{aligned} \quad (2.35a)$$

$$\dot{\hat{\theta}}(t) = \Gamma\gamma^T(t)C^T(t)\Sigma(t)[y(t) - C(t)\hat{x}(t)] \quad (2.35b)$$

is a global exponential adaptive observer for system (2.25), i.e., for any initial conditions $x(t_0), \hat{x}(t_0), \hat{\theta}(t_0)$ and $\forall \theta \in R^p$, the errors $\hat{x}(t) - x(t)$ and $\hat{\theta}(t) - \theta(t)$ tend to zero exponentially fast when $t \rightarrow \infty$ [30].

The proposed approach is applicable to MIMO linear time-varying systems. In addition to its generality, it is conceptually simple and computationally efficient. The robustness of the proposed adaptive observer and its convergence in the presence of noises have also been established [30].

2.4 Robust Residual Generation in Nonlinear Systems

In the following, we discuss observer-based methods for nonlinear residual generation which are employed if the system to be supervised cannot be represented with

sufficient accuracy by a fixed model. If the nonlinear process under consideration does not operate at a constant operating point but is subject to transients covering a wide range of working conditions, a linearization about a single operating point and the subsequent application of linear observer-based methods can cause false alarms due to model-plant mismatches. Moreover, using linear models in such cases makes the FDI system useless, because it provides a wrong fault isolation as soon as the system deviates from the operating point, owing to the occurrence of a fault. In order to avoid these limitations and difficulties nonlinear models must be used.

The idea of the linear unknown input fault detection observer which has been discussed earlier for linear systems can readily be extended to a certain class of nonlinear systems [15]. This class is described by

$$\begin{aligned}\dot{x} &= Ax + B(y, u) + E_1 d_1 + K_1 f_1 \\ y &= Cx + E_2 d_2 + K_2 f_2\end{aligned}\tag{2.36}$$

where d_1 and d_2 represent unknown inputs and the terms f_1 and f_2 are faults. The drawback of the extension of the linear FDI theory to nonlinear systems in [15] is the fact that the class of systems described by models matching (2.36) is rather small.

In [31], the system model is transformed into

$$\begin{aligned}\dot{x} &= Ax + Bu + Ed + f(x, u) \\ y &= Cx\end{aligned}\tag{2.37}$$

where $f(x, u) \in R^n$ is a nonlinear function of the states and inputs. In [31], the unknown inputs observer approach consists of two stages: in the first stage a change of coordinates is obtained that decouples the nonlinear system into two systems, one is independent of the unknown inputs, another is a linear combination of the outputs and the states of the

first subsystem; and in the second stage, a nonlinear observer is designed for the former.

With the matrices given as

$$T_1^T = \ker(E^T) \in R^{n \times (n-p)} \quad (2.38)$$

$$T_3^T = \ker((CE)^T) \in R^{m \times (m-p)} \quad (2.39)$$

the following undisturbed model exists

$$\dot{\hat{x}}_1 = \hat{A}\hat{x}_1 + \hat{A}_{12}\hat{C}_2^+y + \hat{B}_1u + T_1f(x,u) \quad (2.40)$$

$$\dot{\hat{x}}_2 = \hat{C}_2^+(y - \hat{C}_1\hat{x}_1) \quad (2.41)$$

$$\hat{y} = \hat{C}\hat{x}_1 \quad (2.42)$$

where

$$(C)^+ = (C^T C)^{-1} C^T$$

$$\begin{bmatrix} \hat{x}_1 \\ \hat{x}_2 \end{bmatrix} = \begin{bmatrix} T_1 \\ E^+ \end{bmatrix} x,$$

$$\hat{A} = (\hat{A}_{11} - \hat{A}_{12}\hat{C}_2^+\hat{C}_1),$$

$$\hat{C} = T_3\hat{C}_1,$$

$$\begin{bmatrix} \hat{A}_{11} & \hat{A}_{12} \\ \hat{A}_{21} & \hat{A}_{22} \end{bmatrix} = \begin{bmatrix} T_1 \\ E^+ \end{bmatrix} A \begin{bmatrix} T_1^T & E \end{bmatrix},$$

$$\begin{bmatrix} \hat{C}_1 & \hat{C}_2 \end{bmatrix} = C \begin{bmatrix} T_1^T & E \end{bmatrix} \begin{bmatrix} \hat{B}_1 \\ \hat{B}_2 \end{bmatrix} = \begin{bmatrix} T_1 \\ E^+ \end{bmatrix} B$$

$$(E)^+ = (E^T E)^{-1} E^T$$

An estimator is designed as

$$\dot{z} = \hat{A}z + \hat{A}_{12}\hat{C}_2^+y + \hat{B}_1u + T_1f(\hat{x},u) + S^{-1}(\theta)\hat{C}^T(\hat{y} - \hat{C}z) \quad (2.43)$$

where

$$\hat{A}^T S(\theta) + S(\theta)\hat{A} - \hat{C}^T\hat{C} + \theta S(\theta) = 0. \quad (2.44)$$

The residual is then generated as

$$r = \hat{C}z - \hat{y} \quad (2.45)$$

This proposed approach generalizes the early results of the unknown input approach to a class of nonlinear systems.

2.5 Adaptive Residual Generation in Nonlinear Systems

As explained in Section 2.3, adaptive observers can be used in uncertain dynamic systems. A robust nonlinear fault diagnosis scheme developed in [32] described an algorithm for a class of nonlinear dynamic systems with modeling uncertainties when not all states of the system are measurable. The main idea behind this approach is to monitor the plant for any off-nominal system behavior due to fault utilizing a nonlinear approximator with adjustable parameters. The online approximator only uses the system input and output measurements. A nonlinear estimator model and learning algorithm are described so that the online approximator provides an estimate of the fault.

Consider a single output dynamic system described by the differential equation

$$\dot{x} = \xi(x) + \rho(x, u) + \eta(x, u, t) + \beta(t - T)f(x, u) \quad (2.46a)$$

$$y = h(x) \quad (2.46b)$$

where $x \in R^n$ is the state of the system, $u \in R^m$ is the input of the system, $y \in R$ is the measurable output of the system, T denotes the unknown fault occurrence time. ξ, ρ, f, η are smooth vector fields and h is a smooth function, with η representing the modeling uncertainty, f characterizing the change in the system due to a failure, and β is a function representing the time profile of faults. The system

$$\dot{x}_N = \xi(x_N) + \rho(x_N, u) \quad (2.47a)$$

$$y_N = h(x_N) \quad (2.47b)$$

represents the known nominal model dynamics. Based on certain assumption [32], system (2.46) can be transformed using a known local diffeomorphism $z = \psi(x)$ into a new coordinate system as

$$\dot{z} = Az + \alpha(y, u) + \varphi(z, u, t) + \beta(t - T)\phi(y, u),^0 \quad z(0) = z^0 \quad (2.48a)$$

$$y = Cz \quad (2.48b)$$

where ϕ represents the unknown fault vector field in the new coordinate system given by

$$\phi = \left(\frac{\partial \psi}{\partial x} \right) f, \text{ and } \varphi \text{ represents the modeling uncertainties in the new coordinate}$$

system, given by

$$\varphi(z, u, t) = \frac{\partial \psi(x)}{\partial x} \eta(x, u, t) \Big|_{x=\psi^{-1}(z)}.$$

Based on system representation (2.48), the nonlinear estimation is chosen as

$$\dot{\hat{z}} = (A - KC)\hat{z} + \alpha(y, u) + Ky + \hat{\phi}(y, u, \hat{\theta}) + \Omega \dot{\hat{\theta}}, \quad \hat{z}(0) = z^0 \quad (2.49)$$

where K is a design constant vector chosen such that $A_0 := A - KC$ is Hurwitz, $\hat{\phi}$

represents an online approximation model and $\hat{\theta}$ represents the adjustable parameters of

the online approximator. The $n \times q$ matrix Ω is computed as the solution of the filter

$$\dot{\Omega} = A_0 \Omega + Z(y, u, \hat{\theta}), \quad \Omega(0) = 0 \quad (2.50)$$

where Z is the gradient of the online approximator with respect to its adjustable

parameter, i.e.

$$Z := \frac{\partial \hat{\phi}(y, u, \hat{\theta})}{\partial \hat{\theta}}. \quad (2.51)$$

Based on the estimation model (2.49) and the filter (2.50), the following parameter adaptive law is considered:

$$\dot{\hat{\theta}} = P\{\Gamma\Omega^T C^T D[e_y]\}, \quad \hat{\theta}(0) = \hat{\theta}_0 \quad (2.52)$$

where $\Gamma = \Gamma^T$ is a positive definite learning rate matrix and $e_y := y - C\hat{z}$ is the output estimation error. The dead-zone operator $D[\cdot]$ is defined as

$$D[e_y] := \begin{cases} 0, & |e_y| < \varepsilon \\ e_y & otherwise \end{cases} \quad (2.53)$$

In [33], Zhang presents a robust fault diagnosis scheme for abrupt and incipient faults in nonlinear uncertain dynamics. A detection and approximation estimator is used for online health monitoring. Once a fault is detected, a bank of isolation estimators are activated for the purpose of fault isolation. A key design issue of the scheme is the adaptive residual threshold associated with each isolation estimator. The following N nonlinear adaptive estimators are used as isolation estimators:

$$\begin{aligned} \dot{\hat{x}}^s &= -A^s(\hat{x}^s - x) + f(x, u) + \hat{\phi}^s(x, u, \hat{\theta}^s) \\ \hat{\phi}^s(x, u, \hat{\theta}^s) &= [(\hat{\theta}_1^s)^T g_1^s(x, u), \dots, (\hat{\theta}_n^s)^T g_n^s(x, u)]^T \end{aligned} \quad (2.54)$$

where $\hat{\theta}_i^s, i = 1, \dots, n, s = 1, \dots, N$, is the estimate of the fault parameter vector in the i th state variable and $H^s = \text{diag}(\lambda_1^s, \dots, \lambda_n^s)$, where $-\lambda_i^s < 0$ is a constant that represents the estimator pole locations.

Each isolation estimator corresponds to one of the possible types of nonlinear faults belonging to the fault class. The adaptation in the isolation estimators arises due to the unknown parameter vector θ_i^s . The adaptive law for updating each $\hat{\theta}_i^s$ is derived by using the Lyapunov synthesis approach, with the projection operator restricting $\hat{\theta}_i^s$ to the

corresponding known set Θ_i^s . Specifically, if we let $\epsilon_i^s = x_i - \hat{x}_i^s$ be the i th component of the state estimation error vector of the s th estimator, then the learning algorithm is chosen as

$$\dot{\hat{\theta}}_i^s = P\{\Gamma_i^s g_i^s(x, u) \epsilon_i^s\}. \quad (2.55)$$

The fault isolation and decision scheme: if, for each $r \in \{1, \dots, N\} \setminus \{s\}$, there exist some finite time $t^r > T_d$ and some $i \in \{1, \dots, n\}$ such that $|\epsilon_i^r(t^r)| > \mu_i^r(t^r)$, then the occurrence of the fault s is deduced. The absolute fault isolation time is defined as $T_{isol}^s = \max\{t^r, r \in \{1, \dots, N\} \setminus \{s\}\}$.

2.6 Knowledge-based Residual Generation in Dynamic Systems

Design of model-based FDI scheme depends heavily on system model. Generally speaking, it is rather difficult to design model-based FDI for nonlinear or uncertain systems. To tackle this problem, knowledge-based methods have been proposed and studied. Without the need for a complete analytical model, these methods rely on data-driven and knowledge-based techniques to estimate the system dynamics. Some of the knowledge-based methods also use certain “models” built by neural networks, fuzzy systems, or expert systems, for mapping the inputs and outputs of the unknown system. Residual signals are then generated to detect and locate the faults in a similar fashion as model-based methods.

Zhao in [34] developed a real-time FDI scheme by integrating the signal processing technique with neural network design. Wavelet analysis is applied to capture the fault-

induced transients of the measured signals in real-time and the decomposed signals are pre-processed to extract details about a fault. A regional self-organizing feature map (R-SOM) neural network is synthesized to classify the fault types. The system structure is clearly depicted in the Fig. 2-1, which also demonstrates the design and operation process. The FDI system can be divided into the offline learning and the online recognition procedures. The R-SOM neural network is trained offline with the normal conditions and all pre-assumed faults. In the online recognition process, the neural network matched the online features to the known patterns in the knowledge base.

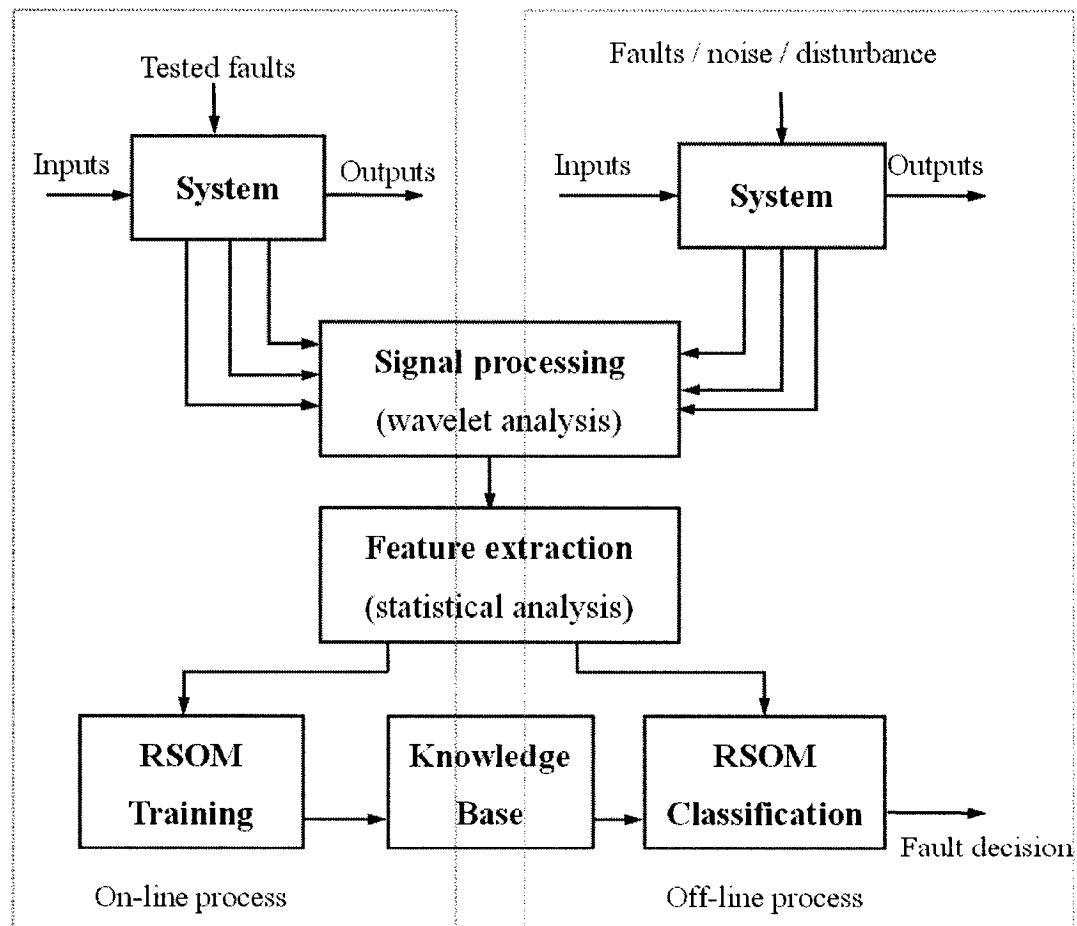


Figure 2-1 System Structure of a regional self-organizing scheme [34]

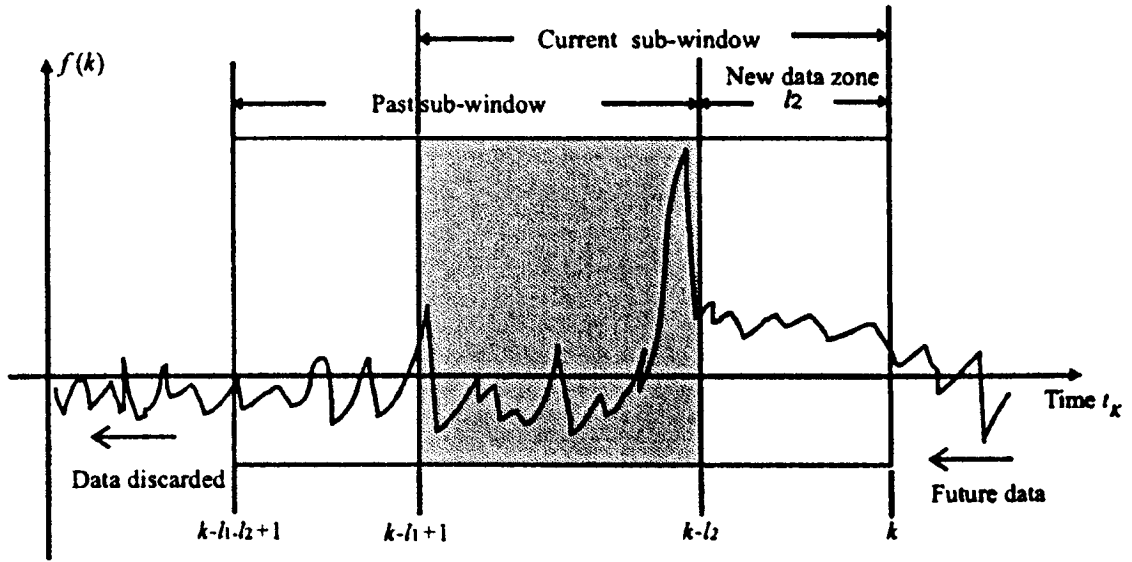


Figure 2-2 Sliding data window [34]

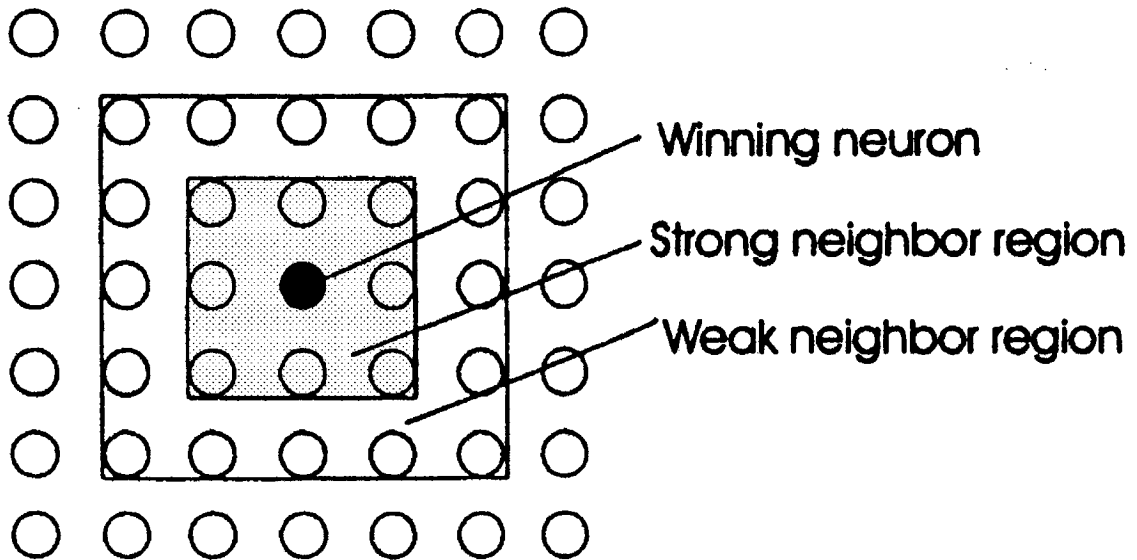


Figure 2-3 Two neighbor regions [34]

In order to achieve the online and real-time fault detection, it needs signal analysis tools that are sensitive to the transient phenomena of the system. For this reason, the

wavelet analysis method and the sliding window techniques are applied to detect signal variations including possible fault-induced transients. The wavelet transform is

$$Wf(u, s) = \frac{1}{\sqrt{s}} \int_{-\infty}^{\infty} f(t) \Psi^* \left(\frac{t-u}{s} \right) dt \quad (2.56)$$

A sliding data window shown in Fig. 2-2 is used for online and real processing. The data window contains two overlapped sub-windows of same length l_1 , labeled as past and current sub-windows, S_p and S_c :

$$S_p = [f(k-l_2), f(k-l_2-1), \dots, f(k-l_1-l_2+1)] \quad (2.57)$$

while

$$S_c = [f(k), f(k-1), \dots, f(k-l_1+1)]. \quad (2.58)$$

The self-organizing neural network, a type of Kohonen network [34], has the capability of learning and adaptation without supervision. Fig. 2-3 shows the two neighbor regions around the winning neuron in the 2-D array, i.e., the strong neighbor region and the weak neighbor region. The weights in the strong neighbor region R_s and the weak neighbor region R_w are adjusted separately as follows:

$$w_{ij}^k(t+1) = w_{ij}^k(t) + \eta(t)[a_{ik} - w_{ij}^k(t)], \quad i, j \in R_s \quad (2.59)$$

$$w_{ij}^k(t+1) = w_{ij}^k(t) + \mu(t)\eta(t)[a_{ik} - w_{ij}^k(t)], \quad i, j \in R_w \quad (2.60)$$

The learning rate $\eta(t)$ is chosen as an exponential function that declines quickly at the beginning and the slowly converge to zero

$$\eta(t) = \eta_0 e^{-\alpha \frac{t}{T}}. \quad (2.61)$$

The R-SOM network has two learning processes: 1) quick rough learning (by the neurons in the strong neighbor region) to capture the major properties of the input model and 2)

the slow fine-tuning (by the neurons in the weak neighbor region) to reveal the minor details of input feature. The exponential rate affects the speed of these two processes.

Most of the design techniques for knowledge-based FDI scheme are application specific, the effort to design a general knowledge-based FDI scheme has been made in [34]. A fuzzy-neural network with a general parameter (GP) learning algorithm and heuristic model structure determination is also proposed in [35] by taking advantage of fuzzy systems and neural networks.

2.7 Conclusion

To detect and isolate faults in a dynamic system by using analytical model, a declarative or residual signal must be generated, which is derived from a combination of real measurements and estimates (generated by the model). The robustness problem can be tackled by defining independent sensitivities of the residual to uncertainties and faults. A robust FDI scheme is one whose residual is insensitive to uncertainties whilst sensitive to faults. The aim of robust design for a FDI scheme is to reduce the effects of uncertainties on the residual, and (or) to enhance the effects of faults acting on the residuals. A primary requirement of residuals for successful diagnosis is the robustness with respect to modeling uncertainty. In this thesis, we will discuss the fault diagnosis for a class of two time-scaled systems with actuator faults.

Chapter 3

Model Order Reduction and Composite Observer

In this chapter, we will develop high-order reduced subsystem models for a linear two time-scale system governed by

$$\dot{x}_1 = A_{11}x_1 + A_{12}x_2 + B_1u, \quad x_1 \in R^n \quad (3.1)$$

$$\varepsilon \dot{x}_2 = A_{21}x_1 + A_{22}x_2 + B_2u, \quad x_2 \in R^m, u \in R, \varepsilon > 0 \quad (3.2)$$

$$y = C_1x_1 + C_2x_2 \quad (3.3)$$

and discuss how to design a composite observer for the original full-order system based on the reduced order observers for the subsystems. This chapter also serves as the preparation for the next chapter, which is about fault diagnosis for the system (3.1)-(3.3) using a geometric approach based on the system model and observers.

3.1 Preliminaries

The singular perturbation model of a finite-dimensional dynamic system has been extensively studied in the mathematical literature, and was used in control and

systems theory. This model is in the explicit state-space representation form in which the derivative of some of the states are multiplied by a small scalar ε , that is

$$\dot{x}_1 = f(x_1, x_2, u, t, \varepsilon) \quad (3.4)$$

$$\varepsilon \dot{x}_2 = g(x_1, x_2, u, t, \varepsilon) \quad (3.5)$$

where $\varepsilon > 0$ and x_1, x_2 and u are n, m and r dimensional vectors, respectively.

As functions of time, the solutions $x_1(t, \varepsilon)$, $x_2(t, \varepsilon)$ of the system (3.4)-(3.5) consist of a fast boundary layer and a slow quasi-steady-state. The layer is significant only in $x_2(t, \varepsilon)$, while $x_1(t, \varepsilon)$ is predominantly slow since its layer is not larger than $O(\varepsilon)$. In the $(n+m)$ -dimensional state space of x_1 and x_2 , an n -dimensional manifold M_ε which depends on the scalar parameter ε can be defined by the expression

$$M_\varepsilon : x_2 = \phi(x_1, u, \varepsilon). \quad (3.6)$$

M_ε is an invariant manifold of (3.4)-(3.5) if when it holds for $t = t^*$

$$x_2(t^*, \varepsilon) = \phi(x_1(t^*, \varepsilon), \varepsilon) \Rightarrow x_2(t, \varepsilon) = \phi(x_1(t, \varepsilon), \varepsilon) \quad \forall t \geq t^*. \quad (3.7)$$

An approximation to $\phi(x_1, u, \varepsilon)$ can be obtained by expanding $\phi(x_1, u, \varepsilon)$, f , g in a power series about $\varepsilon = 0$ [18],

$$\phi(x_1, u, \varepsilon) = \phi_0(x_1, u) + \varepsilon \phi_1(x_1, u) + \dots \quad (3.8)$$

The uncorrected slow manifold at $\varepsilon = 0$ is defined as

$$M_0 : x_2 = \phi_0(x_1, u). \quad (3.9)$$

The deviation of the exact fast variables from this manifold is defined by

$$x_f^0 = x_2 - \phi_0(x_1, u). \quad (3.10)$$

By defining the fast time scale as

$$\tau = \frac{1}{\varepsilon} \quad (3.11)$$

the uncorrected slow and fast systems are obtained as [18]

$$\frac{dx_1}{dt} = f(x_1, \phi_0 + x_f^0, u, 0) \quad (3.12)$$

$$\frac{dx_f^0}{d\tau} = g(x_1, \phi_0 + x_f^0, u, 0) \quad (3.13)$$

The first-order-corrected manifold at $\varepsilon^2 = 0$ is defined as

$$M_1 : x_2 = \phi_0(x_1, u) + \varepsilon\phi_1(x_1, u). \quad (3.14)$$

The deviation of the exact fast variables from this manifold is defined by

$$x_f^1 = x_2 - \phi_0(x_1, u) - \varepsilon\phi_1(x_1, u). \quad (3.15)$$

and the first-order-corrected slow and fast subsystems are obtained as

$$\frac{dx_1}{dt} = f(x_1, \phi_0 + \varepsilon\phi_1 + x_f^1, u, 0) \quad (3.16)$$

$$\frac{dx_f^1}{d\tau} = g(x_1, \phi_0 + \varepsilon\phi_1 + x_f^1, u, 0) \quad (3.17)$$

Higher order corrections, $\varepsilon^2\phi_2(x_1, u)$, etc. are manifold defined likewise. At the n -th stage one obtains an $O(\varepsilon^n)$ approximation closer to the exact manifold M_ε as compared to uncorrected manifold.

3.2 Uncorrected Slow and Fast Models

In this and next sections, we develop slow and fast models for a class of singularly perturbed systems. It is shown in these two sections that the derivative of the inputs plays an important role in high-order slow and fast models. This leads to reduced order models of the original full-order system which may prove more useful for control system design than either the full-order model or the uncorrected models.

We consider a linear singularly perturbed system

$$\dot{x}_1 = A_{11}x_1 + A_{12}x_2 + B_1u, \quad x_1 \in R^n \quad (3.18)$$

$$\varepsilon \dot{x}_2 = A_{21}x_1 + A_{22}x_2 + B_2u, \quad x_2 \in R^m, u \in R, \varepsilon > 0 \quad (3.19)$$

$$y = C_1x_1 + C_2x_2 \quad (3.20)$$

where

$$f(x_1, x_2, u, t, \varepsilon) = A_{11}x_1 + A_{12}x_2 + B_1u,$$

$$g(x_1, x_2, u, t, \varepsilon) = A_{21}x_1 + A_{22}x_2 + B_2u.$$

At $\varepsilon = 0$ and setting $u = u_s + u_f$ with $u_f(\varepsilon = 0) = 0$, we obtain

$$\begin{aligned} A_{21}x_1 + A_{22}\phi_0 + B_2u_s &= 0 \\ \Rightarrow \phi_0 &= -(A_{22})^{-1}(A_{21}x_1 + B_2u_s) \end{aligned} \quad (3.21)$$

Therefore, using $\eta + \phi_0 = x_2$ or $x_f^0 = x_2 - \phi_0$ we get

$$\begin{aligned} \dot{x}_1 &= f(x_1, \phi_0 + x_f^0, u) \\ &= A_{11}x_1 + A_{12}(\phi_0 + \eta) + B_1(u_s + u_f) \\ &= A_{11}x_1 - A_{12}(A_{22})^{-1}(A_{21}x_1 + B_2u_s) + B_1u_s + A_{12}x_f^0 + B_1u_f \\ &= [A_{11} - A_{12}(A_{22})^{-1}A_{21}]x_1 + [B_1 - A_{12}(A_{22})^{-1}B_2]u_s + A_{12}x_f^0 + B_1u_f \end{aligned} \quad (3.22)$$

which is represented as

$$\dot{x}_1 = A_s^0 x_1 + B_s^0 u_s + A_{12}x_f^0 + B_1u_f \quad (3.23)$$

where

$$A_s^0 = A_{11} - A_{12}(A_{22})^{-1}A_{21}, \quad B_s^0 = B_1 - A_{12}(A_{22})^{-1}B_2,$$

And for the fast dynamics

$$\begin{aligned} \varepsilon \dot{x}_f^0 &= g(x_1, \phi_0 + x_f^0, u) \\ &= A_{21}x_1 + A_{22}(x_f^0 + \phi_0) + B_2(u_s + u_f) \\ &= A_{21}x_1 + A_{22}x_f^0 - A_{21}x_1 - B_2u_s + B_2u_s + B_2u_f \end{aligned}$$

$$= A_{22}x_f^0 + B_2u_f \quad (3.24)$$

which is re-written as

$$\frac{dx_f^0}{d\tau} = A_{22}x_f^0 + B_2u_f \quad (3.25)$$

In order to eliminate x_f^0 in (3.22), express x_f^0 in terms of $\varepsilon\dot{x}_f^0$, use (3.24) and substitute it into (3.22)

$$\begin{aligned} \dot{x}_1 - A_{12}x_f^0 - B_1u_f &= A_s^0x_1 + B_s^0u_s \\ \Rightarrow \dot{x}_1 - \varepsilon A_{12}A_{22}^{-1}\dot{x}_f^0 - (B_1 - A_{12}A_{22}^{-1}B_2)u_f &= A_s^0x_1 + B_s^0u_s \\ \Rightarrow \dot{x}_1 - \varepsilon A_{12}A_{22}^{-1}\dot{x}_f^0 - B_s^0u_f &= A_s^0x_1 + B_s^0u_s. \end{aligned} \quad (3.26)$$

A new variable is now defined as

$$x_s^0 = x_1 - \varepsilon A_{12}A_{22}^{-1}\dot{x}_f^0 - B_s^0 \int u_f dt \quad (3.27)$$

then

$$\dot{x}_s^0 = A_s^0(x_s^0 + \varepsilon A_{12}A_{22}^{-1}\dot{x}_f^0 + B_s^0 \int u_f dt) + B_s^0u_s, \quad (\varepsilon = 0, u_f = 0) \quad (3.28)$$

For the output definition of the system, we define slow and fast outputs according to

$$y_s^0 = y|_{\varepsilon=0} = C_1x_s^0 + C_2\phi_0 = (C_1 - C_2A_{22}^{-1}A_{21})x_s^0 - C_2A_{22}^{-1}B_2u_s \quad (3.29)$$

$$\begin{aligned} y_f^0 &= y - y_s^0 \\ &= C_1x_s^0 + C_2(\eta + \phi_0) - (C_1 - C_2A_{22}^{-1}A_{21})x_s^0 - C_2A_{22}^{-1}B_2u_s \\ &= C_2\eta \end{aligned} \quad (3.30)$$

Therefore, the uncorrected slow subsystem is governed by

$$\dot{x}_s^0 = A_s^0x_s^0 + B_s^0u_s \quad (3.31)$$

$$y_s^0 = C_s^0x_s^0 + D_s^0u_s \quad (3.32)$$

where

$$A_s^0 = A_{11} - A_{12}A_{22}^{-1}A_{21}, \quad B_s^0 = B_1 - A_{12}A_{22}^{-1}B_2,$$

$$C_s^0 = C_1 - C_2A_{22}^{-1}A_{21}, \quad D_s^0 = -C_2A_{22}^{-1}B_2.$$

And the uncorrected fast subsystem is governed by

$$\frac{dx_f^0}{d\tau} = A_{22}x_f^0 + B_2u_f \quad (3.33)$$

$$y_f^0 = C_2x_f^0. \quad (3.34)$$

3.3 High-order Slow and Fast Models

In order to obtain models that are closer to the full-order system, for the singularly perturbed system (3.18)-(3.20), at $\varepsilon^2 = 0$, we obtain higher-order slow and fast subsystems.

$$\begin{aligned} \phi_1(x_1, u) &= \left(\frac{\partial g}{\partial x_2} \right)_{x_2=\phi_0}^{-1} \left(\frac{\partial \phi_0}{\partial x_1} f(x_1, \phi_0) + \frac{\partial \phi_0}{\partial u_s} \dot{u}_s \right) \\ &= -A_{22}^{-2} [A_{21}(A_{11}x_1 + A_{12}\phi_0 + B_1u_s) + B_2\dot{u}_s] \\ &= -A_{22}^{-1} [A_{21}(A_{11} - A_{12}A_{22}^{-1}A_{21})x_1 + A_{21}(B_1 - A_{12}A_{22}^{-1}B_2)u_s + B_2\dot{u}_s] \end{aligned} \quad (3.35)$$

Therefore, the dynamics associated with x_1 become

$$\begin{aligned} \dot{x}_1 &= f(x_1, \phi_0 + \varepsilon\phi_1 + x_f^1, u) \\ &= A_{11}x_1 + A_{12}(\phi_0 + \varepsilon\phi_1 + x_f^1) + B_1(u_s + u_f) \\ &= A_{11}x_1 - A_{12}A_{22}^{-1}(A_{21}x_1 + B_2u_s) + B_1u_s + A_{12}x_f^1 - \varepsilon A_{12}A_{22}^{-2}(A_{21}A_s^0x_1 + A_{21}B_s^0u_s + B_2\dot{u}_s) + B_1u_f \\ &= A_{11}x_1 + A_{12}(\phi_0 + \varepsilon\phi_1 + x_f^1) + B_1(u_s + u_f) \end{aligned} \quad (3.36)$$

which is re-written as

$$\dot{x}_1 = A_s^1x_1 + B_s^1u_s - \varepsilon A_{12}A_{22}^{-2}B_2\dot{u}_s + A_{12}x_f^1 + B_1u_f \quad (3.37)$$

where

$$A_s^1 = A_s^0 - \varepsilon A_{12} A_{22}^{-2} A_{21} A_s^0, \quad B_s^1 = B_s^0 - \varepsilon A_{12} A_{22}^{-2} A_{21} B_s^0.$$

For the fast variable x_2 we now obtain

$$\begin{aligned} \varepsilon \dot{x}_f^1 &= g(x_1, \phi_0 + \varepsilon \phi_1 + x_f^1) - \varepsilon \left(\frac{\partial \phi_0}{\partial x} f(x_1, \phi_0 + x_f^1) + \frac{\partial \phi_0}{\partial u_s} \dot{u}_s \right) \\ &= A_{21} x_1 + A_{22} (\phi_0 + \varepsilon \phi_1 + x_f^1) + B_2 (u_s + u_f) - \varepsilon \{ -A_{22}^{-1} A_{21} [A_{11} x_1 + \\ &\quad A_{12} (\phi_0 + x_f^1) + B_1 (u_s + u_f)] - A_{22}^{-1} B_2 \dot{u}_s \} \\ &= B_2 u_f - \varepsilon A_{22}^{-1} (A_{21} A_s^0 x_1 + A_{21} B_s^0 u_s + B_2 \dot{u}_s) + A_{22} x_f^1 + \\ &\quad \varepsilon A_{22}^{-1} (A_{21} A_s^0 x_1 + A_{21} B_s^0 u_s + A_{21} A_{12} x_f^1 + B_2 \dot{u}_s + A_{21} B_1 u_f) \\ &= (A_{22} + \varepsilon A_{22}^{-1} A_{21} A_{12}) x_f^1 + (B_2 + \varepsilon A_{22}^{-1} A_{21} B_1) u_f \end{aligned} \quad (3.38)$$

which is re-written as

$$\varepsilon \dot{x}_f^1 = A_f^1 x_f^1 + B_f^1 u_f \quad (3.39)$$

where

$$A_f^1 = A_{22} + \varepsilon A_{22}^{-1} A_{21} A_{12}, \quad B_f^1 = B_2 + \varepsilon A_{22}^{-1} A_{21} B_1.$$

Let us now define a new variable as

$$x_s^1 = x_1 - \varepsilon A_{12} A_{22}^{-1} x_f^1 - \varepsilon^2 A_s^1 A_{12} A_{22}^{-2} x_f^1 \quad (3.40)$$

This implies that its dynamics is governed by

$$\begin{aligned} \dot{x}_s^1 &= A_s^1 (x_s^1 + \varepsilon^2 A_s^1 A_{12} A_{22}^{-2} x_f^1) + B_s^1 u_s - \varepsilon A_{12} A_{22}^{-2} B_2 \dot{u}_s \\ &= A_s^1 x_s^1 + B_s^1 u_s - \varepsilon A_{12} A_{22}^{-2} B_2 \dot{u}_s \quad (\varepsilon^2 = 0) \end{aligned} \quad (3.41)$$

The corrected slow output of the system is now given by

$$\begin{aligned} y_s^1 &= y|_{\varepsilon^2=0} \\ &= C_1 x_s^1 + C_2 (\phi_0 + \varepsilon \phi_1) \end{aligned}$$

$$\begin{aligned}
&= [(C_1 - C_2 A_{22}^{-1} A_{21}) - \varepsilon C_2 A_{22}^{-2} A_{21} A_s^0] x_s^1 - \\
&(C_2 A_{22}^{-1} B_2 + \varepsilon C_2 A_{22}^{-2} A_{21} B_s^0) u_s - \varepsilon C_2 A_{22}^{-2} B_2 \dot{u}_s
\end{aligned} \tag{3.42}$$

and the corrected fast output of the system is given by

$$\begin{aligned}
y_f^1 &= y - y_s^1 \\
&= C_1 x_s^1 + C_2 (\phi_0 + \varepsilon \phi_1 + x_f^1) - [(C_1 - C_2 A_{22}^{-1} A_{21}) - \varepsilon C_2 A_{22}^{-2} A_{21} A_s^0] x_s^1 \\
&\quad + (C_2 A_{22}^{-1} B_2 + \varepsilon C_2 A_{22}^{-2} A_{21} B_s^0) u_s + \varepsilon C_2 A_{22}^{-2} B_2 \dot{u}_s \\
&= C_2 x_f^1
\end{aligned} \tag{3.43}$$

To summarize, the 1st-order corrected slow and fast subsystems are governed by

$$\dot{x}_s^1 = A_s^1 x_s^1 + B_s^1 u_s \tag{3.44}$$

$$y_s^1 = C_s^1 x_s^1 + D_s^1 u_s - \varepsilon C_2 A_{22}^{-2} B_2 \dot{u}_s \tag{3.45}$$

where

$$\begin{aligned}
A_s^1 &= A_s^0 - \varepsilon A_{12} A_{22}^{-2} A_{21} A_s^0, \quad B_s^1 = B_s^0 - \varepsilon A_{12} A_{22}^{-2} A_{21} B_s^0, \\
C_s^1 &= C_s^0 - \varepsilon C_2 A_{22}^{-2} A_{21} A_s^0, \quad D_s^1 = D_s^0 - \varepsilon C_2 A_{22}^{-2} A_{21} B_s^0,
\end{aligned}$$

and

$$\frac{dx_f^1}{d\tau} = A_f^1 x_f^1 + B_f^1 u_f \tag{3.46}$$

$$y_f^1 = C_f^1 x_f^1 \tag{3.47}$$

where

$$A_f^1 = A_{22} + \varepsilon A_{22}^{-1} A_{21} A_{12}, \quad B_f^1 = B_2 + \varepsilon A_{22}^{-1} A_{21} B_1, \quad C_f^1 = C_2 + \varepsilon C_s^0.$$

This process can be continued to define even higher order corrections, e.g. up to $o(\varepsilon^3)$ we compute $\varepsilon^2 \phi_2(x, u)$ as

$$\begin{aligned}
\phi_2 &= (A_{22})^{-1} \dot{\phi}_1 \\
&= -[(A_{22})^{-1}]^3 (A_{21} \ddot{x}_1 + B_2 \ddot{u}_s)
\end{aligned}$$

$$= -[(A_{22})^{-1}]^3 [A_{21}(A_{11} - A_{12}A_{22}^{-1}A_{21})\dot{x} + A_{21}(B_1 - A_{12}A_{22}^{-1}B_2)\dot{u}_s + B_2\ddot{u}_s] \quad (3.48)$$

At the n th stage, we obtain

$$\phi_n = A_{22}^{-1} \dot{\phi}_{n-1}. \quad (3.49)$$

3.4 Composite Observer Based on Uncorrected Models

A composite observer is first designed by J.O'Reilly [36] for the original full-order system (3.18)-(3.20) based on the observers for the uncorrected slow and fast models (3.31)-(3.34). This composite observer, which is the application of singular perturbation methods in control theory and control system design, is used to reconstruct the states of the original system through observer design in separate time-scales corresponding to decoupled subsystems.

For the original full-order system (3.18)-(3.20), a full-order observer is given by

$$\dot{\hat{x}} = (A - GC)\hat{x} + Gy + Bu, \quad (3.50)$$

$$\hat{y} = C\hat{x} \quad (3.51)$$

where

$$x = \begin{bmatrix} x_1 \\ x_2 \end{bmatrix}, A = \begin{bmatrix} A_{11} & A_{12} \\ \frac{A_{21}}{\varepsilon} & \frac{A_{22}}{\varepsilon} \end{bmatrix}, B = \begin{bmatrix} B_1 \\ B_2 \\ \varepsilon \end{bmatrix}, G = \begin{bmatrix} G_1 \\ G_2 \\ \varepsilon \end{bmatrix}, C = [C_1 \quad C_2]$$

In other words,

$$\begin{bmatrix} \dot{\hat{x}}_1 \\ \varepsilon \dot{\hat{x}}_2 \end{bmatrix} = \begin{bmatrix} \hat{A}_{11} & \hat{A}_{12} \\ \hat{A}_{21} & \hat{A}_{22} \end{bmatrix} \hat{x} + \begin{bmatrix} G_1 \\ G_2 \end{bmatrix} y + \begin{bmatrix} B_1 \\ B_2 \end{bmatrix} u, \quad (3.52)$$

where

$$\hat{A}_{11} = A_{11} - G_1 C_1, \quad \hat{A}_{12} = A_{12} - G_1 C_2, \quad \hat{A}_{21} = A_{21} - G_2 C_1, \quad \hat{A}_{22} = A_{22} - G_2 C_2.$$

The state error vector is defined by

$$e = \hat{x} - x \quad (3.53)$$

which satisfies the dynamical system

$$\dot{e} = (A - GC)e \quad (3.54)$$

that is

$$\begin{bmatrix} \dot{e}_1 \\ \varepsilon \dot{e}_2 \end{bmatrix} = \begin{bmatrix} \hat{A}_{11} & \hat{A}_{12} \\ \hat{A}_{21} & \hat{A}_{22} \end{bmatrix} \begin{bmatrix} e_1 \\ e_2 \end{bmatrix}. \quad (3.55)$$

The original full-order system is separated into uncorrected slow and fast subsystems. And a full-order observer for the uncorrected slow subsystem (3.31)-(3.32) is given as

$$\dot{\hat{x}}_s^0 = (A_s^0 - G_s^0 C_s^0) \hat{x}_s^0 + G_s^0 y_s^0 + (B_s^0 - G_s^0 D_s^0) u_s \quad (3.56)$$

where the state reconstruction error is defined by

$$e_s^0 = \hat{x}_s^0 - x_s^0 \quad (3.57)$$

which satisfies

$$\dot{e}_s^0 = (A_s^0 - G_s^0 C_s^0) e_s^0. \quad (3.58)$$

Similarly, a full-order observer for the uncorrected fast subsystem (3.33)-(3.34) is given by

$$\dot{\hat{x}}_f^0(\tau) = (A_{22} - G_f^0 C_2) \hat{x}_f^0(\tau) + G_f^0 y_f^0(\tau) + B_2 u_f(\tau) \quad (3.59)$$

where the state reconstruction error is defined by

$$e_f^0(\tau) = \hat{x}_f^0(\tau) - x_f^0(\tau) \quad (3.60)$$

and which satisfies

$$\dot{e}_f^0(\tau) = (A_{22} - G_f^0 C_2) e_f^0(\tau). \quad (3.61)$$

According to [36], when the composite observer (3.50)-(3.51) is applied to the original system (3.18)-(3.20) with the observer gains selected as

$$G_1 = A_{12} A_{22}^{-1} G_f^0 + G_s^0 (I_m - C_2 A_{22}^{-1} G_f^0), \quad (3.62)$$

$$G_2 = G_f^0, \quad (3.63)$$

this composite observer is uniformly stable for any $\varepsilon \in (0, \varepsilon^*], \varepsilon^* > 0$ (with ε^* selected to guarantee closed-loop stability of the full-order system) if $A_s^0 - G_s^0 C_s^0$ and $A_f^0 - G_f^0 C_f^0$ are uniformly stable. Then for any positive ε sufficiently small, the state reconstruction errors satisfy

$$e_1 = e_s^0 + O(\varepsilon) \quad (3.64)$$

$$e_2 = -(A_{22} - G_2 C_2)^{-1} (A_{21} - G_2 C_1) e_s^0 + e_f(\tau) + O(\varepsilon). \quad (3.65)$$

3.5 Composite Observer Based on First-order Corrected Models

On the condition that the original full-order system is observable, the observability of the slow and fast subsystems may vary due to different model orders. If either the slow or fast uncorrected subsystem is not observable, it is necessary to consider the observability of higher-order models. Therefore, based on the work of [36], we present the procedures to design a composite observer with the first-order corrected slow and fast subsystem models.

A full-order observer for the 1st-order corrected slow subsystem (3.44)-(3.45)

$$\begin{aligned} \dot{x}_s^1 &= A_s^1 x_s^1 + B_s^1 u_s \\ y_s^1 &= C_s^1 x_s^1 + D_s^1 u_s - \varepsilon C_2 A_{22}^{-2} B_2 \dot{u}_s \end{aligned}$$

where

$$\begin{aligned} A_s^1 &= A_s^0 - \varepsilon A_{12} A_{22}^{-2} A_{21} A_s^0, & C_s^1 &= C_s^0 - \varepsilon C_2 A_{22}^{-2} A_{21} A_s^0, \\ B_s^1 &= B_s^0 - \varepsilon A_{12} A_{22}^{-2} A_{21} B_s^0, & D_s^1 &= D_s^0 - \varepsilon C_2 A_{22}^{-2} A_{21} B_s^0. \end{aligned}$$

is given by

$$\dot{\hat{x}}_s^1 = (A_s^1 - G_s^1 C_s^1) \hat{x}_s^1 + G_s^1 y_s^1 + (B_s^1 - G_s^1 D_s^1) u_s - \varepsilon (A_{12} A_{22}^{-2} B_2 - G_s^1 C_2 A_{22}^{-2} B_2) \dot{u}_s \quad (3.66)$$

$$\hat{y}_s^1 = C_s^1 \hat{x}_s^1 + D_s^1 u_s - \varepsilon C_2 A_{22}^{-2} B_2 \dot{u}_s \quad (3.67)$$

where G_s^1 is the gain matrix for the observer. The state error estimation is defined by

$$e_s^1 = \hat{x}_s^1 - x_s^1 \quad (3.68)$$

that satisfies

$$\dot{e}_s^1 = (A_s^1 - G_s^1 C_s^1) e_s^1 \quad (3.69)$$

where

$$A_s^1 - G_s^1 C_s^1 = (A_s^0 - G_s^1 C_s^0) - \varepsilon (A_{12} - G_s^1 C_2) A_{22}^{-2} A_{21} A_s^0. \quad (3.70)$$

Similarly, for the 1st-order corrected fast subsystem (3.46)-(3.47)

$$\frac{dx_f^1}{d\tau} = A_f^1 x_f^1 + B_f^1 u_f$$

$$y_f^1 = C_f^1 x_f^1$$

where

$$A_f^1 = A_{22} + \varepsilon A_{22}^{-1} A_{21} A_{12}, \quad B_f^1 = B_2 + \varepsilon A_{22}^{-1} A_{21} B_1, \quad C_f^1 = C_2 + \varepsilon C_s^0,$$

a full-order observer is given by

$$\dot{\hat{x}}_f^1(\tau) = (A_f^1 - G_f^1 C_f^1) \hat{x}_f^1 + G_f^1 y_f^1 + B_f^1 u_f, \quad (3.71)$$

$$\hat{y}_f^1(\tau) = C_f^1 \hat{x}_f^1, \quad (3.72)$$

where G_f^1 is the gain matrix for the observer. The state error estimation is defined by

$$e_f^1(\tau) = \hat{x}_f^1(\tau) - x_f^1(\tau), \quad (3.73)$$

that satisfies

$$\frac{de_f^1}{d\tau} = (A_f^1 - G_f^1 C_f^1) e_f^1, \quad (3.74)$$

where

$$A_f^1 - G_f^1 C_f^1 = (A_f^0 - G_f^1 C_f^0) + \varepsilon(A_{22}^{-1} A_{21} A_{12} - G_f^1 C_s^0 A_{12} A_{22}^{-1}). \quad (3.75)$$

Theorem 3.1

If $A_s^1 - G_s^1 C_s^1$ and $A_f^1 - G_f^1 C_f^1$ are uniformly stable, the observer (3.50)-(3.51), (3.66)-(3.67) and (3.71)-(3.72) applied to systems (3.18)-(3.20), (3.44)-(3.45) and (3.46)-(3.47) respectively, where the observer gains are selected as

$$G_1 = A_{12} A_{22}^{-1} G_f^1 + G_s^1 (I_m - C_2 A_{22}^{-1} G_f^1), \quad (3.76)$$

$$G_2 = G_f^1, \quad (3.77)$$

will guarantee that for $\varepsilon \in (0, \varepsilon^*]$, $\varepsilon^* > 0$ (with ε^* selected to guarantee closed-loop stability of the full-order system), the estimation error of the original system (3.18)-(3.20) up to $O(\varepsilon^2)$ satisfies the equations

$$e_1 = e_s^1 + \varepsilon[M + \hat{H}_0 e_f^1(\tau)] + o(\varepsilon^2), \quad (3.78)$$

$$e_2 = [-\hat{L}_0 e_s^1 + e_f^1(\tau)] + \varepsilon[N - \hat{L}_0 \hat{H}_0 e_f^1(\tau) - \hat{L}_0 M - \hat{L}_1 e_s^1] + o(\varepsilon^2), \quad (3.79)$$

with the matrices \hat{L} and \hat{H} defined in (3.87)-(3.89), and M and N matrices defined in (3.111)-(3.112).

Proof:

In order to completely separate the slow and fast states of the observer (3.50), a coordinate transformation is applied as

$$\begin{bmatrix} \hat{x}_1 \\ \hat{x}_2 \end{bmatrix} = \begin{bmatrix} I_n & \varepsilon \hat{H} \\ -\hat{L} & I_m - \varepsilon \hat{L} \hat{H} \end{bmatrix} \begin{bmatrix} \hat{x}_s \\ \hat{x}_f \end{bmatrix} \quad (3.80)$$

and

$$\begin{bmatrix} e_1 \\ e_2 \end{bmatrix} = \begin{bmatrix} I_n & \varepsilon \hat{H} \\ -\hat{L} & I_m - \varepsilon \hat{L} \hat{H} \end{bmatrix} \begin{bmatrix} E_s \\ E_f \end{bmatrix}. \quad (3.81)$$

To transform $[e_1 \ e_2]^T$ into new variables $[E_s \ E_f]^T$, with matrices \hat{L} and \hat{H} to be defined subsequently, a complete separation into slow and fast modes is facilitated as:

$$\begin{aligned}
\begin{bmatrix} \dot{E}_s \\ \dot{E}_f \end{bmatrix} &= \begin{bmatrix} I_n & \varepsilon \hat{H} \\ -\hat{L} & I_m - \varepsilon \hat{L} \hat{H} \end{bmatrix}^{-1} \begin{bmatrix} \hat{A}_{11} & \hat{A}_{12} \\ \frac{\hat{A}_{21}}{\varepsilon} & \frac{\hat{A}_{22}}{\varepsilon} \end{bmatrix} \begin{bmatrix} I_n & \varepsilon \hat{H} \\ -\hat{L} & I_m - \varepsilon \hat{L} \hat{H} \end{bmatrix} \begin{bmatrix} E_s \\ E_f \end{bmatrix} \\
&= \begin{bmatrix} (I_n - \varepsilon \hat{L} \hat{H}) \hat{A}_{11} - \hat{H} \hat{A}_{21} & (I_n - \varepsilon \hat{H} \hat{L}) \hat{A}_{22} \\ \hat{L} \hat{A}_{11} + \frac{\hat{A}_{21}}{\varepsilon} & \hat{L} \hat{A}_{12} + \frac{\hat{A}_{22}}{\varepsilon} \end{bmatrix} \begin{bmatrix} I_n & \varepsilon \hat{H} \\ -\hat{L} & I_m - \varepsilon \hat{L} \hat{H} \end{bmatrix} \begin{bmatrix} E_s \\ E_f \end{bmatrix} \\
&= \begin{bmatrix} U(\hat{L}, \hat{H}, \varepsilon) & S(\hat{H}, \varepsilon) \\ R(\hat{L}, \varepsilon) & V(\hat{L}, \hat{H}, \varepsilon) \end{bmatrix} \begin{bmatrix} E_s \\ E_f \end{bmatrix} \tag{3.82}
\end{aligned}$$

where

$$U(\hat{L}, \hat{H}, \varepsilon) = (I_n - \varepsilon \hat{L} \hat{H}) \hat{A}_{11} - \hat{H} \hat{A}_{21} - (I_n - \varepsilon \hat{H} \hat{L}) \hat{A}_{22} \hat{L} \tag{3.83}$$

$$R(\hat{L}, \varepsilon) = \frac{\hat{A}_{21}}{\varepsilon} - \frac{\hat{A}_{22} \hat{L}}{\varepsilon} + \hat{L} \hat{A}_{11} - \hat{L} \hat{A}_{12} \hat{L} \tag{3.84}$$

$$S(\hat{H}, \varepsilon) = (\hat{A}_{11} - \hat{A}_{12} \hat{L}) \hat{H} - \frac{\hat{H}(\hat{A}_{22} + \varepsilon \hat{L} \hat{A}_{12})}{\varepsilon} + \frac{\hat{A}_{12}}{\varepsilon} \tag{3.85}$$

$$V(\hat{L}, \hat{H}, \varepsilon) = \hat{A}_{21} \hat{H} + \hat{L} \hat{A}_{12} - \hat{A}_{22} \hat{L} \hat{H} - \varepsilon \hat{L} \hat{A}_{11} \hat{H} - \varepsilon \hat{L} \hat{A}_{12} \hat{L} \hat{H} + \frac{\hat{A}_{22}}{\varepsilon} \tag{3.86}$$

for any $\varepsilon \in (0, \varepsilon^*], \varepsilon^* > 0$. The matrices $\hat{L}(\varepsilon)$ and $\hat{H}(\varepsilon)$ satisfy the following algebraic equations by completely decoupling E_s and E_f dynamics by setting

$$R(\hat{L}, \varepsilon) = 0 \Rightarrow \hat{A}_{21} - \hat{A}_{22} \hat{L} + \varepsilon \hat{L} \hat{A}_{11} - \varepsilon \hat{L} \hat{A}_{12} \hat{L} = 0 \tag{3.87}$$

$$S(\hat{H}, \varepsilon) = 0 \Rightarrow \varepsilon(\hat{A}_{11} - \hat{A}_{12} \hat{L}) \hat{H} - \hat{H}(\hat{A}_{22} + \varepsilon \hat{L} \hat{A}_{12}) + \hat{A}_{12} = 0 \tag{3.88}$$

By neglecting terms of $O(\varepsilon)$ in (3.87) and (3.88)

$$\hat{L}_0 = \hat{A}_{22}^{-1} \hat{A}_{21} = (A_{22} - G_2 C_2)^{-1} (A_{21} - G_2 C_1) \tag{3.89}$$

$$\hat{H}_0 = \hat{A}_{12} \hat{A}_{22}^{-1} = (A_{12} - G_1 C_2)(A_{22} - G_2 C_2)^{-1}, \tag{3.90}$$

and the uncorrected model of (3.82) is

$$\begin{aligned}
\begin{bmatrix} \dot{E}_s^0 \\ \dot{E}_f^0 \end{bmatrix} &= \begin{bmatrix} \hat{A}_{11} - \hat{A}_{12}\hat{A}_{22}^{-1}\hat{A}_{21} & 0 \\ 0 & \hat{A}_{22} \end{bmatrix} \begin{bmatrix} E_s^0 \\ E_f^0 \end{bmatrix} \\
&= \begin{bmatrix} (A_{11} - G_1C_1) - (A_{12} - G_1C_2)(A_{22} - G_2C_2)^{-1}(A_{21} - G_2C_1) & 0 \\ 0 & A_{22} - G_2C_2 \end{bmatrix} \begin{bmatrix} E_s^0 \\ E_f^0 \end{bmatrix}
\end{aligned} \tag{3.91}$$

Using the identity

$$\begin{aligned}
I_m &= (A_{22} - G_2C_2)^{-1}(A_{22} - G_2C_2) \\
&= (A_{22} - G_2C_2)^{-1}A_{22} - (A_{22} - G_2C_2)^{-1}G_2C_2 \\
&= \hat{A}_{22}^{-1}A_{22} - \hat{A}_{22}^{-1}G_2C_2.
\end{aligned} \tag{3.92}$$

We get

$$\hat{A}_{22}^{-1} = (I_m + \hat{A}_{22}^{-1}G_2C_2)A_{22}^{-1} \tag{3.93}$$

and

$$\begin{aligned}
&(A_{11} - G_1C_1) - (A_{12} - G_1C_2)(A_{22} - G_2C_2)^{-1}(A_{21} - G_2C_1) \\
&= (A_{11} - G_1C_1) - (A_{12} - G_1C_2)[(I_m + \hat{A}_{22}^{-1}G_2C_2)A_{22}^{-1}](A_{21} - G_2C_1) + O(\varepsilon) \\
&= (A_{11} - A_{12}A_{22}^{-1}A_{21}) - G_1(C_1 - C_2A_{22}^{-1}A_{21}) + (A_{12} - G_1C_1)\hat{A}_{22}^{-1}G_2(C_1 - C_2A_{22}^{-1}A_{21}) \\
&= A_s^0 - G_s^0C_s^0 + O(\varepsilon)
\end{aligned} \tag{3.94}$$

where

$$G_s^0 = G_1 - (A_{12} - G_1C_2)\hat{A}_{22}^{-1}G_2 = G_1 - A_{12}\hat{A}_{22}^{-1}G_2 + G_1C_2\hat{A}_{22}^{-1}G_2 \tag{3.95}$$

Also, from (3.95) we get

$$G_1(I + C_2\hat{A}_{22}^{-1}G_2) = G_0 + A_{12}\hat{A}_{22}^{-1}G_2 \tag{3.96}$$

which by invoking the identity

$$(I + C_2\hat{A}_{22}^{-1}G_2)^{-1} = (I - C_2A_{22}^{-1}G_2) \tag{3.97}$$

Equation (3.62) is obtained

$$G_1 = A_{12} A_{22}^{-1} G_f^0 + G_s^0 (I_m - C_2 A_{22}^{-1} G_f^0)$$

Based on above deviations we get

$$(A_{11} - G_1 C_1) - (A_{12} - G_1 C_2)(A_{22} - G_2 C_2)^{-1}(A_{21} - G_2 C_1) = A_s^0 - G_s^0 C_s^0 + O(\varepsilon) \quad (3.98)$$

$$A_{22} - G_2 C_2 = A_{22} - G_f^0 C_2 + O(\varepsilon) \quad (3.99)$$

The above process can be continued by neglecting terms of $O(\varepsilon^2)$ in (3.87)-(3.88) and

obtain

$$\hat{L}_1 = \hat{A}_{22}^{-2} \hat{A}_{21} (\hat{A}_{11} - \hat{A}_{12} \hat{A}_{22}^{-1} \hat{A}_{21}) \quad (3.100)$$

$$\hat{H}_1 = [(\hat{A}_{11} - \hat{A}_{12} \hat{A}_{22}^{-1} \hat{A}_{21}) \hat{H}_0 - \hat{H}_0 \hat{L}_0 \hat{A}_{12}] \hat{A}_{22}^{-1}. \quad (3.101)$$

and the 1st-order corrected model of (3.68) becomes

$$\begin{bmatrix} \dot{E}_s^1 \\ \varepsilon \dot{E}_f^1 \end{bmatrix} = \begin{bmatrix} (I_n - \varepsilon \hat{H}_0 \hat{L}_0)(\hat{A}_{11} - \hat{A}_{12} \hat{A}_{22}^{-1} \hat{A}_{21}) & 0 \\ 0 & \hat{A}_{22} + \varepsilon \hat{A}_{22}^{-1} \hat{A}_{21} \hat{A}_{12} \end{bmatrix} \begin{bmatrix} E_s^1 \\ E_f^1 \end{bmatrix} \quad (3.102)$$

where

$$\begin{aligned} & (I_n - \varepsilon \hat{H}_0 \hat{L}_0)(\hat{A}_{11} - \hat{A}_{12} \hat{A}_{22}^{-1} \hat{A}_{21}) \\ &= (A_{11} - G_1 C_1) - (A_{12} - G_1 C_2)(A_{22} - G_2 C_2)^{-1}(A_{21} - G_2 C_1) \\ & \quad - \varepsilon \hat{H}_0 \hat{L}_0 (\hat{A}_{11} - \hat{A}_{12} \hat{A}_{22}^{-1} \hat{A}_{21}), \end{aligned} \quad (3.103)$$

$$\hat{A}_{22} + \varepsilon \hat{A}_{22}^{-1} \hat{A}_{21} \hat{A}_{12} = (A_{22} - G_2 C_2) + \varepsilon \hat{A}_{22}^{-1} \hat{A}_{21} \hat{A}_{12}. \quad (3.14)$$

For the original full-order system (3.18)-(3.20), let

$$G_1 = A_{12} A_{22}^{-1} G_f^1 + G_s^1 (I_m - C_2 A_{22}^{-1} G_f^1), \quad (3.105)$$

$$G_2 = G_f^1. \quad (3.106)$$

and expand E_s^1 and E_f^1 according to

$$E_s^1 = (A_s^0 - G_s^1 C_s^0) - \varepsilon \hat{H}_0 \hat{L}_0 (\hat{A}_{11} - \hat{A}_{12} \hat{A}_{22}^{-1} \hat{A}_{21}), \quad (3.107)$$

$$E_f^1 = (A_{22} - G_f^1 C_2) + \varepsilon \hat{A}_{22}^{-1} \hat{A}_{21} \hat{A}_{12}. \quad (3.108)$$

Consequently, for the estimation error system (3.57), using (3.68), (3.71) and (3.81), it deduced that

$$e_1 = E_s^1 + \varepsilon H_0 E_f^1 + o(\varepsilon^2) = e_s^1 + \varepsilon [M + H_0 e_f^1(\tau)] + o(\varepsilon^2), \quad (3.109)$$

$$\begin{aligned} e_2 &= -(L_0 + \varepsilon L_1)E_1 + (I_m - \varepsilon L_0 H_0)E_2 + o(\varepsilon^2) \\ &= [-L_0 e_s^1 + e_f^1(\tau)] + \varepsilon [N - L_0 H_0 e_f^1(\tau) - L_0 M - L_1 e_s^1] + o(\varepsilon^2), \end{aligned} \quad (3.110)$$

where

$$M = \hat{H}_0 \hat{L}_0 (\hat{A}_{11} - \hat{A}_{12} \hat{A}_{22}^{-1} \hat{A}_{21}) - (A_{12} - G_s^1 C_2) A_{22}^{-1} A_{21} A_s^0, \quad (3.111)$$

$$N = L_0 A_{12} - G_f^1 C_s^1 H_0 - \hat{A}_{22}^{-1} \hat{A}_{21} \hat{A}_{12}. \quad (3.112)$$

3.6 Conclusion

The design of the observer for the original full-order system does suffer from the higher dimensionality and ill-conditioning resulting from the interaction of slow and fast dynamic modes. In the two time-scaled approach, this stiffness property is taken advantage of by decoupling the original full-order system into two subsystems in separate time scales. This chapter constructs subsystem models of system (3.1)-(3.3). The approximation procedure starts by calculating $\varphi_0(x), \varphi_1(x)$ etc. in (3.8) by equating terms in like powers of ε , which can be continued to any desired power of ε . The observer design can then proceed for each lower-order subsystem, and the results combined to yield a composite observer (3.62)-(3.63), (3.76)-(3.77) for the original full-order system. A main result in this chapter is Theorem 3.1 which provides sufficient and necessary conditions for the stabilization of the original full-order system through observer design in two separate time-scales. An important corollary to this result is the complete observability of the original full-order system through the separate observability of the subsystems in different time-scales.

Chapter 4

A Geometric Approach to Fault Diagnosis

In Chapter 2, we briefly reviewed the model-based approach to fault detection and isolation (FDI) in dynamic systems. In this chapter, we apply a geometric method for FDI a linear two time-scale system. Utilizing the high-order corrected slow and fast subsystem models and the composite observer architectures obtained in Chapter 3, we are able to detect and isolate actuator faults in the reduced-order subsystems and the original full-order system, even if the states in lower-order subsystem models are not observable. Finally, we have included an example which illustrates the capabilities and characteristics of the proposed techniques developed in section 4.3.

4.1 Preliminaries

Beard [19] and Jones [37] first proposed a systematic procedure for designing a special observer that accentuates the effect of failure on the prediction error of the observer. The observer is designed so that, in the absence of component failure,

modeling errors, and system disturbances, the prediction error dies away, while when the system suffers a failure the prediction error increases.

Massoumnia [21, 22] reformulated the Beard-Jones detection filter problem (BJDFP) by a geometric approach, clarified the notions of output separable and mutually detectable families of subspaces, and showed the failure detection filter problem has a computationally simple solution when the failure events satisfy some mild restrictions.

4.2 Failure Modeling and Problem Formulation

A singularly perturbed linear time-invariant (LTI) model can be described as:

$$\begin{cases} \dot{x} = Ax + Bu + \sum_{i=1}^k L_i f_i \\ y = Cx \end{cases} \quad (4.1)$$

where

$$x = \begin{bmatrix} x_1 \\ x_2 \end{bmatrix}, A = \begin{bmatrix} A_{11} & A_{12} \\ A_{21} & A_{22} \\ \varepsilon & \varepsilon \end{bmatrix}, B = \begin{bmatrix} B_1 \\ B_2 \\ \varepsilon \end{bmatrix}, C = [C_1 \quad C_2].$$

In (4.1), u is the known input and y is the known output. The arbitrary function f_i is the unknown actuator failure modes. When no failure occurs, the function f_i is identically zero. The effect of failure in the i th actuator can be represented by $L_i = B_i$, where B_i is the i th column of B . When the actuator has failed, then $f_i(t) = -u_i(t)$ where $u_i(t)$ is the i th component of $u(t)$; and for a bias fault of the same actuator, $f_i(t)$ is taken as some nonzero constant.

Consider the problem of designing a full-order observer of the form given by the system (4.1):

$$\dot{\hat{x}} = (A - GC)\hat{x} + Gy + Bu \quad (4.2)$$

Where

$$G = \begin{bmatrix} G_1 \\ G_2 \\ \varepsilon \end{bmatrix}.$$

Define the state estimation error vector by $e = \hat{x} - x$, with the corresponding error dynamics given by

$$\begin{cases} \dot{e} = (A - GC)e - \sum_{i=1}^k L_i f_i \\ r = Ce \end{cases} \quad (4.3)$$

When the i th actuator fails, $f_i \neq 0$, $e \in V_i = \langle A - GC | L_i \rangle$, and $r \in CV_i$. The failure can be identified by finding the projection of r onto each of the independent subspaces CV_i and comparing the magnitude of this projection to a threshold.

4.3 A Geometric Approach to Actuator Fault Detection and Isolation

4.3.1 A Geometric Formulation and Solution to the BJDFP

The objective of BJDFP is to modify the invariant subspace of $A - GC$ through appropriate selection of the observer gain matrix G . A subspace W is (C, A) -invariant if there exists a map $G : Y \rightarrow X$ such that $(A - GC)W \subseteq W$.

Assuming the filter has the structure given in (4.2), BJDFP can be stated in a geometric language as follows. Given $A, L_i (i \in k)$ and C , find a compatible and output separable family of (C, A) -invariant subspaces $\{W_i, i \in k\}$ such that $L_i \subseteq W_i$. In other words, find $\{W_i, i \in k\}$ such that there exists a G with

$$(A - GC)W_i \subseteq W_i, \quad i \in k \quad (4.4)$$

$$L_i \subseteq W_i, \quad i \in k \quad (4.5)$$

$$CW_i \cap \left(\sum_{j \neq i} CW_j \right) = 0, \quad i \in k \quad (4.6)$$

If there exist a family of subspaces $\{W_i, i \in k\}$ and an observer gain G such that the conditions in (4.4) and (4.5) are satisfied, then the error $e(t)$ due to a nonzero L_i remains inside W_i . Also the condition (4.6) requires the subspaces CW_i to be independent so that the innovation due to different actuator failures is confined to independent subspaces of the output space.

In references [21, 22], a theorem is stated that the BJDFP has a solution if and only if

$$CW_i^* \cap \left(\sum_{j \neq i} CW_j^* \right) = 0, \quad i \in k. \quad (4.7)$$

When $k_i = 1$ (the scalar case) and (C, A) is observable, it follows that

$$W_i^* = L_i \oplus \dots \oplus A^{\mu_i} L_i \quad (4.8)$$

where μ_i is the smallest integer such that $CA^{\mu_i} L_i \neq 0$ (generically $\mu_i = 0$) and \oplus indicates that the “addition” of independent subspaces. Thus, in an appropriate basis the map $W_i : W_i^* \rightarrow X$ is simply $W_i = [L_i, AL_i, \dots, A^{\mu_i} L_i]$.

Define

$$l_i = A^{\mu_i} L_i \quad \text{and} \quad l = [l_1, \dots, l_k] \quad (4.9)$$

Assuming $\{W_i^*, i \in k\}$ is output separable (or equivalently $\text{Rank } Cl = k$), one observer gain G is

$$G = -Al(Cl)^{-1} \quad (4.10)$$

4.3.2 Application to Singularly-Perturbed Systems

Considering the observer dynamics

$$\dot{\hat{x}}_s^i = (A_s^i - G_s^i C_s^i) \hat{x}_s^i + G_s^i y_s^i + (B_s^i - G_s^i D_s^i) u_s \quad (i = 0,1) \quad (4.11)$$

of the slow subsystem model. In this slow model, the diagnoser will be defined as

$$\begin{cases} \dot{e}_s^i = (A_s^i - G_s^i C_s^i) e_s^i - \sum_{j=1}^k L_{sj}^i f_{sj}^i \\ r_s^i = C_s^i e_s^i \end{cases} \quad (4.12)$$

where L_{sj}^i is equal to the j th column of B_s^i , f_{sj}^i is the slow fault in the j th actuator. If

G_s^i satisfies

$$(A_s^i - G_s^i C_s^i) W_{sj}^i \subseteq W_{sj}^i, \quad j \in k \quad (4.13)$$

$$L_{sj}^i \subseteq W_{sj}^i, \quad (4.14)$$

$$C_s^i W_{sj}^i \cap \left(\sum_{g \neq i} C_s^g W_{sg}^g \right) = 0, \quad (4.15)$$

the slow actuator faults can be detected and isolated in the slow subsystem.

Similarly, for the observer dynamics

$$\dot{\hat{x}}_f^i(\tau) = (A_f^i - G_f^i C_f^i) \hat{x}_f^i(\tau) + G_f^i y_f^i(\tau) + B_f^i u_f(\tau) \quad (i = 0,1) \quad (4.16)$$

of the fast subsystem model, the diagnoser will be defined as

$$\begin{cases} \dot{e}_f^i = (A_f^i - G_f^i C_f^i) e_f^i - \sum_{j=1}^k L_{fj}^i f_{fj}^i \\ r_f^i = C_f^i e_f^i \end{cases} \quad (4.17)$$

where L_{fj}^i is equal to the j th column of B_f^i , f_{fj}^i is the fast fault in the j th actuator. If

G_f^i satisfies

$$(A_f^i - G_f^i C_f^i) W_{fj}^i \subseteq W_{fj}^i, \quad j \in k \quad (4.18)$$

$$L_{fj}^i \subseteq W_{fj}^i, \quad (4.19)$$

$$C_f^i W_{fj}^i \cap \left(\sum_{g \neq i} C_f^g W_{fg}^g \right) = 0, \quad (4.20)$$

the fast actuator faults can be detected and isolated in the fast subsystem.

For the original full-order system, the observer (4.2) is given by

$$\dot{\hat{x}} = (A - GC)\hat{x} + Gy + Bu$$

with the gain matrix partitioned into

$$G = \begin{bmatrix} G_1 \\ G_2 \\ \varepsilon \end{bmatrix} \quad (4.21)$$

where

$$G_1 = A_{12} A_{22}^{-1} G_f^i + G_s^i (I_m - C_2 A_{22}^{-1} G_f^i), \quad (i = 0,1) \quad (4.22)$$

$$G_2 = G_f^i. \quad (i = 0,1) \quad (4.23)$$

If the conditions in (4.4)-(4.6) are satisfied for G , then the error dynamics system (4.3)

$$\begin{cases} \dot{e} = (A - GC)e - \sum_{i=1}^k L_i f_i \\ r = Ce \end{cases}$$

is a residual generator for the original full-order system.

We can even relax the conditions (4.4)-(4.6) and require only that the transfer function from $f_i(s)$ to $r_i(s)$ should be nonzero while the transfer function from $f_i(s)$ to $r_j(s) (i \neq j)$ should be zero. But it is not necessarily possible to reconstruct $f_i(t)$ from $r_i(t)$.

4.4 Simulation Results

In this section, our proposed FDI techniques will be illustrated to a singularly perturbed system with matrices described by (4.24) [38] and compare the fault

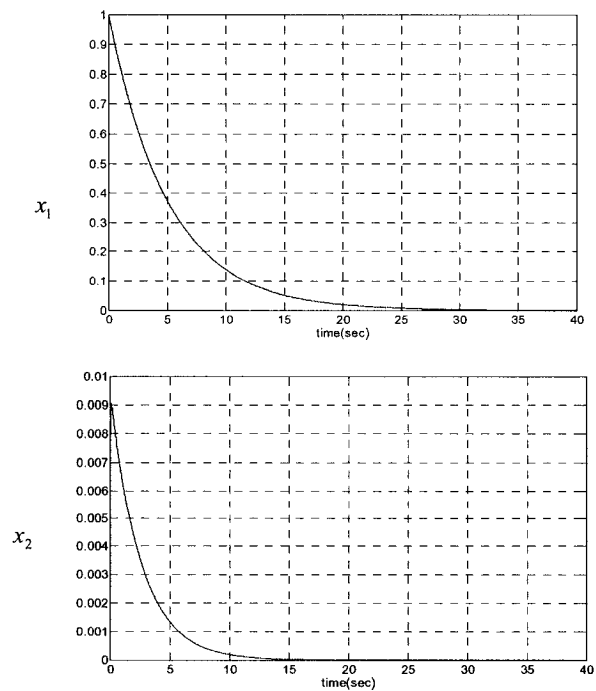
diagnosis simulation results for various values of the singular perturbation parameter as $\varepsilon = 0.01$ and $\varepsilon = 0.5$.

The full-order system matrices are given by

$$A = \begin{bmatrix} -0.2 & 0.4 & 0 & 0 \\ 0 & 0 & 0.345 & 0 \\ 0 & -52.4 & -46.5 & 26.2 \\ 0 & 0 & 0 & -100 \end{bmatrix}, B = \begin{bmatrix} 0 \\ 1 \\ 0 \\ 0 \end{bmatrix}, \quad (4.24)$$

$$C = \begin{bmatrix} 1 & 0 & 0 & 0 \\ 0 & 0 & 1 & 0 \end{bmatrix}.$$

The eigenvalues of A are $\{-0.2, -0.3921, -46.1079, -100\}$. Fig. 4-1 shows the state response of the system with the initial conditions $x_1^0 = 1, x_2^0 = 0, x_3^0 = 1$, and $x_4^0 = 1$.



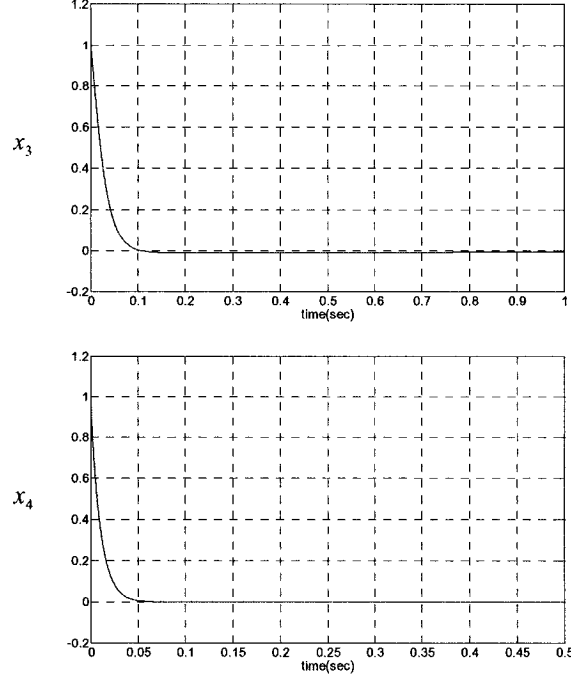


Figure 4-1 The state responses x_1, x_2, x_3, x_4 with $x_1^0 = 1, x_2^0 = 0, x_3^0 = 1, x_4^0 = 1$

4.4.1 Results with $\varepsilon = 0.01$

We design a detection filter for a full-order system having slow and fast dynamics in the standard form (3.18)-(3.20) with $\varepsilon = 0.01$, namely

$$\begin{aligned}
 A_{11}|_{\varepsilon=0.01} &= \begin{bmatrix} -0.2 & 0.4 \\ 0 & 0 \end{bmatrix}, & A_{12}|_{\varepsilon=0.01} &= \begin{bmatrix} 0 & 0 \\ 0.345 & 0 \end{bmatrix}, \\
 A_{21}|_{\varepsilon=0.01} &= \begin{bmatrix} 0 & -0.524 \\ 0 & 0 \end{bmatrix}, & A_{22}|_{\varepsilon=0.01} &= \begin{bmatrix} -0.465 & 0.262 \\ 0 & -1 \end{bmatrix}, \\
 B_1|_{\varepsilon=0.01} &= \begin{bmatrix} 0 \\ 1 \end{bmatrix}, & B_2|_{\varepsilon=0.01} &= \begin{bmatrix} 0 \\ 0 \end{bmatrix}, \\
 C_1|_{\varepsilon=0.01} &= \begin{bmatrix} 1 & 0 \\ 0 & 0 \end{bmatrix}, & C_2|_{\varepsilon=0.01} &= \begin{bmatrix} 0 & 0 \\ 1 & 0 \end{bmatrix}.
 \end{aligned} \tag{4.25}$$

The uncorrected slow subsystem model is given by the matrices

$$\begin{aligned}
A_s^0|_{\varepsilon=0.01} &= \begin{bmatrix} -0.2 & 0.4 \\ 0 & -0.3888 \end{bmatrix}, & B_s^0|_{\varepsilon=0.01} &= \begin{bmatrix} 0 \\ 1 \end{bmatrix}, \\
C_s^0|_{\varepsilon=0.01} &= \begin{bmatrix} 1 & 0 \\ 0 & -1.1269 \end{bmatrix}, & D_s^0|_{\varepsilon=0.01} &= \begin{bmatrix} 0 \\ 0 \end{bmatrix}.
\end{aligned} \tag{4.26}$$

The gain of the slow subsystem dynamics observer given by G_s^0 is selected as

$$G_s^0|_{\varepsilon=0.01} = \begin{bmatrix} 0.8 & -0.355 \\ 0 & -1.4298 \end{bmatrix}, \tag{4.27}$$

and the observer dynamics is given by (3.56) which is given as

$$\dot{\hat{x}}_s^0 = (A_s^0 - G_s^0 C_s^0) \hat{x}_s^0 + G_s^0 y_s^0 + (B_s^0 - G_s^0 D_s^0) u_s$$

This observer gain guarantees to have the poles of $A_s^0 - G_s^0 C_s^0$ placed at $\{-1, -2\}$. A fault detection filter is now designed for the slow subsystem (4.26) with the gain $G_s^0|_{\varepsilon=0.01}$. The residual is generated by the second output of the error system dynamics in this case.

For the uncorrected fast subsystem model is given by

$$\begin{aligned}
A_f^0|_{\varepsilon=0.01} &= \begin{bmatrix} -0.465 & 0.262 \\ 0 & -1 \end{bmatrix}, \\
B_f^0|_{\varepsilon=0.01} &= \begin{bmatrix} 0 \\ 0 \end{bmatrix}, \\
C_f^0|_{\varepsilon=0.01} &= \begin{bmatrix} 0 & 0 \\ 1 & 0 \end{bmatrix}.
\end{aligned} \tag{4.28}$$

Since $B_f^0 = [0 \ 0]^T$, the uncorrected fast subsystem (4.28) is not fault diagnosable, so it is necessary to consider the first-order corrected fast subsystem model which is obtained according to

$$A_f^1|_{\varepsilon=0.01} = \begin{bmatrix} -0.4611 & 0.262 \\ 0 & -1 \end{bmatrix},$$

$$B_f^1 \Big|_{\varepsilon=0.01} = \begin{bmatrix} 0.0113 \\ 0 \end{bmatrix},$$

$$C_f^1 \Big|_{\varepsilon=0.01} = \begin{bmatrix} 0 & 0 \\ 1.0084 & 0.0022 \end{bmatrix}. \quad (4.29)$$

By choosing

$$G_f^1 \Big|_{\varepsilon=0.01} = \begin{bmatrix} 0 & 3.493 \\ 0 & 7.6043 \end{bmatrix}, \quad (4.30)$$

for the observer (3.59)

$$\dot{\hat{x}}_f^0(\tau) = (A_{22} - G_f^0 C_2) \hat{x}_f^0(\tau) + G_f^0 y_f^0(\tau) + B_2 u_f(\tau)$$

The poles of $A_f^1 - G_f^1 C_f^1$ are placed at $\{-2, -3\}$. A detection filter is designed with the gain $G_f^1 \Big|_{\varepsilon=0.01}$.

Fig. 4-2 shows the simulation results corresponding to the following scenario: the actuators u_s and u_f are supposed to provide constant step input equal to $u_s = 1$ and $u_f = 1$. An actuator fault f_s occurs at time $t=20s$ and ends at $t=30s$ [Fig. 4-2(a)] in the slow subsystem and a fault f_f occurs at time $\tau = 20s$ and $\tau = 25s$ [Fig. 4-2(d)] in the fast subsystem. Fig. 4-2(b) is the output of the residual generator of the uncorrected slow model and Fig. 4-2(d) is that of the 1st-order corrected fast subsystem model. It is clear that the residual generator in each subsystem shows the occurrence of the actuator fault and identifies its actual value.

Based on the observer gains (4.27) and (4.30) designed for the slow and fast subsystems, we designed a composite observer for the original full-order system (4.24) by equations (3.76)-(3.77) and obtain the following observer gain

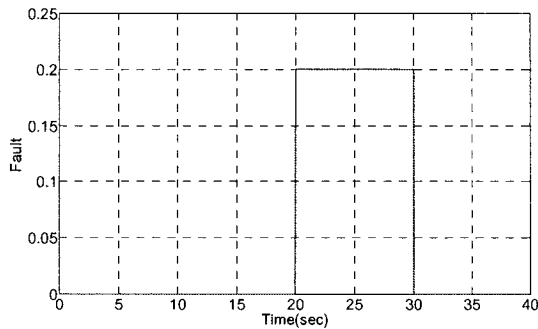
$$G|_{\varepsilon=0.01} = \begin{bmatrix} 0.8 & -4.5422 \\ 0 & -22.3662 \\ 0 & 349.3026 \\ 0 & 760.4272 \end{bmatrix} \quad (4.31)$$

which places the poles of $(A-GC)$ at $\{-1, -1.99, -21151, -28229\}$. In order to compare the simulation results and the performance capabilities, we also designed an observer directly based on the original full-order system (4.24) as

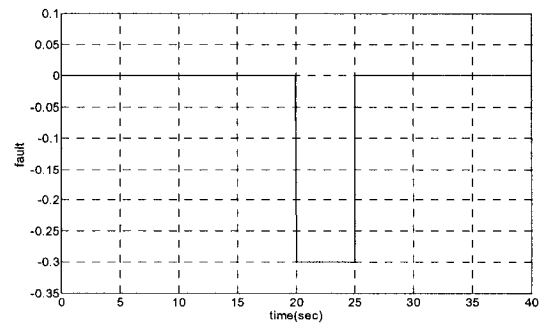
$$G_{or}|_{\varepsilon=0.01} = \begin{bmatrix} 2.9098 & -5.4282 \\ 2.3960 & -11.0242 \\ -52.4009 & 346.3902 \\ -259.8070 & 757.5931 \end{bmatrix} \quad (4.32)$$

which places the poles of $(A-G_{or}C)$ at $\{-1, -2, -211, -282\}$.

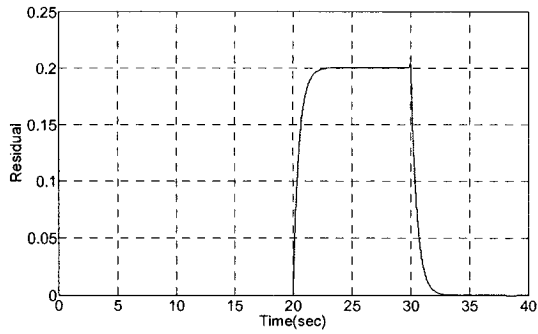
Fig. 4-3(a) shows the simulations for an actuator fault that has occurred in the original full-order system (4.24). Fig. 4-3(b) shows the output of the residual generator designed based on the composite observer, while Fig. 4-3(c) shows the residual generated based on the observer directly designed for the original full-order system. By comparing the error between the fault and the residual in Figs. 4-3 (a) and (b) and that between the fault and the residual in Fig. 4-3(c), Figs. 4-3 (a) and (d) shows that the detection filter based on the composite slow and fast observer has better capability in fault diagnosis than the full-order observer.



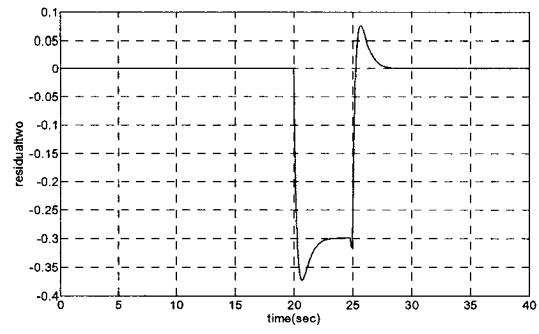
(a) The actuator fault occurs in the slow subsystem



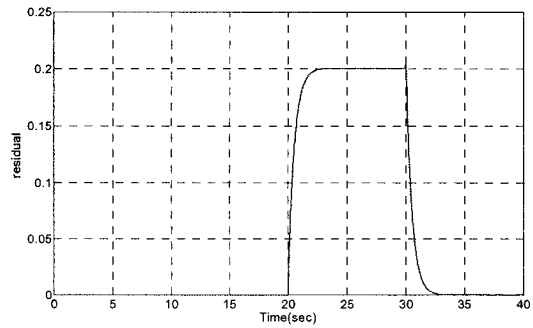
(d) The actuator fault occurs in the fast subsystem



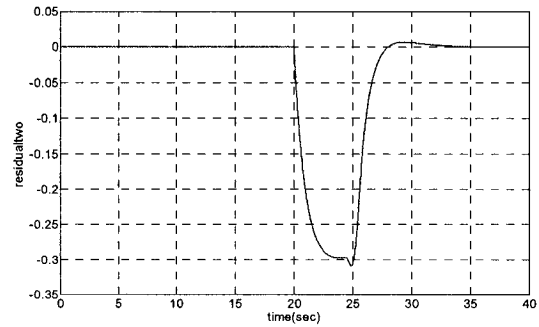
(b) The residual of the uncorrected slow model at $\varepsilon = 0.01$



(e) The residual of the 1st-order corrected fast model at $\varepsilon = 0.01$

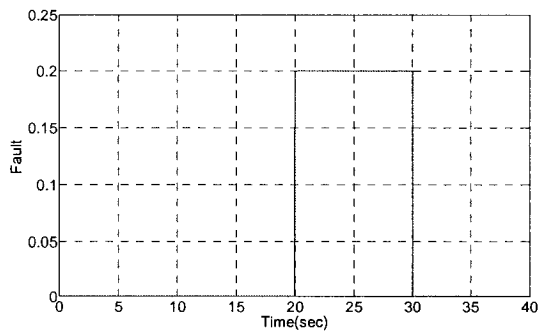


(c) The residual of the uncorrected slow model at $\varepsilon = 0.5$

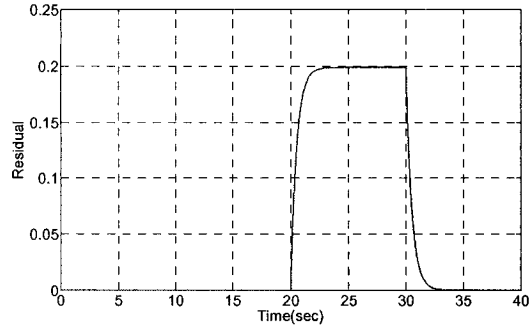


(f) The residual of the 1st-order corrected fast model at $\varepsilon = 0.5$

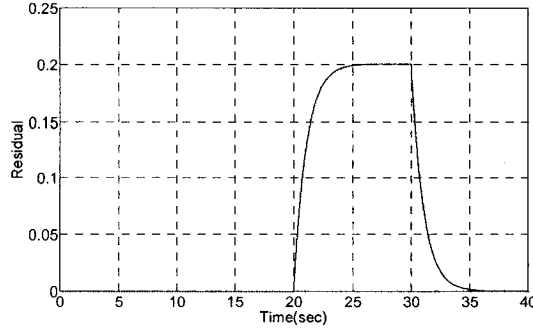
Figure 4-2 Detection and identification of the actuator fault in the slow and fast subsystems at $\varepsilon = 0.01$ and $\varepsilon = 0.5$



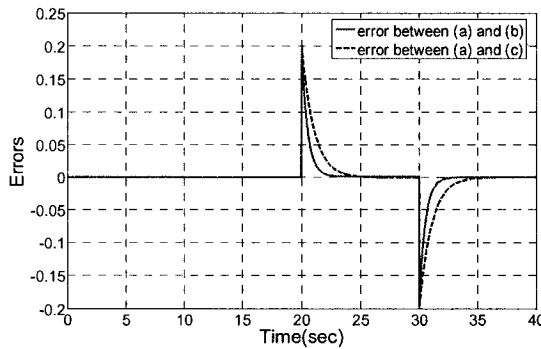
(a) The actuator fault occurs in the original full-order system



(b) The residual with the composite slow and fast subsystem observer gain G



(c) The residual with the gain G_{or} for the full-order observer directly designed



(d) The error comparison

Figure 4-3 The fault in the original system and the residuals with different observers gain at $\varepsilon = 0.01$.

4.4.2 Results with $\varepsilon = 0.5$:

At $\varepsilon = 0.5$, the full-order system matrices are given by

$$A_{11}|_{\varepsilon=0.5} = \begin{bmatrix} -0.2 & 0.4 \\ 0 & 0 \end{bmatrix}, \quad A_{12}|_{\varepsilon=0.5} = \begin{bmatrix} 0 & 0 \\ 0.345 & 0 \end{bmatrix},$$

$$\begin{aligned}
A_{21}|_{\varepsilon=0.5} &= \begin{bmatrix} 0 & -0.262 \\ 0 & 0 \end{bmatrix}, & A_{22}|_{\varepsilon=0.5} &= \begin{bmatrix} -0.233 & 0.131 \\ 0 & -0.5 \end{bmatrix}, \\
B_1|_{\varepsilon=0.5} &= \begin{bmatrix} 0 \\ 1 \end{bmatrix}, & B_2|_{\varepsilon=0.5} &= \begin{bmatrix} 0 \\ 0 \end{bmatrix}, \\
C_1|_{\varepsilon=0.5} &= \begin{bmatrix} 1 & 0 \\ 0 & 0 \end{bmatrix}, & C_2|_{\varepsilon=0.51} &= \begin{bmatrix} 0 & 0 \\ 1 & 0 \end{bmatrix}.
\end{aligned} \tag{4.33}$$

Clearly, the slow subsystem model is the same as that at $\varepsilon = 0.01$, therefore the observer gain can be selected to be the same as in (4.27), namely

$$G_s^0|_{\varepsilon=0.5} = \begin{bmatrix} 0.8 & -0.355 \\ 0 & -1.4298 \end{bmatrix},$$

for placing the poles of $A_s^0 - G_s^0 C_s^0$ at $\{-1, -2\}$. For $\varepsilon = 0.5$, the difference appears in the fast subsystem model given as

$$\begin{aligned}
A_f^0|_{\varepsilon=0.01} &= \begin{bmatrix} -0.233 & 0.131 \\ 0 & -0.5 \end{bmatrix}, \\
B_f^0|_{\varepsilon=0.01} &= \begin{bmatrix} 0 \\ 0 \end{bmatrix}, \\
C_f^0|_{\varepsilon=0.01} &= \begin{bmatrix} 0 & 0 \\ 1 & 0 \end{bmatrix}.
\end{aligned} \tag{4.34}$$

which is not fault diagnosable. Therefore, the first-order corrected fast subsystem model is obtained according to

$$\begin{aligned}
A_f^1|_{\varepsilon=0.01} &= \begin{bmatrix} -0.0381 & 0.131 \\ 0 & -0.5 \end{bmatrix}, & B_f^1|_{\varepsilon=0.01} &= \begin{bmatrix} 0.2634 \\ 0 \end{bmatrix}, \\
C_f^1|_{\varepsilon=0.01} &= \begin{bmatrix} 0 & 0 \\ 1.8361 & 0.2191 \end{bmatrix}.
\end{aligned} \tag{4.35}$$

where we have chosen the observer gain as

$$G_f^1|_{\varepsilon=0.5} = \begin{bmatrix} 0 & 0.4725 \\ 0 & 0.4306 \end{bmatrix}, \tag{4.36}$$

to place the poles of $A_f^1 - G_f^1 C_f^1$ at $\{-0.7, -0.8\}$.

Considering the same as that scenario described in Figs. 4-2 (a) and (d), Fig. 4-2(c) is the output of the residual generator of the uncorrected slow subsystem model at $\varepsilon = 0.5$ and Fig. 4-2(f) is that of the 1st-order corrected fast subsystem model $\varepsilon = 0.5$. It is clear that the residual generators for the subsystems with different values of ε are able to detect the occurrence of the actuator fault and identify its actual value.

For the original full-order observer, based on the observers (4.27) and (4.36) designed for the slow and fast subsystems, a composite observer gain may now be selected as

$$G|_{\varepsilon=0.5} = \begin{bmatrix} 0.8 & -4.5422 \\ 0 & -22.3662 \\ 0 & 349.3026 \\ 0 & 760.4272 \end{bmatrix} \quad (4.37)$$

which places the poles of $(A-GC)$ at $\{-1, -1.96 - 34.67 \pm 24.11j\}$. In order to compare the capability and performance of the proposed diagnoses with a brute force design, an observer is directly designed based on the original full-order system (4.24) according to

$$G_{or}|_{\varepsilon=0.5} = 10^3 \times \begin{bmatrix} 0.0036 & 0 \\ 0.0061 & 0.0003 \\ -0.3896 & -0.0249 \\ 1.1947 & 0.0604 \end{bmatrix} \quad (4.38)$$

which places the poles of $(A - G_{or}C)$ at $\{-1, -1.2, -3, -3\}$.

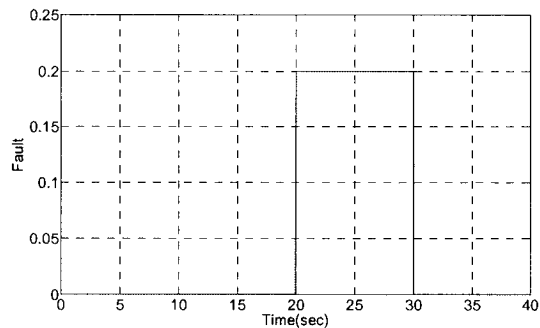
Fig. 4-4(a) shows the simulations for an actuator fault that has occurred in the original full-order system (4.24). Fig. 4-4(b) shows the output of the residual generator designed based on the composite observer, while Fig. 4-4(c) depicts the residual generated based on the observer directly designed for the original full-order

system. By comparing the error between the fault and the residual in Figs. 4-4 (a) and (b) and that between the fault and the residual in Fig. 4-4(c), Fig. 4-4(d) shows that the detection designed filter based on the composite observer has better capability in fault diagnosis as compared to the full-order observer.

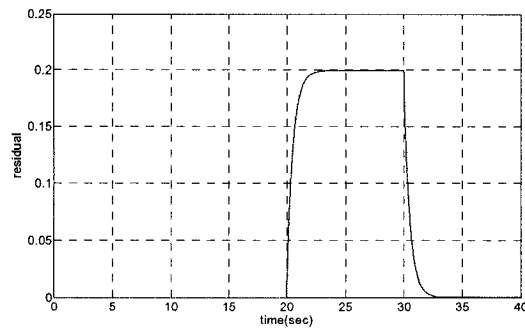
4.5 Conclusion

In this chapter, a geometric approach is applied to the fault diagnosis of the two time-scaled systems. Given that the observability of the slow and fast subsystems may vary due to the order of accuracy of the models, it is necessary to consider the observability of the models with different accuracy orders. For the slow and fast subsystems, the necessary and sufficient conditions (4.4)-(4.6) of the geometric approach can be used to design the observers which will detect and isolate faults in the subsystems. However, for the composite observer G for the original full-order system, it may not be possible to find a subspace W_f which satisfies the condition (4.6).

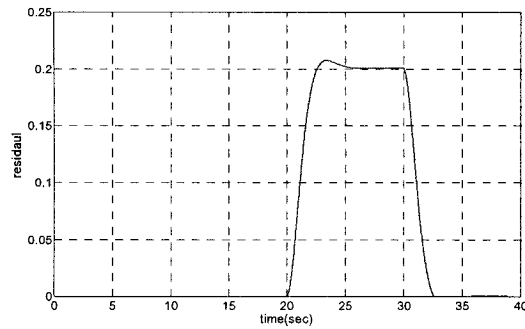
Consider the numerical example given by (4.24) which is a single-input-two-output system. The original full-order system was decoupled into uncorrected slow and fast subsystems. Since $B_f^0 = [0 \ 0]^T$, the uncorrected fast subsystem (4.28) is not



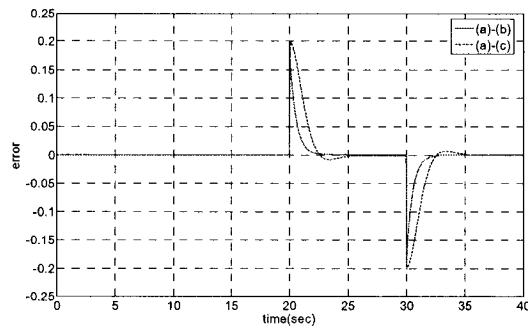
(a) The actuator fault occurs in the original full-order system



(b) The residual with the composite observer gain G



(c) The residual with the gain G_{or} for the observer directly designed for the full-order system



(d) error comparison

Figure 4-4 The fault in the original full-order system and the residuals for different observers with gains at $\varepsilon = 0.5$.

fault diagnosable. Therefore, we need to investigate the observability of the 1st-order fast subsystem. Furthermore, observers for the uncorrected slow subsystem and 1st-order fast subsystem based on the geometric approach were constructed. A composite observer is then obtained for the original full-order system.

We compared simulation results of fault diagnosis between the original full-order system with the composite observer and the observer directly-designed for the

original full-order system. We concluded that the composite observer has better capability in fault diagnosis as compared to the full-order observer. Furthermore, as ε increases, the advantage of the composite observer becomes more obvious.

Chapter 5

Validation of the Proposed FDI Schemes to Two Applications

In this chapter, we apply the preceding ideas to a detailed model of the longitudinal dynamics of an F-8 aircraft [39] and the four degree of freedom (DOF) gyroscope. For the F-8 aircraft model, it is necessary to design observers for both subsystems and a composite observer in order to detect and isolate actuator faults in the subsystems and the original full-order system. However, for the DOF gyroscope, only the slow states are needed to be estimated for the fault diagnosis purpose since the fast subsystem is neither observable nor diagnosable.

5.1 Two Time-scale Aircraft Longitudinal Dynamics

5.1.1 System Model

In this section we apply the preceding ideas to a detailed model of the longitudinal dynamics of an F-8 aircraft [39]. The equations of an airplane are nonlinear equations of

the longitudinal and lateral states. The linearized equations are approximately decoupled into separate longitudinal and lateral dynamics.

The aircraft's longitudinal variables are

$$x = [V \quad \gamma \quad \alpha \quad q]^T, u = \delta_e,$$

where

V denotes the horizontal-velocity deviation in feet/second;

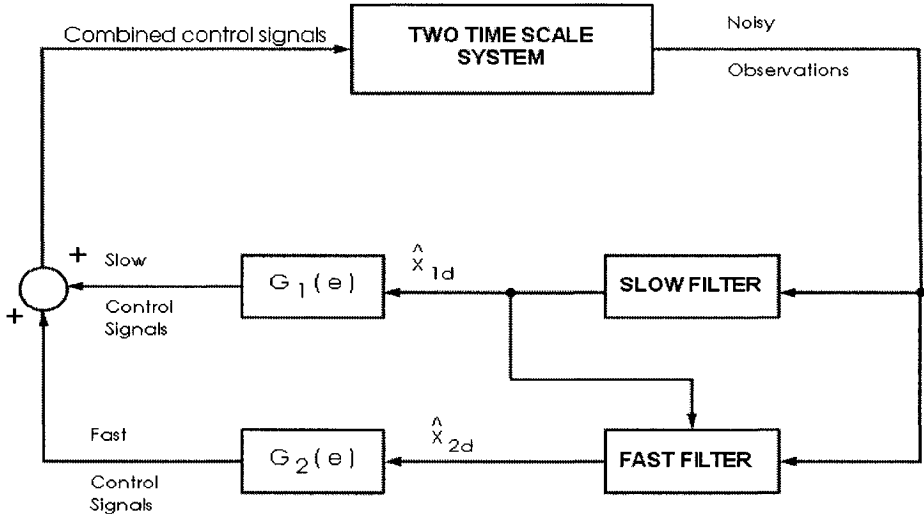
γ denotes the flight-path angle in radians;

α denotes the angle of attack in radians;

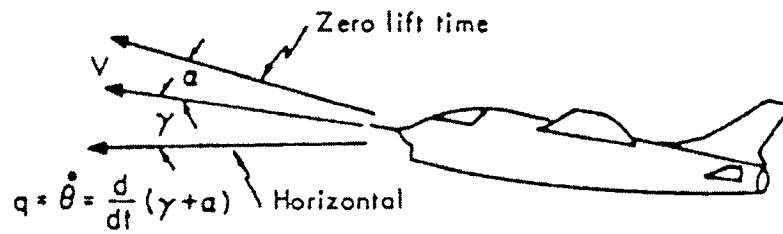
q denotes the pitch rate in radians/second;

δ_e denotes the elevator deflection in radians.

The physical interpretation for these variables is given in Fig.5-1.



Asymptotically optimal two time-scale controller



Aircraft longitudinal variables.

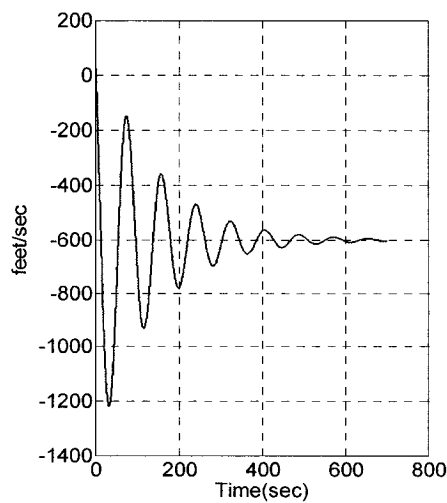
Figure 5-1 Two Time-scale Aircraft Longitudinal Dynamics [39]

The LTI state-space system matrices are given by

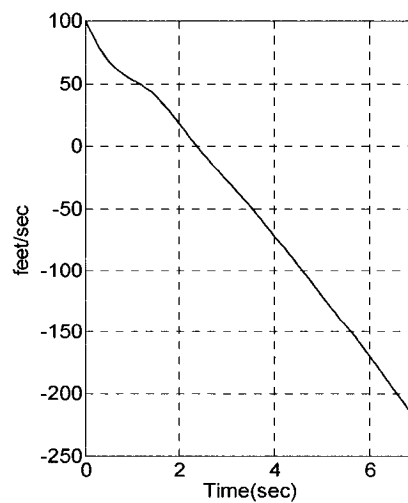
$$A = \begin{bmatrix} -1.357 \times 10^{-2} & -3.220 \times 10^1 & -4.630 \times 10^1 & 0.000 \\ 1.200 \times 10^{-4} & 0.000 & 1.214 & 0.000 \\ -1.212 \times 10^{-4} & 0.000 & -1.214 & 1.000 \\ 5.700 \times 10^{-4} & 0.000 & -.9010 & -6.696 \times 10^{-1} \end{bmatrix}$$

$$B = \begin{bmatrix} -4.330 \times 10^{-1} \\ 1.394 \times 10^{-1} \\ -1.394 \times 10^{-1} \\ -1.577 \times 10^{-1} \end{bmatrix}, \quad C = \begin{bmatrix} 0.0 & 0.0 & 0.0 & 1.0 \\ 1.0 & 0.0 & 0.0 & 0.0 \end{bmatrix}. \quad (5.1)$$

Fig. 5-2 and Fig. 5-3 show the response to an initial velocity error $V(0) = 100 \text{ ft/s}$, an initial flight-path angle $\gamma(0) = 1 \text{ rad}$, and an initial angle of attack $\alpha(0) = 1 \text{ rad}$. The two time-scale behavior is clearly illustrated here.



V



V

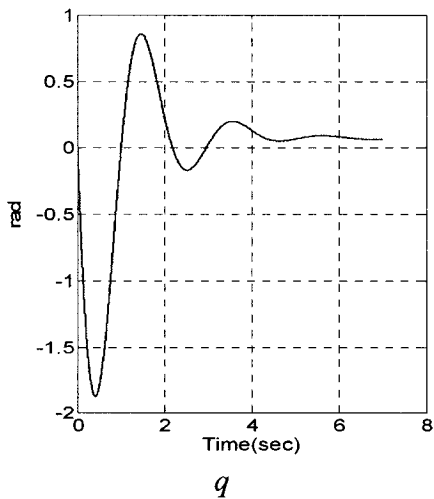
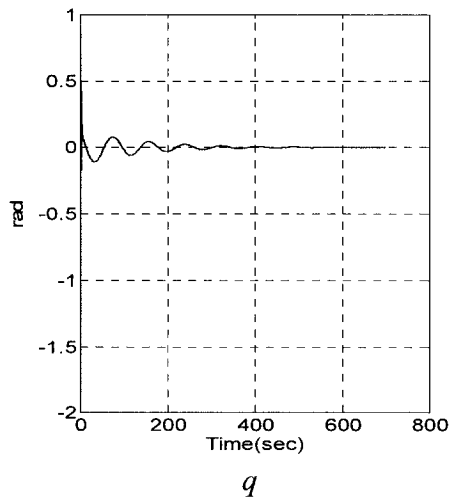
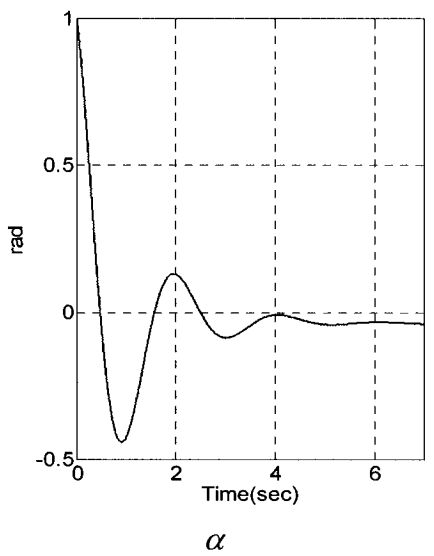
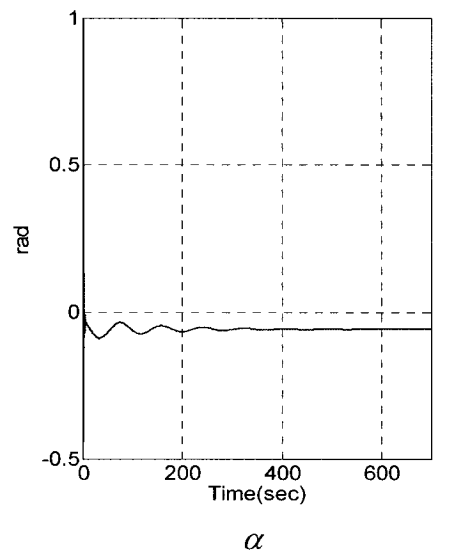
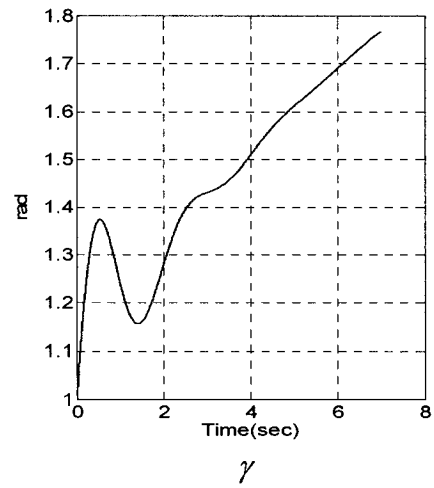
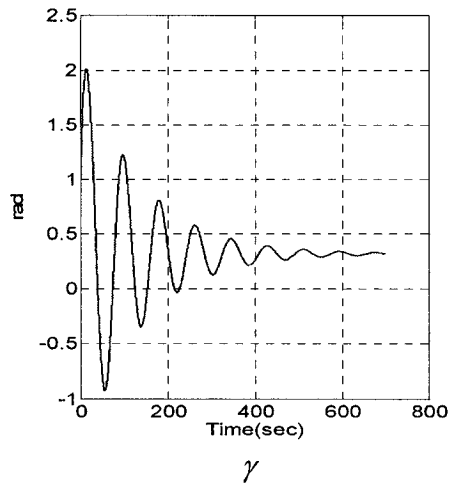


Figure 5-2 Aircraft response in slow time scale

Figure 5-3 Aircraft response in fast time scale

The eigenvalues of A are given by $\{-0.99411 \pm 2.9878i, -0.0075 \pm 0.0759i\}$. The states and equations for V and γ represent the slow dynamics, and the states and equations for α and q represent the fast dynamics. Therefore, we set

$$\begin{bmatrix} x_1 \\ x_2 \end{bmatrix} = \begin{bmatrix} V \\ \gamma \end{bmatrix}, \quad \begin{bmatrix} z_1 \\ z_2 \end{bmatrix} = \begin{bmatrix} \alpha \\ q \end{bmatrix}.$$

Choosing $\varepsilon = 0.01$, the system (5.1) can be written in the standard form of the system (3.18)-(3.20) where

$$\begin{aligned} A_{11} &= \begin{bmatrix} -0.0136 & -32.2000 \\ 0.0001 & 0 \end{bmatrix}, & A_{12} &= \begin{bmatrix} -46.3000 & 0 \\ 1.2140 & 0 \end{bmatrix}, \\ A_{21} &= 10^{-5} \times \begin{bmatrix} -0.1212 & 0 \\ 0.5700 & 0 \end{bmatrix}, & A_{22} &= \begin{bmatrix} -0.0121 & 0.0100 \\ -0.0901 & -0.0067 \end{bmatrix}, \\ B_1 &= \begin{bmatrix} -0.4330 \\ 0.1394 \end{bmatrix}, & B_2 &= \begin{bmatrix} -0.0014 \\ -0.0016 \end{bmatrix}, \\ C_1 &= \begin{bmatrix} 0 & 0 \\ 1 & 0 \end{bmatrix}, & C_2 &= \begin{bmatrix} 0 & 1 \\ 0 & 0 \end{bmatrix}. \end{aligned} \tag{5.2}$$

By setting $\varepsilon = 0$, the uncorrected slow subsystem model is given by

$$\begin{aligned} A_s^0|_{\varepsilon=0.01} &= \begin{bmatrix} -0.0159 & -32.2000 \\ 0.0002 & 0 \end{bmatrix}, & B_s^0|_{\varepsilon=0.01} &= \begin{bmatrix} 0.7503 \\ 0.1084 \end{bmatrix}, \\ C_s^0|_{\varepsilon=0.01} &= \begin{bmatrix} 0.0002 & 0 \\ 1.0000 & 0 \end{bmatrix}, & D_s^0|_{\varepsilon=0.01} &= \begin{bmatrix} 0.1084 \\ 0 \end{bmatrix}. \end{aligned} \tag{5.3}$$

The uncorrected fast subsystem model is given by

$$\begin{aligned} A_f^0|_{\varepsilon=0.01} &= \begin{bmatrix} -0.0121 & 0.0100 \\ -0.0901 & -0.0067 \end{bmatrix}, \\ B_f^0|_{\varepsilon=0.01} &= \begin{bmatrix} -0.0014 \\ -0.0016 \end{bmatrix}, \end{aligned}$$

$$C_f^0|_{\varepsilon=0.01} = \begin{bmatrix} 0 & 1 \\ 0 & 0 \end{bmatrix}. \quad (5.4)$$

By computing the first order corrected slow and fast subsystem models by setting $\varepsilon^2 = 0$ and taking into account $O(\varepsilon)$, we obtained

$$\begin{aligned} A_s^1|_{\varepsilon=0.01} &= \begin{bmatrix} -0.0159 & -32.2326 \\ 0.0002 & 0.0009 \end{bmatrix}, & B_s^1|_{\varepsilon=0.01} &= \begin{bmatrix} 0.7510 \\ 0.1084 \end{bmatrix}, \\ C_s^1|_{\varepsilon=0.01} &= \begin{bmatrix} 0.0002 & -0.0007 \\ 1.000 & 0 \end{bmatrix}, & D_s^1|_{\varepsilon=0.01} &= \begin{bmatrix} 0.1084 \\ 0 \end{bmatrix}, \end{aligned} \quad (5.5)$$

and

$$\begin{aligned} A_f^1|_{\varepsilon=0.01} &= \begin{bmatrix} -0.0121 & 0.0100 \\ -0.0900 & -0.0067 \end{bmatrix}, \\ B_f^1|_{\varepsilon=0.01} &= \begin{bmatrix} -0.0014 \\ -0.0016 \end{bmatrix}, \\ C_f^1|_{\varepsilon=0.01} &= \begin{bmatrix} 0.0006 & 1.0009 \\ 3.1561 & 4.7135 \end{bmatrix}. \end{aligned} \quad (5.6)$$

In order to investigate the influence of ε on system (5.2), we compute the uncorrected and first-order corrected models for system (5.2) at $\varepsilon = 0.05$. The uncorrected models are the same as those at $\varepsilon = 0.01$, which implies

$$\begin{aligned} A_s^0|_{\varepsilon=0.05} &= A_s^0|_{\varepsilon=0.01}, & B_s^0|_{\varepsilon=0.05} &= B_s^0|_{\varepsilon=0.01}, & C_s^0|_{\varepsilon=0.05} &= C_s^0|_{\varepsilon=0.01}, & D_s^0|_{\varepsilon=0.05} &= D_s^0|_{\varepsilon=0.01}; \\ A_f^0|_{\varepsilon=0.05} &= A_f^0|_{\varepsilon=0.01}, & B_f^0|_{\varepsilon=0.05} &= B_f^0|_{\varepsilon=0.01}, & C_f^0|_{\varepsilon=0.05} &= C_f^0|_{\varepsilon=0.01}. \end{aligned} \quad (5.7)$$

For the first-order corrected models, we have

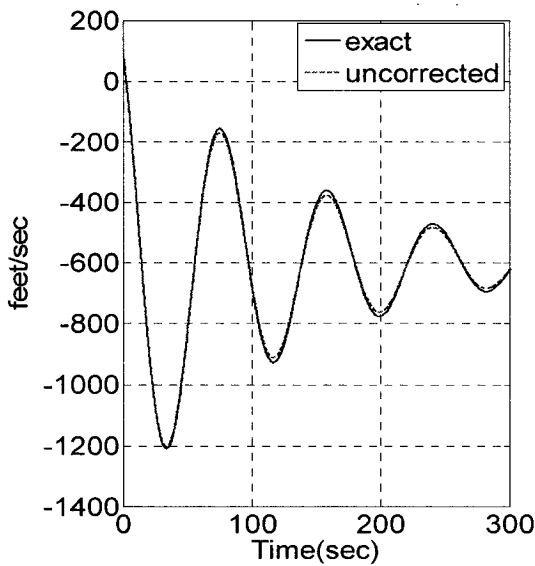
$$\begin{aligned} A_s^1|_{\varepsilon=0.05} &= \begin{bmatrix} -0.0161 & -32.3630 \\ 0.0002 & 0.0040 \end{bmatrix}, & B_s^1|_{\varepsilon=0.05} &= \begin{bmatrix} 0.7674 \\ 0.1103 \end{bmatrix}, \\ C_s^1|_{\varepsilon=0.05} &= \begin{bmatrix} 0.0002 & -0.0038 \\ 1.000 & 0 \end{bmatrix}, & D_s^1|_{\varepsilon=0.05} &= \begin{bmatrix} 0.1088 \\ 0 \end{bmatrix}, \end{aligned} \quad (5.8)$$

and

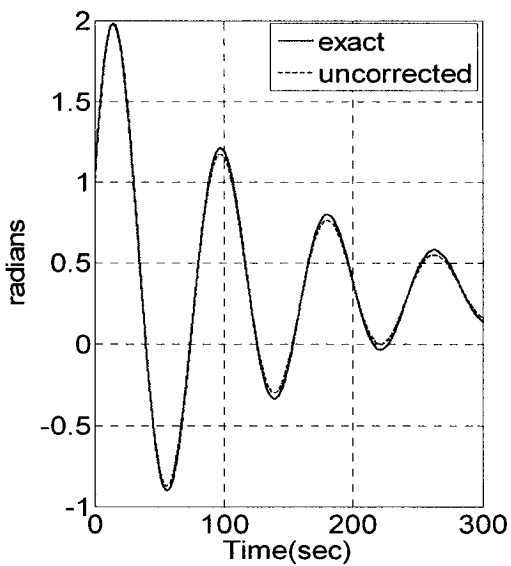
$$A_f^1|_{\varepsilon=0.05} = \begin{bmatrix} -0.0120 & 0.0100 \\ -0.0897 & -0.0067 \end{bmatrix}, \quad B_f^1|_{\varepsilon=0.05} = \begin{bmatrix} -0.0014 \\ -0.0016 \end{bmatrix},$$

$$C_f^1|_{\varepsilon=0.05} = \begin{bmatrix} 0.0029 & 1.0043 \\ 15.7937 & 23.5727 \end{bmatrix}. \quad (5.9)$$

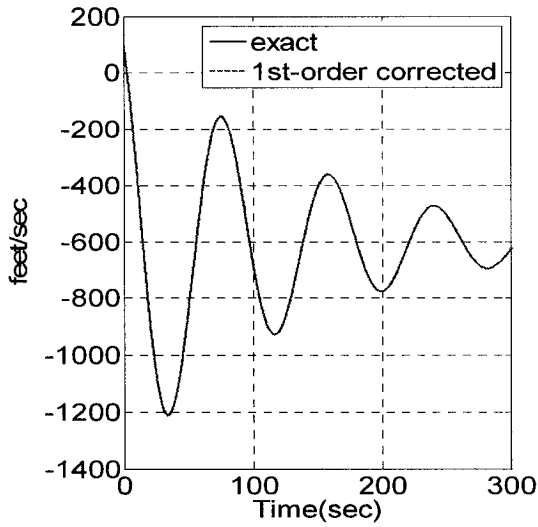
The exact solution, the uncorrected solution and the 1st-order corrected solution of the slow states V and γ are shown comparatively in Figure 5-4 and Figure 5-5 at $\varepsilon = 0.01$ and $\varepsilon = 0.05$, respectively. It can be seen that the 1st-order corrected solution agrees more with the exact in contrast to the case of the uncorrected solution. As ε increases, the advantage of the 1st-order corrected solution become even further clear.



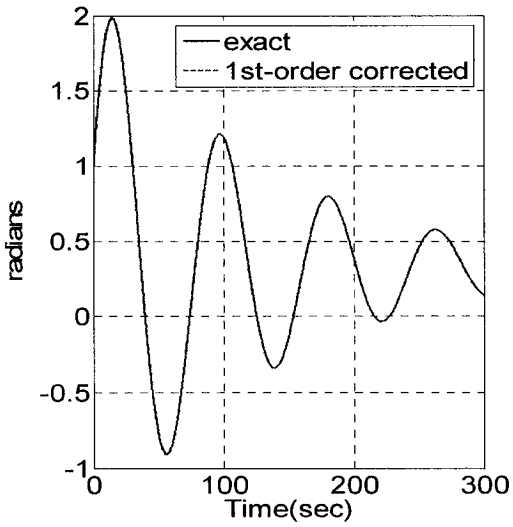
(a) The exact solution vs. the uncorrected solution of x_1



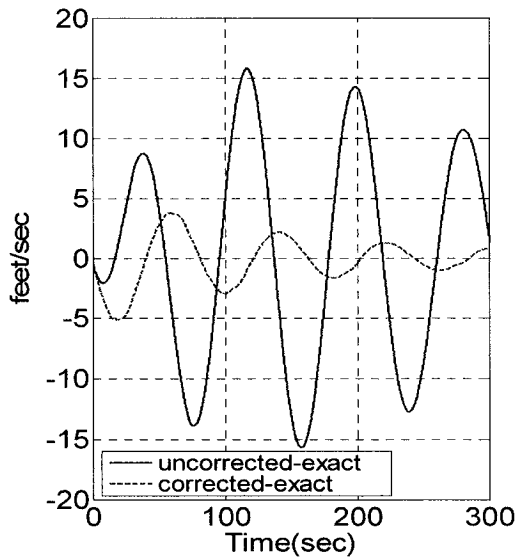
(d) The exact solution vs. the uncorrected solution of x_2



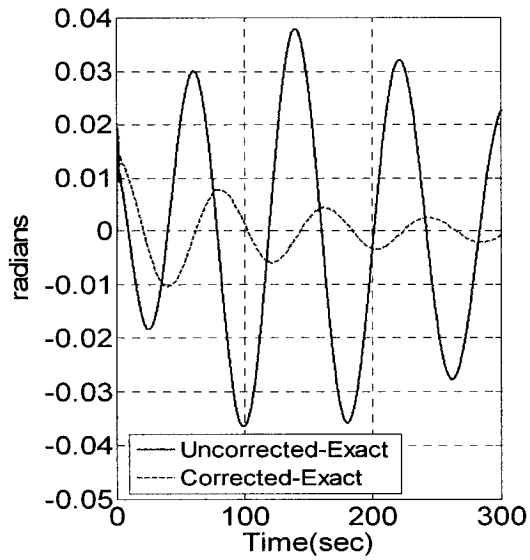
(b) The exact solution vs. the 1st order corrected solution of x_1



(e) The exact solution vs. the 1st order corrected solution of x_2

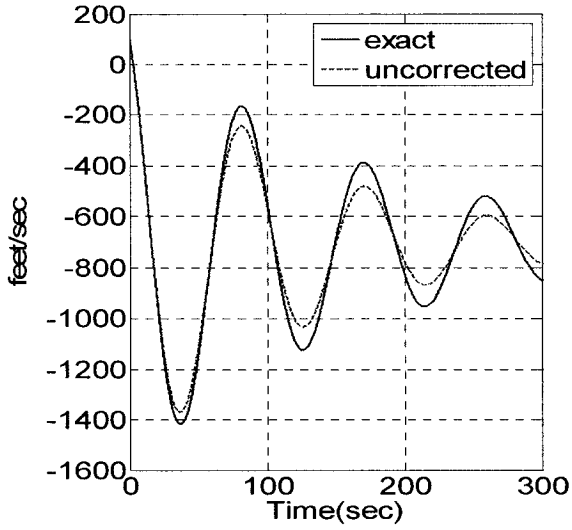


(c) The error of different solutions of x_1

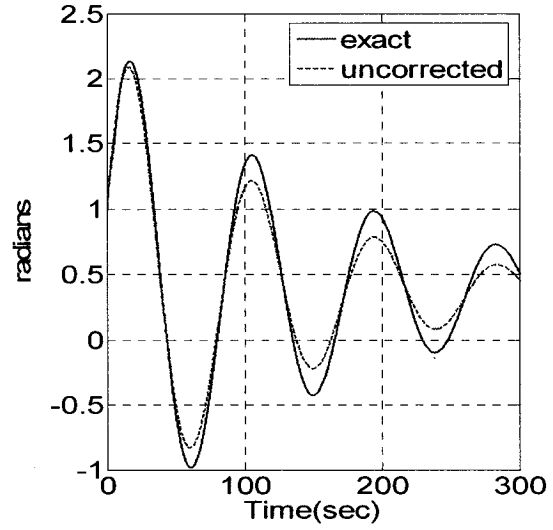


(f) The error of different solutions of x_2

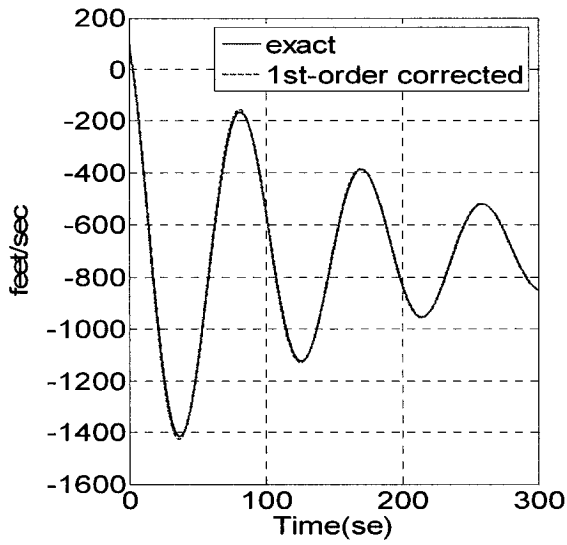
Figure 5-4 The exact solution vs. the uncorrected solution and 1st-order corrected solution at $\varepsilon = 0.01$ and $u(t) = 1, x_1^0 = 100 \text{ feet/sec}, x_2^0 = 1 \text{ rad}$



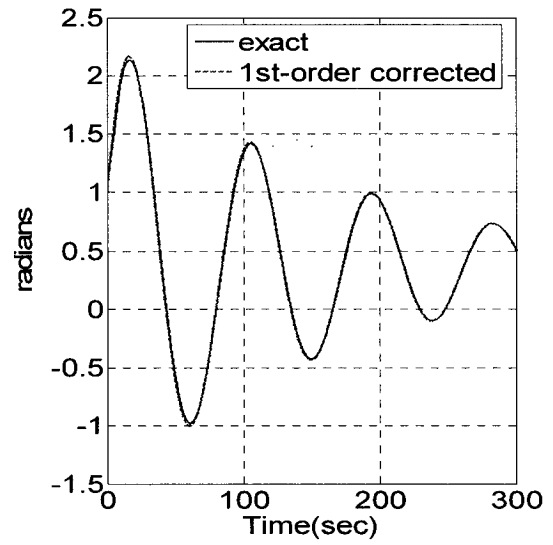
(a) The exact solution vs. the uncorrected solution of x_1



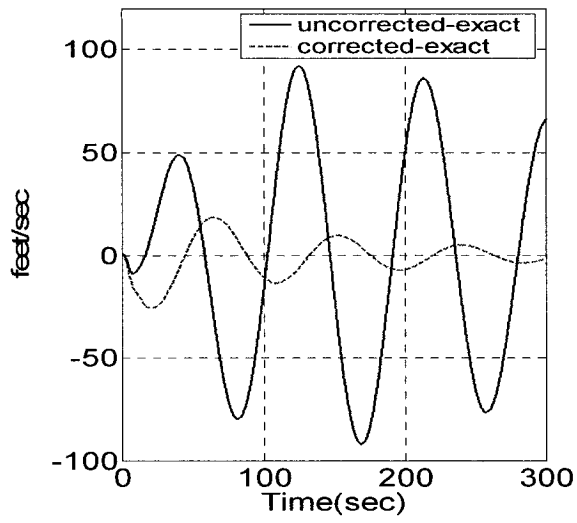
(d) The exact solution vs. the uncorrected solution of x_2



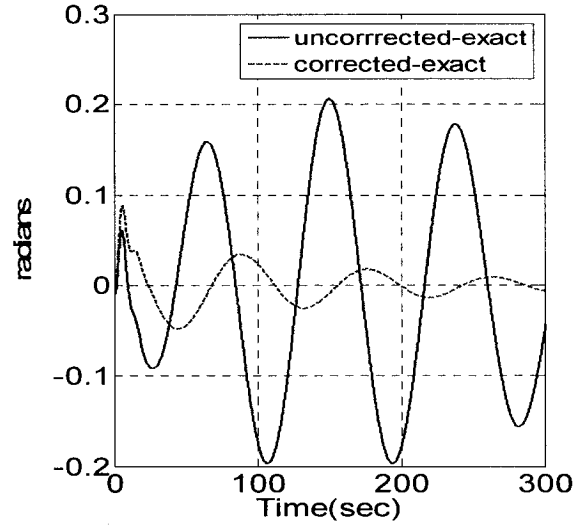
(b) The exact solution vs. the 1st order corrected solution of x_1



(e) The exact solution vs. the 1st order corrected solution of x_2



(c) The error of different solutions of x_1



(f) The error of different solutions of x_2

Figure 5-5 The exact solution vs. uncorrected solution and the 1st-order corrected solution at $\varepsilon = 0.05$ and $u(t) = 1, x_1^0 = 100 \text{ feet/sec}, x_2^0 = 1 \text{ rad}$

5.1.2 Composite Observer Design

We continue to design a composite observer for the two time-scale aircraft longitudinal dynamics. The detailed procedures are shown as below.

For the uncorrected slow model (5.3) we have

$$A_s^0|_{\varepsilon=0.01} = \begin{bmatrix} -0.0159 & -32.2000 \\ 0.0002 & 0 \end{bmatrix}, \quad B_s^0|_{\varepsilon=0.01} = \begin{bmatrix} 0.7503 \\ 0.1084 \end{bmatrix},$$

$$C_s^0|_{\varepsilon=0.01} = \begin{bmatrix} 0.0002 & 0 \\ 1.0000 & 0 \end{bmatrix}, \quad D_s^0|_{\varepsilon=0.01} = \begin{bmatrix} 0.1084 \\ 0 \end{bmatrix}$$

where we chose

$$G_s^0 = \begin{bmatrix} 0.0001 & 0.4041 \\ 0 & -0.0012 \end{bmatrix} \quad (5.10)$$

which places the poles of $(A_s^0 - G_s^0 C_s^0)$ at $\{-0.22, -0.2\}$.

For the uncorrected fast model (5.4) we have

$$A_f^0|_{\varepsilon=0.01} = \begin{bmatrix} -0.0121 & 0.0100 \\ -0.0901 & -0.0067 \end{bmatrix}, \quad B_f^0|_{\varepsilon=0.01} = \begin{bmatrix} -0.0014 \\ -0.0016 \end{bmatrix},$$

$$C_f^0|_{\varepsilon=0.01} = \begin{bmatrix} 0 & 1 \\ 0 & 0 \end{bmatrix}$$

where we chose

$$G_f^0 = \begin{bmatrix} 0.0067 & 0 \\ 0.0402 & 0 \end{bmatrix} \quad (5.11)$$

which places the poles of $(A_f^0 - G_f^0 C_f^0)$ at $\{-0.029, -0.03\}$.

Then by simply following equations (4.14)-(4.15), for the original model (5.1), we have a composite observer gain matrix given by

$$G = \begin{bmatrix} 21.4367 & 0.4042 \\ -0.5527 & -0.0012 \\ 0.6658 & 0 \\ 4.0164 & 0 \end{bmatrix} \quad (5.12)$$

and that places the poles of $(A - GC)$ at $\{-0.2099 \pm 0.0008i, -2.8955, -3.0025\}$.

For comparison, we also design an observer directly for the original full-order model (5.1) with the gain matrix G_{or} given by

$$G_{or} = \begin{bmatrix} 26.865 & -2.0048 \\ -0.5974 & 0.0831 \\ 1.7726 & -0.1193 \\ 6.3076 & -0.9957 \end{bmatrix} \quad (5.13)$$

which places the poles of $(A - G_{or}C)$ at $\{-2.9 \pm 2i, -0.2 \pm 0.2i\}$.

To design a closed-loop stable system, a state feedback control of the form $u = -K\hat{x}$ is then designed where the feedback gain K is selected as

$$K = [-0.0013 \quad 1.8274 \quad -26.1108 \quad -5.1216] \quad (5.14)$$

in order to place the poles of the closed loop matrix $(A - BK)$ at $\{-2.6, -3.8, -0.1 \pm 0.11i\}$.

Fig.5-6 and Fig.5-7 show the responses for states V and q of the closed-loop system with the composite observer G and the full-order model observer G_{or} . It is clear that using the same feedback control, the closed-loop system with either G or G_{or} is stable and the output responses are very close.

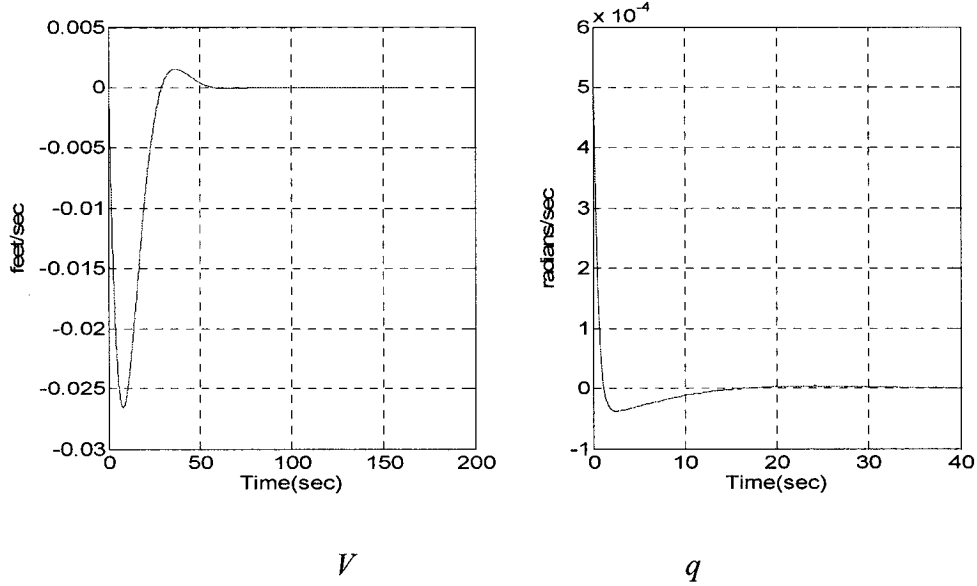


Figure 5-6 The responses of V and q for the closed-loop system with the composite full-order model observer G

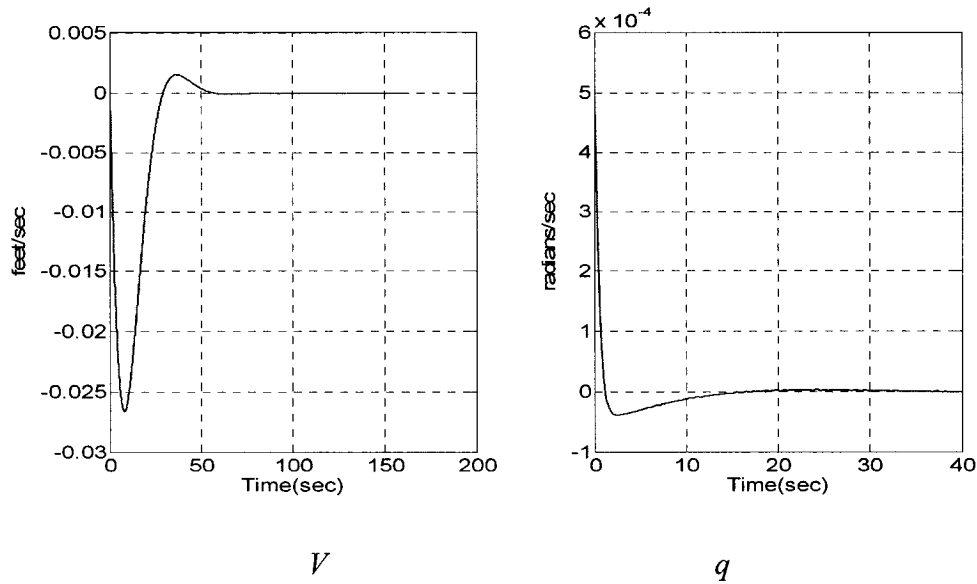


Figure 5-7 The responses of V and q for the closed-loop system with the composite observer G_{or}

5.1.3 Actuator Fault Diagnosis and Simulation Results

Consider the uncorrected slow subsystem model (5.3) with the matrices

$$A_s^0|_{\varepsilon=0.01} = \begin{bmatrix} -0.0159 & -32.2000 \\ 0.0002 & 0 \end{bmatrix}, \quad B_s^0|_{\varepsilon=0.01} = \begin{bmatrix} 0.7503 \\ 0.1084 \end{bmatrix},$$

$$C_s^0|_{\varepsilon=0.01} = \begin{bmatrix} 0.0002 & 0 \\ 1.0000 & 0 \end{bmatrix}, \quad D_s^0|_{\varepsilon=0.01} = \begin{bmatrix} 0.1084 \\ 0 \end{bmatrix}$$

and the uncorrected fast subsystem model (5.4) with the matrices

$$A_f^0|_{\varepsilon=0.01} = \begin{bmatrix} -0.0121 & 0.0100 \\ -0.0901 & -0.0067 \end{bmatrix}, \quad B_f^0|_{\varepsilon=0.01} = \begin{bmatrix} -0.0014 \\ -0.0016 \end{bmatrix},$$

$$C_f^0|_{\varepsilon=0.01} = \begin{bmatrix} 0 & 1 \\ 0 & 0 \end{bmatrix}.$$

Both the subsystems have a single input and two outputs systems. This implies that the innovation due to the actuator fault in each system is confined to a subspace of the system's output space and it is not necessary to consider the fault isolation problem. Therefore, we utilize G_s^0 and G_f^0 to the error dynamics system for each subsystem and choose the second output of the error system dynamics as the residual.

Fig. 5-8 shows the simulation results corresponding to the following scenario: the actuators u_s and u_f are supposed to ideally provide constant unit step input, that is $u_s = 1$ and $u_f = 1$. An actuator fault f_s occurs at time $t=150s$ and ends at $t=200s$ [as shown in Fig. 5-8(a)] in the slow subsystem and a fault f_f occurs at time $\tau = 200s$ and $\tau = 250s$ [as shown in Fig. 5-8(c)] in the fast subsystem. Fig. 5-8(b) depicts the output of the residual generator corresponding to the uncorrected slow model and Fig. 5-8(d)

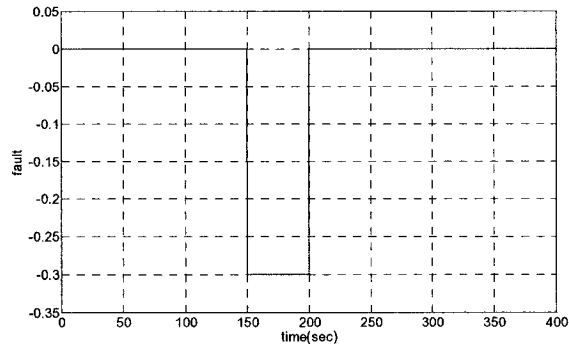
shows that of the uncorrected fast model. It is clear that the residual generator in each subsystem indicates the occurrence of the actuator fault and identifies its actual value.

For the original system (5.1), there is the composite observer with the gain (5.12) and the observer directly designed with the gain (5.13). We generate an actuator fault f which occurs between time $t=200$ and $t=250$ s [as shown in Fig. 5-9(a)]. Fig. 5-9(b) is the residual of the error system using G and Fig. 5-9(c) is the residual of the error dynamics system using G_{or} . Fig. 5-9(d) shows the comparison between the two residuals in Fig.5-9 (b) and (c). It shows the residual of the error dynamics system with G_{or} is closer to the real fault than that with the composite observer gain G .

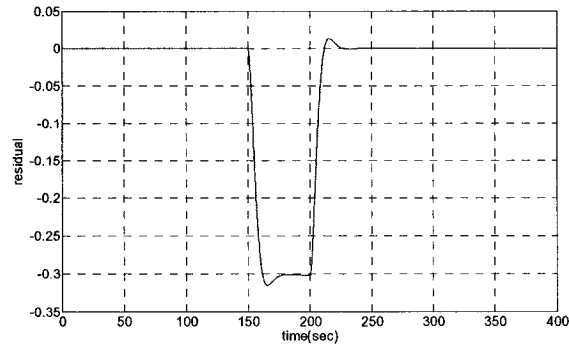
5.2 The Four Degree of Freedom (DOF) Gyroscope

5.2.1 System Model [40]

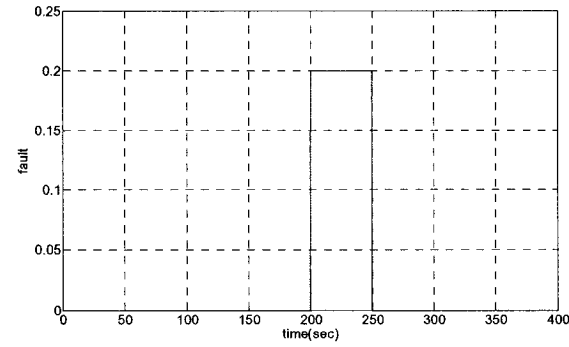
Figure 5-10 shows a 4 DOF gyroscope comprised of gimbals (A , B , and C) along with an axisymmetric disk (D). Dextral sets of orthogonal unit vectors a_i, b_i, c_i and $d_i (i=1,2,3)$ are fixed in A , B , C , and D , respectively. An inertial (or Newtonian) reference frame is defined as N , in which a dextral set of orthogonal unit vector $N_i (i=1,2,3)$ are fixed. Four angles specify the configuration of the system. The angular travel of D in C in the direction d_2 is defined as q_1 . However, the displacement of the rotor is typically not used explicitly in the dynamics and control study of this system- rather, the speed of D in C , ω_1 , will generally be considered. The angle q_2 is defined as



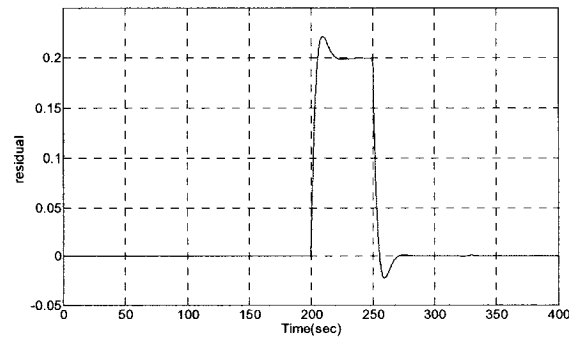
(a) The actuator fault occurs in the slow subsystem



(b) The residual of the uncorrected slow subsystem model

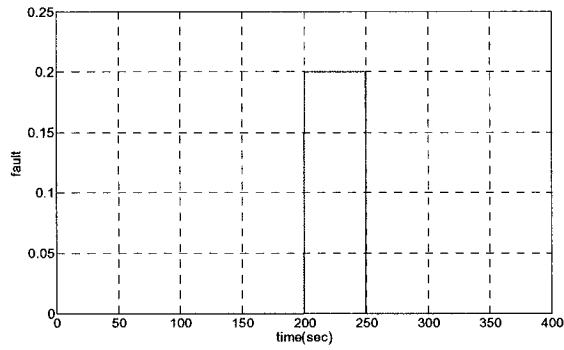


(c) The actuator fault occurs in the fast subsystem model

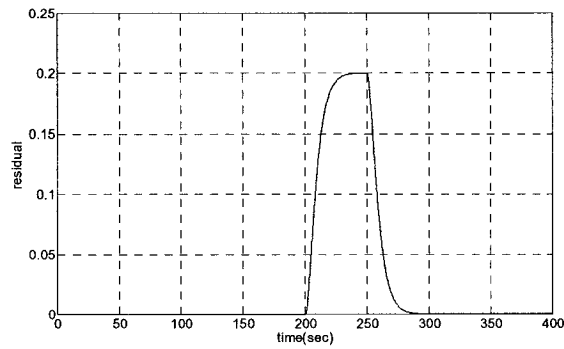


(d) The residual of the uncorrected fast subsystem model

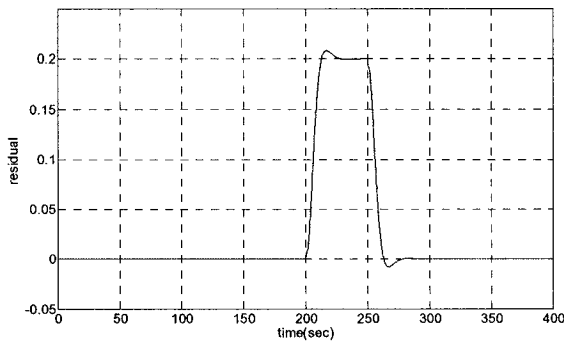
Figure 5-8 The faults in the slow and fast subsystems and the residuals associated with the uncorrected models



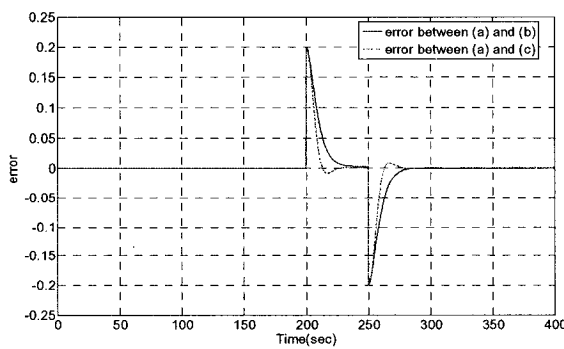
(a) The actuator fault occurs in the original system



(b) The residual with the composite observer gain G



(c) The residual with the gain G_{or} of the observer directly designed



(d) Error comparison

Figure 5-9 The fault in the original system and the residuals using different observer gain

the angular rotation about a_3 of A relative to N . The configuration shown in Fig. 5-10 reflects $q_i = 0$ ($i = 1, 2, 3$).

For this system, the mass centers of all bodies comprising the system are at the center of the disk (D) which is also the center of all the gimbal axes. Only rotational dynamics are considered in the following analysis and the effects of gravity are neglected.

The central inertia matrices of the bodies comprising the system are given below. Each matrix is given in the coordinate frame attached to the respective body. The I_x, J_x, K_x ($x = A, B, C$ and D) elements are the scalar moments of inertia about the i^{th} ($i=1, 2, 3$) direction respectively in bodies A, B, C , and D .

$$\begin{aligned}
 I^A &= \begin{bmatrix} I_A & 0 & 0 \\ 0 & J_A & 0 \\ 0 & 0 & K_A \end{bmatrix} & I^B &= \begin{bmatrix} I_B & 0 & 0 \\ 0 & J_B & 0 \\ 0 & 0 & K_B \end{bmatrix} \\
 I^C &= \begin{bmatrix} I_C & 0 & 0 \\ 0 & J_C & 0 \\ 0 & 0 & K_C \end{bmatrix} & I^D &= \begin{bmatrix} I_D & 0 & 0 \\ 0 & J_D & 0 \\ 0 & 0 & K_D \end{bmatrix} \quad (5.15)
 \end{aligned}$$

The only moments of inertia are considered while products of inertia are set to zero. This simplification is valid for most dynamic and control modeling purpose.

The rectilinear velocities of the mass centers of all the bodies comprising the system are zero since all the mass centers are fixed in N . Only angular velocities are considered in the present analysis. The angular velocity of A in N is given as

$${}^N \omega^A = \omega_4 a_3 \quad (5.16)$$

Adopting this notation, the quantities are defined as

$${}^A \omega^B = \omega_3 b_2 \quad (5.17)$$

$${}^B \omega^C = \omega_2 c_1 \quad (5.18)$$

$${}^c \omega^D = \omega_1 d_2 \quad (5.19)$$

The following kinematic differential equations relate the generalized coordinates to the regular speeds.

$$\dot{q}_2 = \omega_2 \quad (5.20)$$

$$\dot{q}_3 = \omega_3 \quad (5.21)$$

$$\dot{q}_4 = \omega_4 \quad (5.22)$$

Finally, the coordinates of any of the body frames may be transformed to the inertial frame through the following transformation matrices. These follow from inspection of Figure 5-10.

$$\begin{bmatrix} n_1 \\ n_2 \\ n_3 \end{bmatrix} = \begin{bmatrix} \cos q_4 & -\sin q_4 & 0 \\ \sin q_4 & \cos q_4 & 0 \\ 0 & 0 & 1 \end{bmatrix} \begin{bmatrix} a_1 \\ a_2 \\ a_3 \end{bmatrix} \quad (5.23)$$

$$\begin{bmatrix} a_1 \\ a_2 \\ a_3 \end{bmatrix} = \begin{bmatrix} \cos q_3 & 0 & \sin q_3 \\ 0 & 1 & 0 \\ -\sin q_3 & 0 & \cos q_3 \end{bmatrix} \begin{bmatrix} b_1 \\ b_2 \\ b_3 \end{bmatrix} \quad (5.24)$$

$$\begin{bmatrix} b_1 \\ b_2 \\ b_3 \end{bmatrix} = \begin{bmatrix} 1 & 0 & 0 \\ 0 & \cos q_2 & -\sin q_2 \\ 0 & \sin q_2 & \cos q_2 \end{bmatrix} \begin{bmatrix} c_1 \\ c_2 \\ c_3 \end{bmatrix} \quad (5.25)$$

$$c_2 = d_2 \quad (5.26)$$

This simplified expression of equations (5.26) results from the axial symmetry of D and by recognizing that only angular velocity of the rotor (ω_1) – not its position (q_1) – is needed in the dynamics and control study of this system.

Two inputs are considered for this system. The first is a torque, T_1 , applied to D by C (via the rotor spin motor) which results in the following torques on D and C

$$T^D = T_1 d_2 \quad (5.27)$$

$$T^C = -T_1 d_2 \quad (5.28)$$

The second input is a torque, T_2 , applied to C by B (via a gimbal motor/capstan drive) which results in the following torques on C and B

$$T^C = T_2 c_1 \quad (5.29)$$

$$T^B = -T_2 c_1 \quad (5.30)$$

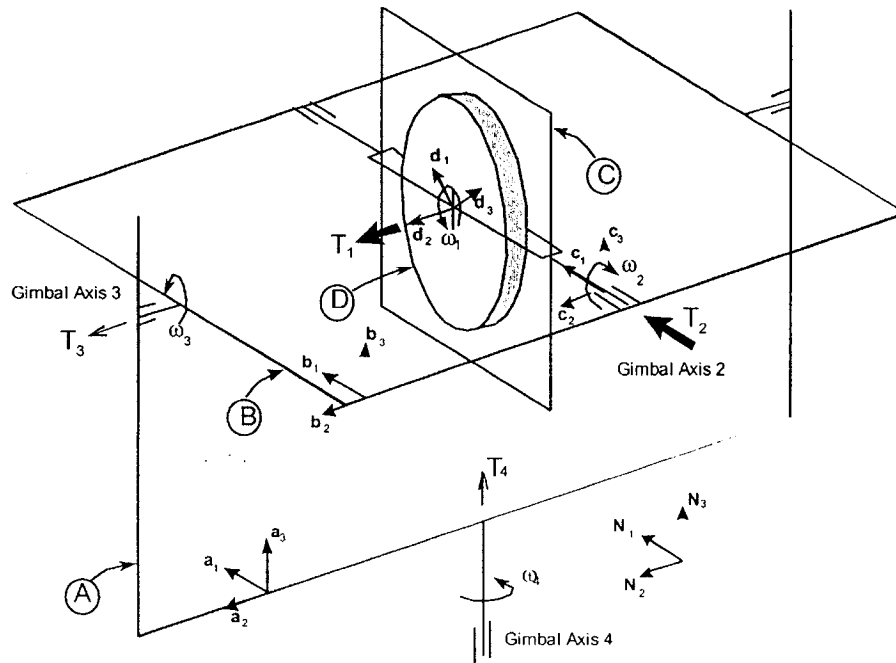


Figure 5-10 The Four Degree of Freedom Gyroscope [40]

5.2.2 Special Case: All Gimbals Free (Reaction & Gyroscopic Torques Acting)

In this special case which is depicted in Figure 5-11, the dynamics are simplified as all gimbals are Free. The operating point is about $q_{2_0} = 0, q_{3_0} = 0, \omega_1 = \Omega$. Here Ω is the spin speed of the rotor disk (D). The unit vectors c_1 and d_2 are normal to a_3 (i.e. T_1 and T_2 are directed horizontally).

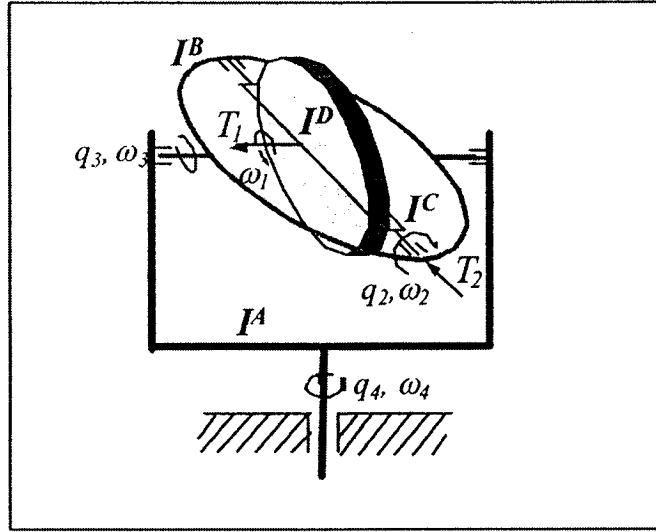


Figure 5-11 All gimbals free configuration ($q_{2_0} = 0, q_{3_0} = 0$) [40]

For the purpose of controls design, the plant dynamic model is represented as

$$x = \begin{bmatrix} q_2 \\ q_3 \\ q_4 \\ \omega_1 \\ \omega_2 \\ \omega_3 \\ \omega_4 \end{bmatrix}, \quad A = \begin{bmatrix} 0 & 0 & 0 & 0 & 1 & 0 & 0 \\ 0 & 0 & 0 & 0 & 0 & 1 & 0 \\ 0 & 0 & 0 & 0 & 0 & 0 & 1 \\ 0 & 0 & 0 & 0 & 0 & 0 & 0 \\ 0 & 0 & 0 & 0 & 0 & 0 & 72.68 \\ 0 & 0 & 0 & 0 & 0 & 0 & 0 \\ 0 & 0 & 0 & 0 & -5.630 & 0 & 0 \end{bmatrix}, \quad B = \begin{bmatrix} 0 & 0 \\ 0 & 0 \\ 0 & 0 \\ 44.70 & 0 \\ 0 & 470.7 \\ -43.06 & 0 \\ 0 & 0 \end{bmatrix} \quad (5.31)$$

$$C = \begin{bmatrix} 0 & 1 & 0 & 0 & 0 & 0 & 0 \\ 0 & 0 & 1 & 0 & 0 & 0 & 0 \end{bmatrix} \quad (5.32)$$

with the following transfer functions

$$\frac{q_3}{T_1} = \frac{-43.06}{s^2} \quad (5.33)$$

$$\frac{q_4}{T_2} = \frac{2650}{s^3 + 409.2s} \quad (5.34)$$

$$\frac{q_2}{T_2} = \frac{-470.7}{s^2 + 409.2} \quad (5.35)$$

The overall system is seventh order. An eigenvalue evaluation of the result in one rigid-body mode (two poles are at zero), three additional poles at the origin representing the kinematic differential equations, and two complex poles $\{\pm 20.2284i\}$ corresponding to the natural frequency and associated oscillatory mode that couples gimbals ω_2 and ω_4 .

In order for the diagnose to converge to a unique solution and for there to be no unobservable or uncontrollable states, the plant model must be represented in its minimal form, which is specified according to:

$$\begin{aligned}
 x' &= \begin{bmatrix} q_3 \\ q_4 \\ \omega_3 \\ \omega_2 \\ \omega_4 \end{bmatrix}, & A' &= \begin{bmatrix} 0 & 0 & 1 & 0 & 0 \\ 0 & 0 & 0 & 0 & 1 \\ 0 & 0 & 0 & 0 & 0 \\ 0 & 0 & 0 & 0 & 72.68 \\ 0 & 0 & 0 & -5.63 & 0 \end{bmatrix}, & B' &= \begin{bmatrix} 0 & 0 \\ 0 & 0 \\ -43.06 & 0 \\ 0 & 470.1 \\ 0 & 0 \end{bmatrix}, \\
 C' &= \begin{bmatrix} 1 & 0 & 0 & 0 & 0 \\ 0 & 1 & 0 & 0 & 0 \end{bmatrix}. \tag{5.36}
 \end{aligned}$$

The eigenvalues of A' are located at $\{0,0,0,\pm 20.2284i\}$. The dynamics for the states q_3, q_4 and ω_3 are slow dynamics and these for ω_2 and ω_4 are fast. Using $\varepsilon = 0.05$, the model (5.36) may be expressed in a standard singularly perturbed form

$$\begin{aligned}
 x_1 &= \begin{bmatrix} q_3 \\ q_4 \\ \omega_3 \end{bmatrix}, & A_{11} &= \begin{bmatrix} 0 & 0 & 1 \\ 0 & 0 & 0 \\ 0 & 0 & 0 \end{bmatrix}, \\
 A_{12} &= \begin{bmatrix} 0 & 0 \\ 0 & 1 \\ 0 & 0 \end{bmatrix}, & B_1 &= \begin{bmatrix} 0 & 0 \\ 0 & 0 \\ -43.06 & 0 \end{bmatrix}, \\
 x_2 &= \begin{bmatrix} \omega_2 \\ \omega_4 \end{bmatrix}, & A_{21} &= \begin{bmatrix} 0 & 0 & 0 \\ 0 & 0 & 0 \end{bmatrix},
 \end{aligned}$$

$$\begin{aligned}
A_{22} &= \begin{bmatrix} 0 & 3.63 \\ -0.28 & 0 \end{bmatrix}, & B_2 &= \begin{bmatrix} 0 & 23.5 \\ 0 & 0 \end{bmatrix}, \\
C_1 &= \begin{bmatrix} 1 & 0 & 0 \\ 0 & 1 & 0 \end{bmatrix}, & C_2 &= \begin{bmatrix} 0 & 0 \\ 0 & 0 \end{bmatrix}.
\end{aligned} \tag{5.37}$$

5.2.3 Composite Observer Design

In this section, it is shown that the original full-order model and the uncorrected slow model are both observable, but the uncorrected fast model is unobservable. Therefore, in order to design a composite observer for the original model, it is necessary to consider higher-order fast subsystem models and their observability properties.

For the original full-order system (5.36), we may directly design an observer with the gain matrix as

$$G_{or} = 10^3 \times \begin{bmatrix} 0.006 & 0 \\ 0 & 0.1220 \\ 0.0050 & 0 \\ 0.0025 & 7.9078 \\ 0.0018 & 2.5308 \end{bmatrix}, \tag{5.38}$$

which places the poles of $(A' - G_{or} C')$ at $\{-90, -30, -5, -2, -1\}$.

At $\varepsilon = 0$, the uncorrected slow subsystem is given by the following matrices

$$\begin{aligned}
A_s^0 \Big|_{\varepsilon=0.05} &= \begin{bmatrix} 0 & 0 & 1 \\ 0 & 0 & 0 \\ 0 & 0 & 0 \end{bmatrix}, & B_s^0 \Big|_{\varepsilon=0.05} &= \begin{bmatrix} 0 & 0 \\ 0 & -6.468 \\ -43.06 & 0 \end{bmatrix}, \\
C_s^0 \Big|_{\varepsilon=0.05} &= \begin{bmatrix} 1 & 0 & 0 \\ 0 & 1 & 0 \end{bmatrix}, & D_s^0 \Big|_{\varepsilon=0.05} &= \begin{bmatrix} 0 & 0 \\ 0 & 0 \end{bmatrix}.
\end{aligned} \tag{5.39}$$

The resulting observer gain is now obtained as

$$G_s^0|_{\varepsilon=0.05} = \begin{bmatrix} 6 & 0 \\ 0 & 10 \\ 5 & 0 \end{bmatrix}, \quad (5.40)$$

which places the poles of $(A_s^0 - G_s^0 C_s^0)$ at $\{-10, -5, -1\}$. For the slow subsystem, there is no correction in the higher order models, since $A_{21} = 0$ which makes all the ε -terms equal to zero. Therefore, we set $G_s^1 = G_s^0$.

The uncorrected fast subsystem is now given by

$$\begin{aligned} A_f^0|_{\varepsilon=0.05} &= \begin{bmatrix} 0 & 3.634 \\ -0.2815 & 0 \end{bmatrix}, & B_f^0|_{\varepsilon=0.05} &= \begin{bmatrix} 0 & 23.51 \\ 0 & 0 \end{bmatrix}, \\ C_f^0|_{\varepsilon=0.05} &= \begin{bmatrix} 0 & 0 \\ 0 & 0 \end{bmatrix}. \end{aligned} \quad (5.41)$$

Since $\text{rank}[C_2 \ C_2 A_{22}]^T = 0$, the uncorrected associated fast model (5.41) is not observable, and therefore no observer can be designed for this system. Thus, for the fast subsystem, we obtain the first-order corrected model which is easily described as

$$\begin{aligned} A_f^1|_{\varepsilon=0.05} &= \begin{bmatrix} 0 & 3.634 \\ -0.2815 & 0 \end{bmatrix}, \\ B_f^1|_{\varepsilon=0.05} &= \begin{bmatrix} 0 & 23.51 \\ 0 & 0 \end{bmatrix}, \\ C_f^1|_{\varepsilon=0.05} &= \begin{bmatrix} 0 & 0 \\ 0.0138 & 0 \end{bmatrix}. \end{aligned} \quad (5.42)$$

and is now clearly observable. Hence we choose the observer gain matrix as

$$G_f^1|_{\varepsilon=0.05} = \begin{bmatrix} 0 & 363.4 \\ 0 & 99.54 \end{bmatrix}. \quad (5.43)$$

which places the poles of $(A_f^1 - G_f^1 C_f^1)$ at $\{-2, -3\}$.

By applying the expression (3.76)-(3.77), a composite observer is now obtained

as

$$G = 10^3 \times \begin{bmatrix} 0.006 & 0 \\ 0 & 0.11 \\ 0.005 & 0 \\ 0 & 7.268 \\ 0 & 1.99 \end{bmatrix} \quad (5.44)$$

which locates the poles of $(A' - GC')$ at $\{-80.99, -27.15, -5, -1.86, -1\}$.

Using the state feedback gain $[T_1 \ T_2]^T = -K\hat{x}$, the roots of the pole-placement design are given by $\{-2, -3, -4, -30, -90\}$ when

$$K = \begin{bmatrix} -4.7265 & 1.5729 & -1.6404 & -0.7808 & 0.9944 \\ 0.1645 & -0.1751 & 0.0543 & 0.1242 & 0.0270 \end{bmatrix} \quad (5.45)$$

The plots in Figure 5-12 correspond to the output responses q_3 and q_4 of the closed-loop system with the composite observer G (solid lines) and the observer G_{or} (dashed lines) that are directly designed for the original full-order system. These plots show that the responses obtained by using G and G_{or} match closely asymptotically increases (that is, as t approaches to infinity).

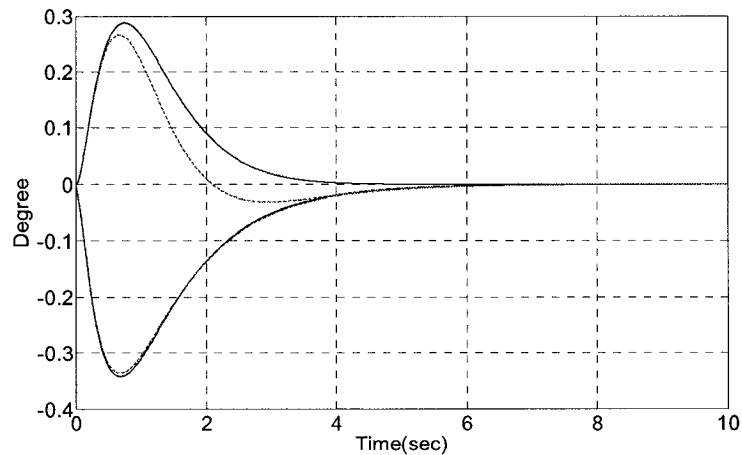


Figure 5-12 Performance comparison of the output responses (q_3, q_4) of the closed-loop system with the composite observer G (solid lines) and the observer G_{or} (dashed lines) directly designed for the original full-order system

5.2.4 Actuator Fault Diagnosis and Simulation Results

The system (5.36) is a 2-input-2-output system, so it is necessary to consider the fault separation problem first. Following the procedures outlined in Section 4.3.1, we have

$$l_1 = [0 \ 0 \ -43.06 \ 0 \ 0]^T \quad (5.46)$$

$$l_2 = [0 \ 0 \ 470.1 \ 0 \ 0]^T \quad (5.47)$$

$$l = [Al_1 \ A^2l_2] = 10^5 \times \begin{bmatrix} 0.0004 & 0 \\ 0 & -0.0265 \\ 0 & 0 \\ 0 & -1.9236 \\ 0 & 0 \end{bmatrix} \quad (5.48)$$

Since

$$R = \text{rank}(Cl) = \text{rank} \left(\begin{bmatrix} -43.1 & 0 \\ 0 & -2646.7 \end{bmatrix} \right) = 2, \quad (5.49)$$

the two possible actuator faults in the system (5.36) are seperable.

As already obtained in Section 5.2.3, we have

$$B_f^0|_{\epsilon=0.05} = B_f^1|_{\epsilon=0.05} = \begin{bmatrix} 0 & 23.51 \\ 0 & 0 \end{bmatrix},$$

$$C_f^0|_{\epsilon=0.05} = \begin{bmatrix} 0 & 0 \\ 0 & 0 \end{bmatrix}, \quad C_f^1|_{\epsilon=0.05} = \begin{bmatrix} 0 & 0 \\ 0.0138 & 0 \end{bmatrix},$$

so that the uncorrected fast subsystem model is not observable and the 1st-order corrected fast model is observable but not actuator fault diagnosable. Furthermore, since in the original full-order system

$$y' = C'x' = \begin{bmatrix} 1 & 0 & 0 & 0 & 0 \\ 0 & 1 & 0 & 0 & 0 \end{bmatrix} = \begin{bmatrix} q_3 \\ q_4 \end{bmatrix} \quad (5.50)$$

where q_3 and q_4 are slow states, we can use the observer for the slow subsystem

$$\dot{\hat{x}}_s^0 = (A_s^0 - G_s^0 C_s^0) \hat{x}_s^0 + B_s^0 u_s + G_s^0 y_s^0 \quad (5.51)$$

$$\hat{y}_s^0 = C_s^0 \hat{x}_s^0 \quad (5.52)$$

to estimator q_3, q_4 and construct the residual generator as

$$r = [r_1 \quad r_2]^T = \hat{y}_s^0 - y', \quad (5.53)$$

For comparison, we also consider the observer designed with the gain matrix

G_{or} for the residual generator. The error dynamics system is described as

$$\dot{e} = (A - G_{or})e - Bf \quad (5.54)$$

$$r = Ce \quad (5.55)$$

with the transfer function

$$\frac{f_1}{r_1} = \frac{43.06}{s^2 + 6s + 5}$$

$$\frac{f_1}{r_2} = 0$$

and the transfer function

$$\frac{f_2}{r_1} = 0$$

$$\frac{f_2}{r_2} = \frac{2647}{s^3 + 110s^2 + 2400s + 4092}$$

Therefore, the residual generator (5.54)-(5.55) is able to detect and isolate faults in the original system.

Fig. 5-13 shows the simulation results corresponding to the following scenario: the actuators are supposed to provide constant step input equal to $T_1 = 1$ and $T_2 = 1$. An actuator fault in the 1st actuator f_1 occurs at time $t=200$ and ends at $t=300$ s [as shown in Fig. 5-13(a)]. Fig. 5-13(b) depicts the output of the simple residual generator

(5.40) based on the slow subsystem observer. Fig. 5-13(c) shows the output of the residual generator using with the gain G_{or} .

From the behavior of the error between the residual and the real fault as shown in [Fig. 5-13(d)], it is clear that the residual of the generator using G_{or} is closer to the real fault. However, design of an observer for the reduced-order slow subsystem is easier to accomplish when compared to a full-order observer for the original system.

5.3 Conclusion

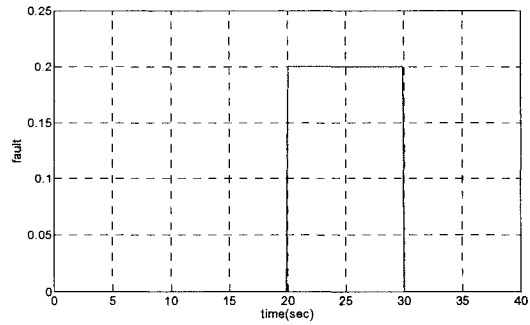
The proposed FDI schemes were validated to two applications: a two time-scaled aircraft longitudinal dynamical models and a four degree of freedom gyroscope system.

For the two time-scaled aircraft longitudinal dynamics, simulations of the open loop responses of a detailed model show that the uncorrected model accurately does model the full-order system when the singular perturbation parameter ε is small, but as ε increases, the higher-order models are needed to approximate the full-order system. For the fault diagnose purpose, a composite observer is obtained based on the observers designed for the uncorrected slow and fast subsystem models. Consequently, the observer design for the high-order system were simplified by designing two lower-order observers for the slow and fast subsystem models.

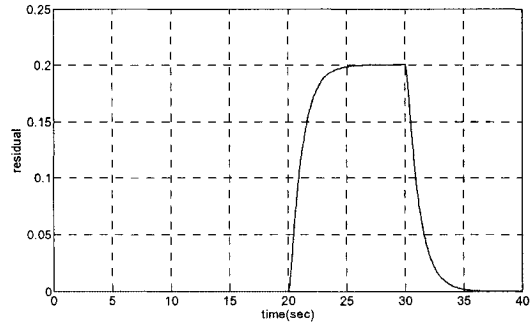
For the four degree of freedom gyroscope system, we compared the outputs of the closed-loop systems with the composite observer G and the observer G_{or} directly designed for the original full-order system. Simulation results show that the responses obtained by using G and G_{or} match closely asymptotically. Since the fast subsystem is not fault diagnosable up to the 1st-order model and the outputs of the original full-

order system are the two slow states q_3, q_4 , we can therefore use the observer for the slow subsystem to and construct the residual generator (5.53). The simulation results show the residual generator (5.53) can diagnose the fault in the full-order system effectively.

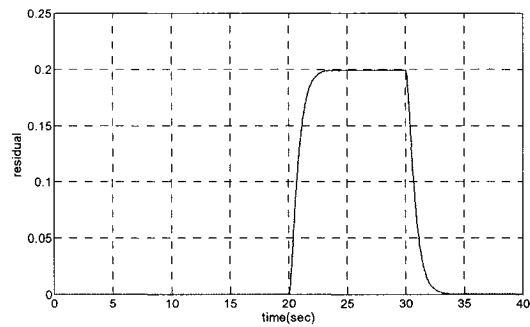
In conclusion, the observer design for a two time-scaled system can be simplified by investigating the observability of the slow and fast subsystem models.



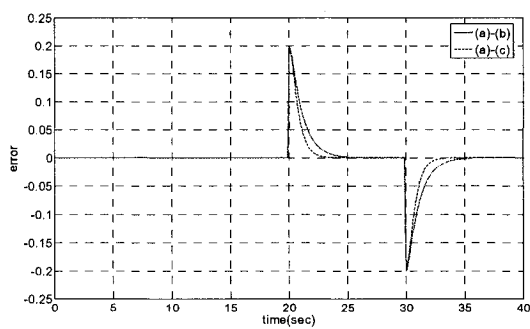
(a) The fault occurs in the 1st actuator of the original system



(b) The 1st output of the simple residual generator (5.26)



(c) The 1st output of the residual generator with G_{or}



(d) The error between the real fault and the residual

Figure 5-13 The actuator fault in the original system and the residuals of different generators

Chapter 6

Conclusions and Future Work

6.1 Conclusions and Contributions

In this thesis, a composite observer was developed as a residual generator and applied to a two time-scale aircraft longitudinal dynamics and the four degree of freedom gyroscope, both of which are singularly perturbed systems. The original full-order system is first decoupled into slow and fast subsystem models and the observers are designed to detect and isolate the actuator faults in the subsystems. An observer is then decoupled to diagnose the actuator faults in the original system. The performance and capabilities of the observer and the observer designed directly for the original full-order system are compared and analyzed.

In Chapter 2, we review approaches for fault detection and isolation in automatic processes using analytical and knowledge-based redundancy and discuss some recent new results from the literature. The principles for model-based methods are outlined, and robust residual generation for both linear and nonlinear systems is discussed. Furthermore, we also present some knowledge-based redundancy methods in case the linear model of the system is not precisely given or known.

In Chapter 3, slow and fast models (3.44)-(3.47) associated with a class of linear singularly perturbed systems are provided and it is shown that the derivative of the input plays an important role in the characterization and definition of higher-order subsystem models. As the singular perturbation parameter ε increases, higher-order corrected systems are utilized as they agree more closely with the original full-order system as compared to the uncorrected subsystems. Furthermore, we reviewed J.O'Reilly's work [36] for designing a composite observer for the original full-order model and discussed the necessity to develop this composite observer based on the observers for the high-order slow and fast subsystem models. A theorem is proved to determine sufficient conditions for designing the composite observer and expressions (3.18)-(3.20) which the state estimation errors satisfy.

In Chapter 4, we considered a geometric method [24, 25] that provides the sufficient and necessary conditions for solving the linear fault detection and isolation problem. If the subsystem models satisfy the sufficient and necessary conditions, observers can be designed as the residual generators to detect and isolate the actuator faults in the subsystems. Furthermore, based on the composite observers, residual generators can be designed to solve the FDI problem in the original system. It is essential to consider the observability and fault diagnosability of the subsystems and thus higher-order corrected models are necessary to develop.

Chapter 5 deals with the application of the techniques developed in previous chapters illustrated to practical singularly perturbed systems. The two time-scale aircraft longitudinal dynamics is first studied. The uncorrected slow and fast models are both observable and fault diagnosable, so observers are designed to detect and isolate the actuator faults in the slow and fast subsystems. An observer is then designed composed as a residual generator for the original full-order system. Thus, we

avoid designing a high-order observer by designing two lower-order observers and obtaining a composite one for the original full-order system. For the four degree of freedom gyroscope, there is no correction to higher-order slow models. The uncorrected slow and subsystem is fault diagnosable but the fast subsystem is not fault diagnosable. The outputs of the original full-order system are the two slow states. Therefore, we simply used the error between the output of the original system and that of the observer of the slow subsystem as the fault residual. The FDI procedure was thus simplified in this case. Therefore, a composite observer is not always needed if the output of the original full-order system can be estimated by the observer of an observable subsystem model.

In the thesis, we developed the high-order corrections of the slow and fast models of a singularly perturbed system with inputs, and constructed a full-order diagnoser for the original full-order system based on the diagnosers designed separately for the slow and fast high-order models. By investigating the observability of the subsystem models, we simplified the observer design for a high-order two time-scaled system. And by using the geometric approach, we detected and isolated actuator faults in the full-order system and the slow and fast subsystems.

6.2 Future Direction of Research

Singularly perturbed systems often occur naturally due to the presence of small “parasitic” parameters, typically small time constants, masses etc., multiplying time derivatives which gives rise to coupled system with slow and fast dynamical modes. Using the singular perturbation approach, system analysis and design may be carried out in two separated and decoupled stages, namely one for the slow modes and the other for the fast. In this way, through system design in two separate time-scales, both

high dimensionality and stiffness problems are alleviated while retaining an approximation to the original coupled system's behavior.

Following the procedures in Chapter 3, we can formulate conditions for which a composite observer-based controller stabilizes the original full-order system. The composite observer-based controller will be synthesized from observer-based controllers for the two separate subsystems in different time-scales and forms the basis of a dynamical controller design using a full-order observer.

Another interesting topic for future investigation is the FDI problem for more general singularly-perturbed systems, for example, under what conditions the composite observer can be used as the residual generator for the original system if observers for the subsystems satisfy the sufficient and necessary conditions of the geometric approach.

Thirdly, most real-life singularly perturbed systems demonstrate nonlinear dynamic behaviors. Observer design and fault diagnosis for nonlinear two time-scale systems also need considerable attention when linear models are not sufficiently accurate. The composite observer method, introduced in Chapter 3 for linear systems, can be extended to nonlinear autonomous systems. The design is sequential in general, since the observer design for the fast subsystem depends on that of the slow subsystem. Like linear systems, the fundamental question of the fault diagnosis of nonlinear systems is still what additional conditions will guarantee the asymptotic stability of the original full-order system for a sufficiently small singular perturbation parameter ε assuming that the associate slow and fast systems are each asymptotically stable.

Bibliography

- [1] J. Chen, R.J. Patton, "*Robust model-based fault diagnosis for dynamic systems*", Kluwer Academic Publishers, pp. 2, 1999.
- [2] R. J. Patton, P. M. Frank, R. N. Clark, "*Issues of fault diagnosis for dynamic systems*", Springer-Verlag London Limited, 2000.
- [3] Y. Xiong, M. Saif, "*Robust and nonlinear fault diagnosis using sliding mode observers*", Proceedings of the 40th IEEE Conference on Decision and Control, Florida, 2001.
- [4] P. M. Frank, "*Fault diagnosis in dynamic systems using analytical and knowledge-based redundancy – a survey and some new results*", Automatica, vol. 26, pp. 459-474, 1990.
- [5] J. J. Gertler, "*Survey of model-based failure detection and isolation in complex plants*," IEEE Contr. Sys. Mag., vol. 8, pp.3-11, 1988.
- [6] R. Iserman, "*Process fault detection based on modeling and estimation methods: a survey*", Automatica, vol. 20, pp. 387-404, 1984.
- [7] A. S. Willsky, "*A survey of design methods for failure detection in dynamic systems*", Automatica, vol. 12, pp. 601-611, 1976.
- [8] D. Koenig, S. Nowakowski, A. Bourjij, "*New design of robust observers for fault detection and isolation*", Proceedings of the 35th Conference on Decision and Control, Kobe, 1996.

- [9] H. Hammouri, M. Kinnaert, E. H. El Yaagoubi, “*Observer-based approach to fault detection and isolation for nonlinear systems*”, IEEE Transactions on Automatic Control, vol. 44, pp.1879-1884, 1999.
- [10] M. Staroswiecki, B. Jiang, “*Fault identification for a class of linear systems based on adaptive observer*”, Proceedings of the 40th IEEE Conference on Decision and Control, Florida, 2001.
- [11] E. Y. Chow, A. S. Willsky, “*Analytical redundancy and the design of robust detection systems*”, IEEE Transactions on Automatic Control, vol. 29, pp. 603-614, 1984.
- [12] J. Gertler, “*Fault detection and isolation using parity relations*”, Control Engineering Practice, vol. 5, pp. 653-661,1997.
- [13] M. M. Polycarpou, A. T. Vemuri, “*Learning approach to fault tolerant control: an overview*”, Proceedings of the 1998 IEEE ISIC/CIRA/ISAS Joint Conference Gaithersburg, MD, 1998.
- [14] Y. Wang, C.W. Chan, K. C. Cheung, W.C. Chan, “*Fault estimation for a class of nonlinear dynamical systems*”, Proceedings of the 38th Conference on Decision and Control, Arizona, 1999.
- [15] P. M. Frank, “*On-line fault detection in uncertain nonlinear systems using diagnostic observers: a survey*”, INT. J. SYSTEMS SCI., vol. 25, pp.2129-2154, 1994.
- [16] P. V. Kokotovic, R. E. O’Malley, P. Sannuti, “*Singular perturbation and order reduction in control theory – an overview*”, Automatica, vol. 12, pp.123-132, 1976.
- [17] V. R. Saksena, J. O’Reilly, P. V. Kokotovic, “*Singular perturbation and time-scale methods in control theory: survey 1976-1983*”, Automatica, vol. 20, pp. 273-293, 1984.

- [18] P. V. Kokotovic, H. K. Khalil, J. O'Reilly, "*Singular perturbation methods in control analysis and design*", SIAM edition, Academic Press, London, 1986.
- [19] R. V. Beard, "*Failure accommodation in linear systems through self-reorganization*," Ph.D. dissertation, Dep. Aeronautics and Astronautics, Mass. Inst. Technol., Cambridge, MA, Feb. 1971.
- [20] K. Khorasani, "*Nonlinear noninteracting control with stability: a high gain control approach*", Proceedings of the 29th Conference on Decision and Control, vol. 6, pp. 3385-3387, 1990.
- [21] M. A. Massoumnia, "*A geometric approach to failure detection and identification in linear systems*", Ph.D. dissertation, Dep. Aeronautics and Astronautics, Mass. Inst. Technol., Cambridge, 1986.
- [22] M. A. Massoumina, "*A geometric approach to the synthesis of failure detection filters*", IEEE Transactions on Automatic Control, vol. 31, pp. 839-846, Sep, 1986.
- [23] J. H. Yang, F. L. Lian, L. C. Fu, "*Adaptive hybrid position/force control for robotic manipulators with compliant links*", Robotics and Automation, vol.1, pp. 603-608, 1995.
- [24] J. Lin, T. S. Chiang, "*A new design of hierarchical fuzzy hybrid position/force control for flexible link robot arm*", American Control Conference , vol. 6, pp. 5239-5244, 2003.
- [25] J. Wunnenberg, "*Observer-based fault detection in dynamic systems*", PhD thesis, University of Duisburg, VDI-Fortschrittsber, Reihe 8, Nr 222.
- [26] R. J. Patton, J. Chen, "*A re-examination of the relationships between parity space and observer-based approaches in fault diagnosis*", Revue Europeenne Diagnostic et Surete de fonctionnement, 1(2), 183-200, 1990.
- [27] C. Christophe, V. Cocoquempot, B. Jiang, "*Link between high gain observer-*

based residual and parity space one”, Proceedings of the American Control Conference Anchorage, AK, pp. 2100-2105, 2002.

[28] T. G. Park, K. S. Lee, “ *Process fault isolation for linear systems with unknown inputs*”, IEE Proceedings Control Theory Appl., Vol. 151, No. 6, pp. 720-726, 2004.

[29] M. Staroswiecki, B. Jiang, “ *Fault identification for a class of linear systems based on adaptive observer*”, Proceedings of the 40th IEEE Conference on Decision and Control, pp. 2283-2288, 2001.

[30] Q. H. Zhang, “ *Adaptive observer for multiple-input-multiple-output linear time-varying systems*”, IEEE Transactions on Automatic Control, vol. 47, 2002.

[31] D. Koenig, S. Mammar, “ *Design of a class of reduced order unknown inputs nonlinear observer for fault diagnosis*”, Proceeding of the American Control Conference, pp. 2142-2147, 2001.

[32] A. T. Vemuri, M. M. Polycarpou, “ *Robust nonlinear fault diagnosis in input-output systems*”, INT. J. CONTROL, vol. 68, pp. 343-360, 1997.

[33] X. D. Zhang, M. M. Polycarpou, “ *A robust detection and isolation scheme for abrupt and incipient faults in nonlinear systems*”, IEEE Transactions on Automatic Control, vol. 47, pp. 576-593, 2002.

[34] Q. Zhao, Z.H. Xu, “ *Design of a novel knowledge-based fault detection and isolation scheme*”, IEEE Transaction on Systems, Man and Cybernetics, vol.34, pp.1089-1096, 2004.

[35] D. F. Akhmetov, Y. Dote, “ *Fuzzy neural network with general parameter adaptation for modeling of nonlinear time-series*”, IEEE Transactions on Neural Networks, vol. 12, pp.148-153, 2001.

[36] J.O'Reilly, “ *Observers for singularly perturbed linear time-varying system*”, Int. J. Control, vol. 30, pp. 745-754, 1979..

- [37] H. L. Jones, “ *Failure detection in linear systems*”, Ph.D. dissertation, Dep. Aeronautics and Astronautics, Mass. Inst. Technol., Cambridge, MA, 1973.
- [38] J. H. Chow and P. V. Kokotovic, “ *A decomposition of near-optimum regulator for systems with slow and fast modes*”, IEEE Transactions on Automatic Control , vol. 21, pp.701 – 705, 1976.
- [39] T. Demosthenis, Nils R.Sandell, “*Linear regulator design for stochastic systems by a multiple time-scales method*”, IEEE Transactions on Automatic Control, vol. 22, pp. 615-621, 1977.
- [40] User’s Manual of the Model 750 Control Moment Gyroscope System, Educational Control Products, 1999.